Nitric Oxide Generating Polymers (NOGPs)

by

Sang-yeul Hwang

A dissertation submitted in partial fulfillment
of the requirements for the degree of
Doctor of Philosophy
(Chemistry)
in The University of Michigan
2007

Doctoral Committee:

Professor Mark E. Meyerhoff, Chair
Assistant Professor Marc J. A. Johnson
Associate Professor Kyoung-Dall Lee
Assistant Professor Melanie S. Sanford

To mother

Park, Mu-Soon

ACKNOWLEDGEMENTS

I would like to thank Dr. Mark Meyerhoff, my advisor, for giving me the opportunity to work with him and inspiring me with his endless energy for research. I am very grateful for his patience and thoughtful support so that I could pursue the research described in this dissertation. Especially, the research of nitric oxide performed under his guidance has definitely affected my scientific career, goals, and even point of view on chemical biology.

I want to acknowledge Drs. Marc Johnson, Kyoung-Dall Lee, and Melanie Sanford for being members of my dissertation members and also for providing references of recommendation letters as needed. I also want to thank Dr. Joerg Lahann in Chemical Engineering Department of the University of Michigan, who has collaborated on one of the projects regarding nitric oxide generating polymers. I am grateful to Dr. Scott Merz at MC3 Inc. for supporting this research. I am appreciative of Dr. Paul Rasmussen for his financial support during my initial research rotation as well as for always showing kindness to me.

I am indebted to my collaborators. Dr. Wansik Cha helped me to prepare the amperometric RSNO sensor. Yongjae Kang taught me to properly operate the UV spectrophotometer and spin coater. Nathan Lafayette in the Dr. Bartlett group at the Medical Center of the University of Michigan prepared the blood samples for the sensor work. Dr. Ted Huston in the Geological Department of the University of Michigan

performed the analysis of copper and tellurium using the ICP-HRMS in a timely manner and with kindness. Dr. Eugenio Alvarado instructed me on how to analyze the organoditelluride compound via the NMR. Dr. James Windak guided me in operating the MS and EPR instruments. My dissertation research could not have been carried out without the help of these collaborators.

I also want to show gratitude to many past and all the present members of the Meyerhoff research group for their support and friendship. Special thanks go to Jason Bennett, Natalie Walker, Yiduo Wu, Laura Zimmerman, Jeremy Mitchell-Koch, and Biyun Wu for their revisions of this dissertation and previous manuscripts. I truly enjoyed discussing chemistry and working together with Yongjae Kang, Wansik Cha, and Zhengrong Zhou. I am thankful to Qinyi Yan, Jun Yang, Maxim Burgman, Lin Wang, Dongxuan Shen, Ayman Eldourghamy, and Megan Frost, who have worked together with friendship.

Finally, I am really obliged for the support of all my family; my parents (Mu-Soon Park, Hyoung-Jun Hwang), parents-in-law (Dong-Geon Kweon, Byoung-Wha Cha), as well as my brothers and sisters (particularly, Kywe-Hwan Hwang). My sincere and special thanks go to Dr. Hye Kyong Kweon (wise wife), Jae Chan Hwang (proud son), and Min Su Hwang (loving daughter).

TABLE OF CONTENTS

DEDICATION · ii

ACKNOWLEDGEMENTS · iii

LIST OF FIGURES · vii

LIST OF SCHEMES · xiii

LIST OF TABLES · xiv

LIST OF ABBREVIATIONS · xv

ABSTRACT · xix

CHAPTER

1. Introduction · **1**

1.1. Biological roles of NO · 2
1.2. NO releasing polymers vs. NO generating polymers · · · · · · · · · · 4
1.3. Biological NO production · 7
1.4. Endogenous S-nitrosothiols as potential substrates for NOGPs · · · · · 9
1.5. Potential catalysts for NOGPs · · · · · · · · · · · · · · · · · · · 11
1.6. Statement of dissertation research · · · · · · · · · · · · · · · · · 16
1.7. References · 20

2. Polymethacrylates with Covalently Linked Copper(II)-Cyclen Complex for In Situ Generation of Nitric Oxide from Nitrosothiols in Blood · · · · · · · **29**

2.1. Introduction · 29
2.2. Experimental · 32
2.3. Results and discussion · 40
2.4. Conclusions · 51
2.5. References · 52

3. Polyurethanes with a Tethered Copper(II)-Cyclen Complex: Synthesis and Catalytic Generation of Nitric Oxide From S-Nitrosothiols · · · · · · · · 55
3.1. Introduction · 55
3.2. Experimental · 58
3.3. Results and discussion · 66
3.4. Conclusions · 78
3.5. References · 80

4. Organoditelluride-Mediated Catalytic S-Nitrosothiol Decomposition to Nitric Oxide · 82
4.1. Introduction · 82
4.2. Experimental · 85
4.3. Results and discussion · 88
4.4. Conclusions · 98
4.5. References · 100

5. Organoditelluride-Tethered Polymeric Materials as New Nitric Oxide Generating Polymers · 102
5.1. Introduction · 102
5.2. Experimental · 104
5.3. Results and discussion · 110
5.4. Conclusions · 123
5.5. References · 125

6. Amperometric Nitrosothiol Sensor Using Immobilized Organoditelluride Species as Selective Catalyst · 128
6.1. Introduction · 128
6.2. Experimental · 133
6.3. Results and discussion · 136
6.4. Conclusions · 147
6.5. References · 149

7. Conclusions and Future Directions · · · · · · · · · · · · · · · · · · · 153
7.1. Conclusions · 153
7.2. Future directions · 158
7.3. Considerations for future research and applications of NOGPs · · · · 162
7.4. References · 165

LIST OF FIGURES

Figure

1.1 Scheme of NO production by nitric oxide synthase in the endothelial cell (eNOS). . . . 3

1.2 Schemes for NO releasing polymers in contact with blood; two different types of NO donors; (1) proton-mediated NO release from diazeniumdiloates and (2) light-initiated NO release from S-nitrosothiols. . . . 5

1.3 Depiction of a NO generating polymer (NOGP). . . . 6

1.4 Three typical pathways of NO production in biological systems in which various enzymes such as NOS (nitric oxide synthase), NiR (nitrite reductase), NR (nitrate reductase), PDI (protein disulfide-isomerase), GPx (glutathione peroxidase), and Trxn (thioredoxin) are involved in the NO formation from various NO sources such as L-Arg (L-arginine), NO_2^- (nitrite), NO_3^- (nitrate), RSNOs (S-nitrosothiols). . . . 7

1.5 Structures of low molecular weight S-nitrosothiols (RSNOs) such as S-nitrosoglutathione (GSNO) and S-nitrosocysteine (CySNO) found in blood. . . . 8

1.6 Biological pathways for S-nitrosothiol (RSNO) formation from NO and free thiols (RSHs) through (i) oxidative products (N_xO_y) such as nitrogen dioxide (NO_2), dinitrogen trioxide (N_2O_3), and peroxynitrite $(ONOO)^{\bullet -}$; (ii) the formation of an radical intermediate, (RS-$N^{\bullet}$-OH); or (iii) nitrosylated metal centers such as copper or iron. . . . 9

1.7 The redox chemistry of Cu(II/I) in generating NO from RSNOs. . . . 12

1.8 Examples of copper ion-complexes liberating NO from RSNOs in the presence of reducing agents (DTTCT= dibenzo[e,k]-2,3,8,9-tetrapheny-1,4,7,10-tetraaza-cyclododeca-1,3,7,9-tetraene; cyclen= 1,4,7,10-tetraazacyclododecane). . . . 13

2.1 A general experimental configuration for NO measurements via a chemiluminescence nitric oxide analyzer (NOA). . . . 37

2.2 The configuration of amperometric NO sensor used for the direct detection of RSNOs in fresh sheep blood. 40

2.3 EPR spectra of $Cu(cyclen)Cl_2$ and Cu(II)-cyclen-pHEMA **7** in DI water or PBS buffer, pH 7.4 at 77K. 42

2.4 The pictures of a crosslinked pHEMA and Cu(II)-cyclen-pHMEA 7 with various copper content after being hydrated in DI water. 43

2.5 The profiles of NO generation for the following disk polymers (thickness, 0.3 mm; radius, 2.0 mm) in 2 mL of 10 mM deoxgenated PBS buffer, pH=7.4, monitored with a chemiluminescence NO analyzer (NOA) at RT. 44

2.6 Copper leaching from Cu(II)-cyclen-pHEMA **7** after soaking experiments. . . 47

2.7 The NO generation profiles of Cu(II)-cyclen-pHEMA **7** before and after soaking in the sheep plasma or whole blood over the various time periods were recorded by the NOA. 49

2.8 Calibration responses for RSNO sensor (a) and NO sensor (b) toward the different NO levels. 50

2.9 The direct amperometric detection of endogenous RSNOs in fresh sheep blood using a NO sensor (A) as a control and a RSNO sensor (B) upon injection of 6 mL of fresh sheep blood (→) into 30 mL of 10 mM PBS buffer, pH 7.4, at 37 ˚C under nitrogen stream. 50

3.1 IR spectra of (A) thermoplastic PU (Tecophilic, SP-93A-100); (B) isocyanated intermediate; and (C) aminated PU (**2**). 67

3.2 UV spectra of two films in fully hydrated states: (A) Cu(II)-cyclen-PU (**5**); and (B) cyclen-PU (**4**). 68

3.3 EPR spectra of (A) the polymer of Cu(II)-cyclen-PU (**5**), and (B) the solution of Cu(II)-cyclen complex, both in PBS buffer, pH, 7.4, at 77K. 69

3.4 The NOA measurements of catalytic NO production by small disk-shaped films of Cu(II)-cyclen-PU (**5**), cyclen-PU (**4**), and copper ion-treated $(Boc)_3$-cyclen-PU (**3**). . 71

3.5 Substrate dependency on the NO generation from the film of (Cu(II)-cyclen-PU (**5**)) when sequentially used: (A) reducing agent dependency (10 μM) at a 10 μM GSNO solution; and (B) RSH/RSNO variation with both at 10 μM concentrations in the PBS buffer. 72

3.6 NO generation profiles of a piece of Cu(II)-cyclen-PU (**5**) measured by the NOA before/after soaked in the various conditions such as: (A) continuous uses; (B) soaking in excess of GSH/GSNO; and (C) soaking in a platelet-rich sheep plasma. · · · · · 75

3.7 The calibration curves of both sensors ((A) NO and (B) RSNO) were plotted for their intrinsic direct amperometric responses to NO upon the addition of standard NO solution into 100 mL of 10 mM PBS buffer, pH 7.4, at 36 °C. · · · · · · · · · · · · 77

3.8 The direct detection of endogenous RSNOs in fresh sheep blood using the amperometric (A) NO sensor and (B) RSNO sensor by injecting 30 mL of fresh sheep blood into 70 mL of 10 mM PBS buffer, pH 7.4, at 36 °C. · · · · · · · · · · 78

4.1 The proposed mechanism for thiol peroxidase acivity (glutathione peroxidase mimic) of organoditelluride (RTeTeR). · 83

4.2 The proposed mechanism for organoditelluride-mediated catalytic RSNO decomposition to NO. · 84

4.3 The NMR identification for the regioisomer of organoditelluride **1** via the partial substitution of Te with a deuterium using NaOD. · · · · · · · · · · · · · 87

4.4 (A) UV spectroscopy of 5,5'-ditelluro-2,2'-dithiophenecarboxylic acid (DTDTCA, organoditelluride **1**); (B) calibration curve at maximum absorbance (306 nm); (C) the stability of organoditelluride **1**; (D) the calculated decomposition rate of organoditelluride **1** (first order, $k= 9 \times 10^{-5}$ min^{-1}). · 88

4.5 The measurements of catalytic NO generation by 2.5 μM 5,5'-ditelluro-2,2'-dithiophenecarboxylic acid (DTDTCA, organoditelluride **1**) in a solution of (A) 25 μM GSNO and 100 μM GSH, and (B) 50 μM GSNO and 100 μM GSH in PBS buffer, pH 7.4 (0.5 mM EDTA) via chemiluminescence NO analyzer (NOA). · · · · · · · · 90

4.6 The measurements of catalytic NO generation by 2.5 μM 5,5'-ditelluro-2,2'-dithiophenecarboxylic acid (DTDTCA, organoditelluride **1**) in a solution of 50 μM CySNO and 100 μM CySH in 2 mL of 10 mM PBS buffer, pH 7.4, containing 0.5 mM EDTA, via chemiluminescence NO analyzer (NOA). · · · · · · · · · · · 90

4.7 (A) UV-Vis spectrophotometric data for 5,5'-ditelluro-2,2'-dithiophenecarboxylic acid (organoditelluride **1**; λ_{max}= 306 nm), and various GSH and/or GSNO levels; (B) their absorbance changes (at 306 nm) as a function of time; and (C) absorbance changes (at 311 nm) of each solution. · 92

4.8 ArTeSR species was detected by mass spectrometry (electrospray) from a mixture of 5,5'-ditelluro-2,2'-dithiophenecarboxylic acid (organoditelluride **1**)/GSH (1/14, mole/mole) in CH_3CN/water (1/1, v/v). · · · · · · · · · · · · · · · · · · 93

4.9 pH dependent NO generation of 1.25 μM 5,5'-ditelluro-2,2'-dithiophenecarboxylic acid (DTDTCA, organoditelluride **1**) depending on the various pH values of test solution (a= pH 6, b= pH 7, or c= pH 8) in 2 mL buffer containing 0.5 mM EDTA with 25 μM GSH and GSNO. · 94

4.10 The measurements of NO generation by 2.5 μM 5,5'-ditelluro-2,2'-dithiophenecarboxylic acid (DTDTCA, organoditelluride **1**) in a solution of 50 μM GSNO and 100 μM ascorbate (Asc) in 2 mL of 10 mM PBS buffer, pH 7.4, containing 0.5 mM EDTA. · 94

4.11 The GSH/GSNO concentration-dependent NO generation of 5,5'-ditelluro-2,2'-dithiophenecarboxylic acid (DTDTCA, organoditelluride **1**). · · · · · · · · · 95

4.12 The current changes of amperometric NO sensor mounted with an organoditelluride **1**-immobilized membrane upon adding 20 μL of 5 mM GSNO solutions into 100 mL PBS buffer containing 50μM GSH and 0.1 mM EDTA under ambient oxygen. · · 96

5.1 Comparison of IR spectra between 5,5'-ditelluro-2,2'-dithiophenecarboxylic acid; DTDTCA, **1** (a), the aminated thermoplastic PU; polymer **2** (b), and the conjugated product with (a) and (b); polymer **3** (c). · · · · · · · · · · · · · · · · · 111

5.2 IR and UV spectra of polymer **4**, PAH, and DTDTCA (**1**). · · · · · · · · 112

5.3 Scanning electron microscopy (SEM) image of a part of the intersected polymer **5** film in a dried state after gold coating; the blank (A), L (B), M (C), H (D) film. Polymer **4** is scattered everywhere (bulk phase and surface) in the L, M, and H film (the polymer **5**) in proportional to the amount of polymer **4** loaded in the polymerization process. · 114

5.4 The catalytic NO generation mediated by a piece (ca. 3.9 mg and 3.2 cm^2) of polymer **3** in a solution of 100 μM GSH and 25 μM GSNO in PBS buffer, pH 7.4, (with 0.5 mM EDTA) was monitored using a chemiluminescence NO analyzer. · · · · · · · 116

5.5 The complete denitrosations of S-nitrosothiols (10 μM) catalyzed by the water soluble polymer **4** (~0.75 μM DTDTCA, **1**) were observed via the NOA ((a) and (b)); the same amount of poly(allylamine hydrochloride) (PAH) did not catalyze the reaction (c); nitrite (1 mM $NaNO_2$) was not decomposed by polymer **4** (d) (in 2 mL of PBS buffer, pH 7.4, containing 0.5 mM EDTA and 50 μM RSH). · · · · · · · · · · · · · 117

5.6 The NO generation profiles using the blank (A), film L (B), M (C), and H (D) (1 cm x 1 cm x 50 μm, polymer **5**) from GSNO (50 μM) and GSH (50 μM) in the 2 mL of PBS buffer (10 mM), pH 7.4, containing EDTA (0.5 mM) monitored via a chemiluminescence NO analyzer (NOA). · 118

5.7 A plot of soaking time vs. the accumulated Te amount in sample solution which was withdrawn daily from the solution of 10 μM GSH/GSH with the fully immersed polymer **5**, while a fresh solution of 10 μM GSH/GSNO was correspondingly added into the original solution resulting in an increasing concentration of GSH. · · · · · · · 120

5.8 (A) Calibration curves for the inherent NO responses of both RSNO (a) and NO sensors (b) in the PBS buffer (pH 7.4, 100 mL) at 35 °C; (B) calibration curve for the inherent RSNO response of RSNO sensor (a) in a blood sample (30 mL) diluted in PBS buffer (pH 7.4, 70 mL) at 35 °C. · · · · · · · · · · · · · · · · · · · 122

5.9 The amperometric NO measurements in a fresh sheep whole blood (30 mL) diluted with PBS buffer (70 mL, pH 7.4) at 35 °C using two sensors; RSNO (a) and NO sensor (b), where the amperometric signals were converted to the NO or GSNO equivalents (nM) from their calibration curves. · · · · · · · · · · · · · · · · · · · 122

6.1 (A) Schematic of RSNO detection using the proposed amperometric sensor modified with a NO generating catalytic layer; (B) the schematic structure of organoditelluride-linked hydrogel used in this work. · · · · · · · · · · · · · · · · · · · 132

6.2 The inherent amperometric responses of (a) NO and (b) RSNO sensor monitored by intermittently adding a small aliquots of a standard (A) NO or (B) GSNO solution into the stirred solution of PBS buffer, pH 7.4, containing 0.1 mM EDTA and 50 μM GSH at RT (the working buffer solution). · · · · · · · · · · · · · · · · · · · 137

6.3 The dynamic amperometric response and reversibility of RSNO sensor by exchanging three different concentrations (0, 2, and 4 μM) of GSNO in working buffer solution at RT. · 138

6.4 Stability of RSNO sensor, plotted as relative sensitivity (S_{GSNO}/S_{NO}) of the RSNO sensor as a function of time, where S_{GSNO} is the sensitivity (nA/μM) of RSNO sensor toward GSNO and S_{NO} is the sensitivity (nA/μM) of RSNO sensor toward NO. · · 139

6.5 The typical dynamic amperometric responses detected by the RSNO sensor at low concentrations of various RSNOs, known as endogenous RSNO species in blood ((A) GSNO, (B) CySNO, and (C) AlbSNO) in the working buffer solution at RT. · · 141

6.6 Calibration curves for the representative low molecular weight (LMW) RSNOs with various concentrations ((A) sub μM, (B) μM levels) in the working buffer solution at RT. · 141

6.7 (A) Calibration curves for GSNO, CySNO, and SNAP as measured with new RSNO sensor in the presence of a different reducing agents (GSH or CySH) in the working buffer solution at RT; (B) The real-time measurements of GSNO (4 μM) via the RSNO sensor by injecting GSH or CySH in the working buffer solution at RT. · · · · 143

6.8 Calibration curves of both the (a) RSNO and (b) NO sensors for the individual current responses toward the NO standard solutions added in the working buffer solution at 35 ºC, where the sensitivities were calculated to be 6.8 nA/μM for the NO sensor and 3.3 nA/μM for the RSNO sensor. · 145

6.9 (A) The real-time amperometric detections using both the (a) RSNO and (b) NO sensors for endogenous RSNOs in the sheep whole blood sample in the working buffer solution at 35 ºC (30mL blood, 70 mL PBS buffer, 50 μM GSH, and 0.1 mM EDTA); arrow indicates the moment the fresh sheep whole blood was injected; (B) calibration curves of two ((a) RSNO and (b) NO) sensors for their intrinsic amperometric responses toward GSNO standard solutions added in the same blood sample at 35 ºC. · · · 146

LIST OF SCHEMES

Scheme

2.1 The synthetic scheme for preparing a crosslinked hydrogel, Cu(II)-cyclen-pHEMA **7**. 31

3.1 The typical synthetic scheme for preparing thermoplastic polyurethane (PU). . . 56

3.2 The synthesis of a polyurethane possessing covalently appended Cu(II)-cyclen complex (Cu(II)-cyclen-PU (**5**)) from a modified cyclen derivative (**1**) and aminated PU (**2**). 58

4.1 The synthetic scheme of organoditelluride (**1**), 5,5'-ditelluro-2,2'-dithiophenecarboxylic acid (DTDTCA) using 2-thiophene carboxylic acid. . . . 84

5.1 Synthetic schemes used for preparing new types of nitric oxide generating polymers (NOGPs; polymers **3, 4**, and **5**,) covalently attached with an organoditelluride species (DTDTCA, **1**), where different polymeric matrices are used; hydrophilic thermoplastic polyurethane (PU) for polymer **3**, a water soluble poly(allylamine hydrochloride) (PAH) for polymer **4**, and an interpenetrating polymer network (IPN) consisting of polymer **4** and a cellulose membrane for polymer **5**. 104

7.1 The proposed scheme for the anchoring the Cu(II)-cyclen complex on the surface of stent coated with the functionalized poly-*para*-xylylene (PPX) (**2**) using the cyclen-N-propyl methacrylate monmer (**3**) developed in this research (see **scheme 2.1** in Chapter 2). 159

LIST OF TABLES

Table

1.1 Concentrations of free thiol species in plasma (P) or blood (B). ・ ・ ・ ・ ・ ・ 16

2.1 The correlation between the modified cyclen monomer **5** used in the polymerization reactions and the theoretical and measured copper content of films (Cu(II)-cyclen-pHEMA **7**) as determined by atomic absorption spectrophotometer (AA). ・ ・ ・ ・ 43

5.1 Comparisons of three different polymers (**5**) prepared by altering the amounts of polymer **4** (0.9 wt % (L): 2.7 wt % (M): 9.0 wt % (H)= 1: 3: 10) when loaded in the cellulose membrane (size= 1 cm x 1 cm x 50 μm). ・ ・ ・ ・ ・ ・ ・ ・ ・ ・ ・ ・ 113

LIST OF ABBREVIATIONS

ABBREVIATION

Alb	Albumin
AIBN	2,2'-Azo-bis(isobutyronitrile)
AlbSNO	S-Nitrosoalbumin
$ArSe^-$	Selenolate
ArSeSeAr	Diaryl Diselenide
$ArTe^-$	Tellurolate
ArTeNO	Nitrosotellurol
ArTeSR	Telluro-sulfide
ArTeTeAr	Diaryl ditelluride
BDO	1,4-Butanediol
Boc	tert-Butlycarbonate
BSA	Bovine serum albumin
cAMP	Cyclic adenosine monophosphate
cGMP	Cyclic guanosine 3',5'-monophosphate
csPDI	Cell-surface protein disulfide-isomerase
Cyclen	1,4,7,10-Tetraazacyclododecane
CySH	Cysteine
CySNO	S-Nitrosocysteine
CVD	Chemical vapor deposition
DBTDL	Dibutyltin dilaurate
dHb	Deoxyhemoglobin
DMAC	N,N'-Dimethyl acetamide
DTDTCA	5,5'-Ditelluro-2,2'-dithiophenecarboxylic acid

DTTCT	Dibenzo[e,k]-2,3,8,9-tetrapheny-1,4,7,10-tetraaza-cyclododeca-1,3,7,9-tetraene
EC	Endothelial cell
ECM	Extracellular matrix
ED	Ethylene diamine
EDC	N-(3-Dimethylaminopropyl)-N'-ethylcarbodiimide hydrochloride
EDRF	Endothelium-derived releasing factor
EDTA	Ethylenediamine tetraacetic acid
EGDM	Ethyleneglycol dimethacrylate
GPM	Gas permeable membrane
GPx	Glutathione peroxidase
GSH	Glutathione
GSNO	S-Nitrosoglutathione
GSSG	Glutathione disulfide
GTP	Guanosine 5'-triphosphate
Hb	Hemoglobin
HbSNO	S-Nitrosohemoglobin
HDI	Hexamethylene diisocyanate
HEMA	2-Hydroxyethyl methacrylate
HMDI	Hydrogenated 4,4'-methlyenediphenyl diisocyanate
HMW	High molecular weight
HPU	Hydrophilic polyurethane
HS	Hard segment
ICP-HRMS	Inductively coupled plasma-high resolution mass spectrometry
IP_3	Inositol 1, 4, 5- triphosphate
IPN	Interpenetrating polymer network
LMW	Low molecular weight
MDI	4,4'-Methlyenediphenyl diisocyanate
MTBE	Methyl *tert*-butylether
MWCO	Molecular weight cutoff
NADH	Reduced adenine dinucleotide

NADPH	Nicotinamide adenine dinucleotide phosphate
NAP	N-Acetyl-penicillamine
NHS	N-Hydroxysuccinimide
NiR	Nitrite reductase
NO	Nitric oxide
NOA	Chemiluminescence nitric oxide analyzer
NOGP	Nitric oxide generating polymer
NOS	Nitric oxide synthase
NR	Nitrate reductase
PAAc	Poly(acrylic acid)
PAH	Poly(allylamine hydrochloride)
PBS	Phosphate-buffered saline
PDE	Phosphodiesterase
PDI	Protein disulfide-isomerase
PEG	Poly(ethylene glycol)
PEO	Poly(ethylene oxide)
pHEMA	Poly(2-hydroxyethyl methacrylate)
PKA	Protein kinase A
PKG	Protein kinase
PLA	Poly(lactic acid)
PNIPAAm	Poly(N-isopropyl acrylamide)
PNVP	Poly(N-vinyl pyrrolidone)
PPX	Poly-*para*-xylylene
PTMO	Poly(tetramethyleneoxide)
PU	Polyurethane
PVA	Poly(vinyl alcohol)
PVC	Poly(vinyl chloride)
ROOH	Organic peroxide
RS^-	Thiolate
RSe^-	Selenolate
RSeNO	Nitrososelenol

RSeOH	Selenoic acid
RSeSeR	Organodiselenide
RSeSR	Seleno-sulfide
RSH	Free thiol
RSNO	S-Nitrosothiol
$RSSe^-$	Thio-selenolate
RSSR	Disulfide
$RSTe^-$	Thio-tellurolate
RT	Room temperature
RTeOH	Telluroic acid
RTeTeR	Organoditelluride
SEM	Scanning electron microscopy
sGC	Soluble guanylate cyclase
S_{GSNO}/S_{NO}	Ratio of sensitivity (nA/μM) toward GSNO and NO
SNAP	S-Nitroso-N-acetyl penicillamine
SS	Soft segment
TFA	Trifluoroacetic acid
Trxn	Thioredoxin
XO	Xanthine oxidase

ABSTRACT

Nitric Oxide Generating Polymers (NOGPs)

by

Sang-yeul Hwang

Chair: Mark E. Meyerhoff

Several functional polymers that can catalytically generate nitric oxide (NO) from naturally occurring substrates (S-nitrosothiols; RSNOs) in blood by means of immobilized catalytic sites within the polymers were synthesized and investigated. Such polymers are termed NO generating polymers (NOGPs) and they have the potential to be used as more biocompatible polymeric coatings for biomedical devices (e.g., catheters, vascular grafts, indwelling sensors, etc.) owing to NO's ability to inhibit platelet activation/adhesion and reduce smooth muscle cell proliferation.

In this thesis, two distinctive catalysts were employed to develop the NOGPs: a) Cu(II)-cyclen (cyclen; 1,4,7,10-tetraazacyclododecane) complex, already recognized as

an NO generating catalyst via reductive decomposition of RSNOs; and b) 5,5'-ditelluro-2,2'-dithiophenecarboxylic acid (DTDTCA), a newly synthesized organoditelluride (RTeTeR) species that was discovered, in this thesis work, to exhibit catalytic RSNO denitrosation to NO in the presence of thiol reducing agents (RSHs) at physiological pH. To optimize the catalytic function of the immobilized RTeTeR species, its catalytic mechanism toward RSNO was investigated. Both NO generating catalysts were covalently linked to a variety of polymers including poly(2-hydroxyethyl methacrylate), thermoplastic polyurethane (PU), and poly(allylamine hydrochloride) using standard synthetic methodologies. Loading of catalytic sites on such polymers ranged from 0.04 – 7.5 wt % (Cu or Te content). In addition, some of these catalytic polymers were also employed to create interpenetrating polymer networks using a cellulose membrane or PU base. In all cases, NO generation from RSNOs by the new NOGPs, as measured by chemiluminescence, was found to be proportional to the amount of Cu(II)-cyclen or RTeTeR species linked to the polymeric backbone. Further, it was found that all polymers retained significant catalytic function for at least two weeks, with < 10 -30 % loss of catalytic sites when bathed in buffer containing RSH/RSNO. The ability of each new NOGP to generate NO when in contact with fresh animal blood was also investigated and confirmed by employing the polymers as outer coatings at the distal end of an amperometric NO sensor. Finally, such a measurement configuration was shown to function as a useful RSNO sensor for direct detection of total RSNO species in whole blood samples.

CHAPTER 1

Introduction

Thrombus formation and restenosis are mainly responsible for causing clinical failure in the application of a variety of medical devices such as catheters, vascular grafts, stents, indwelling sensors, and extracorporeal blood-loop circuits when they are in contact with blood.[1-4] The most biocompatible surface known is the host's own intact endothelium that lines the inner walls of all blood vessels. Therefore, mimicking endothelial cellular activity has been suggested as a means to develop more hemocompatible synthetic materials.[5-7] Indeed, since nitric oxide (NO) was recognized as the endothelium-derived releasing factor (EDRF), it has been shown to possess a variety of vasoprotection activities including inhibition of platelet adhesion/activation,[8-10] anti-proliferation of smooth muscle cells,[11] anti-microbial,[12] and wound healing.[13-15] Thus, NO releasing polymers have been developed and proven to exhibit improved blood compatibility.[16-19] However, these polymers have a relatively short use-life because of the rapid depletion of NO from a relatively thin coating of polymeric NO-donor reservoir after they are implanted. Therefore, a new strategy to prepare biomaterials that can produce NO for a prolonged time once implanted *in vivo* is needed. Hence, this thesis introduces a novel idea of using NO generating polymers (NOGPs) that can

biomimetically/catalytically generate NO locally from endogenous substrates in blood for extended periods of time to potentially improve the biocompatibility of implanted biomedical devices.

1.1. Biological roles of NO

Nitric oxide (NO) is one of the most important physiological regulators,[20] playing many biological roles in both cytoprotection and cytotoxicity.[21, 22] For instance, the inhibition of platelet aggregation[8, 10] and smooth muscle cell proliferation,[11] as well as the involvement in angiogensis,[23] are well known examples of NO's cytoprotection in blood vessels. In contrast, the cytotoxicity of NO is associated with peroxynitrite ($ONOO^-$) formation; is neurotoxic[24] as well as DNA damaging.[25] NO also plays a role in killing bacteria[12] and cancer cells.[26] Because NO participates in a variety of biological roles, many NO related studies are still continuing to unravel its complex and wide ranging biological actions, although most of the underlying molecular mechanisms remain poorly understood.

Nonetheless, nitric oxide synthase (NOS) has been generally considered to be the primary source of NO in biological systems. NOS in endothelial cells (eNOS) is the enzyme that catalyzes the conversion of L-arginine and oxygen to L-citrulline and NO with the help of activated calmodulin and nicotinamide adenine dinucleotide phosphate (NADPH) (see **Figure 1.1**). NO generated from eNOS diffuses into the blood (and into platelets) and the surrounding vascular smooth muscle cell, and binds to soluble guanylate cyclase (sGC),[27, 28] a hemoprotein. This binding event activates the enzyme, which catalyzes the conversion of guanosine 5'-triphosphate (GTP) to cyclic guanosine

3',5'-monophosphate (cGMP). This NO/cGMP pathway regulates platelet adhesion and aggregation, as well as smooth muscle cell proliferation and migration.[29-33]

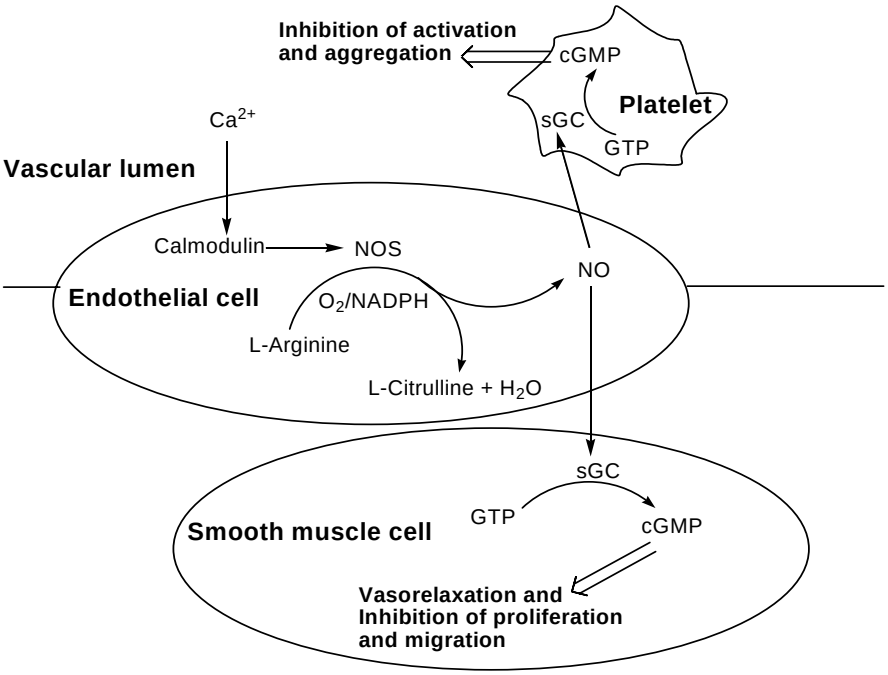

Figure 1.1 Scheme of NO production by nitric oxide synthase in the endothelial cells (eNOS): NO disseminates into vascular lumen and inhibits platelet activation and aggregation. NO also diffuses into the smooth muscle cell and causes vasorelaxation as well as inhibition of proliferation and migration; NADPH (nicotinamide adenine dinucleotide phosphate), sGC (soluble guanylate cyclase), GTP (guanosine 5'-triphosphate), cGMP (cyclic guanosine 3',5'-monophosphate).

The molecular mechanisms responsible for anti-platelet activation/adhesion are not fully known. However, in platelets, it is reported that cGMP activates cGMP-dependent protein kinase (PKG)[34] to phosphorylate an inositol 1, 4, 5- triphosphate (IP_3) receptor,[35] leading to a decrease in intracellular Ca^{2+} concentration, ultimately resulting in the deactivation of the platelet.[36, 37] Indeed, it is known that an increase of intracellular free Ca^{2+} plays a key role during platelet activation.[38] Platelet activation by all stimulatory agonists involves the elevation of intracellular Ca^{2+} levels. Cyclic GMP

also lowers cGMP-regulated phosphodiesterase (PDE) levels, leading to an enhancement in cyclic adenosine monophosphate (cAMP), in sequence, causing a reduction in intracellular Ca^{2+} concentration.[36, 37] Another key process involved is cGMP's ability to modulate the inhibition of a key platelet receptor, glycoprotein IIb/IIIa, which binds with fibrinogen, a critical step for the activation and adhesion of platelets onto surfaces.[39]

With respect to the regulation of vascular smooth cell proliferation, which is mainly responsible for narrowing the lumen of blood vessels in coronary artery disease (i.e. restenosis), the molecular mechanisms involved are even more complicated, and are not well understood.[40, 41] It has been reported that cGMP formed via activation of sGC by NO contributes to the inhibition of cAMP phosphodiesterase (PDE III), and in turn elevates intracellular cAMP concentration and stimulates protein kinase A (PKA).[42, 43] Such NO-dependent activation of PKA is thought to hinder smooth muscle cell proliferation by inhibition of Raf-1, a serine/threonine-specific protein kinase.[44] In addition, the cGMP-independent mechanism of inhibition of cell proliferation by NO is known to be mediated by inhibition of arginase (I and II) and ornithine decarboxylase.[45]

1.2. NO releasing polymers vs. NO generating polymers

From a biomaterial scientist's point of view, NO is a powerful hemostatic regulator, one of the smallest and simplest biosynthetic molecules. Hence, NO is a very attractive agent to adapt into biomaterials to improve persistent hemocompatibility problems. In fact, there are many known NO donors,[16] some of which (e.g., diazeniumdiolates,[19, 46] S-nitrosothiols,[47] etc.) are cost-effective, and can be easily prepared and loaded into polymeric coatings of biomedical devices. For instance, a

diazeniumdiolate-loaded polymer can release 2 equivalents of NO gas (per equivalent of parent diazeniumdiolate) into the blood phase upon contact with 1 equivalent of water via the protonation of amine sites in the polymer phase (see **Figure 1.2**). In the case of polymers with immobilized S-nitrosothiols, NO release from the polymer phase can be initiated by photons, where the NO production is regulated by turning the light on/off (see **Figure 1.2**).

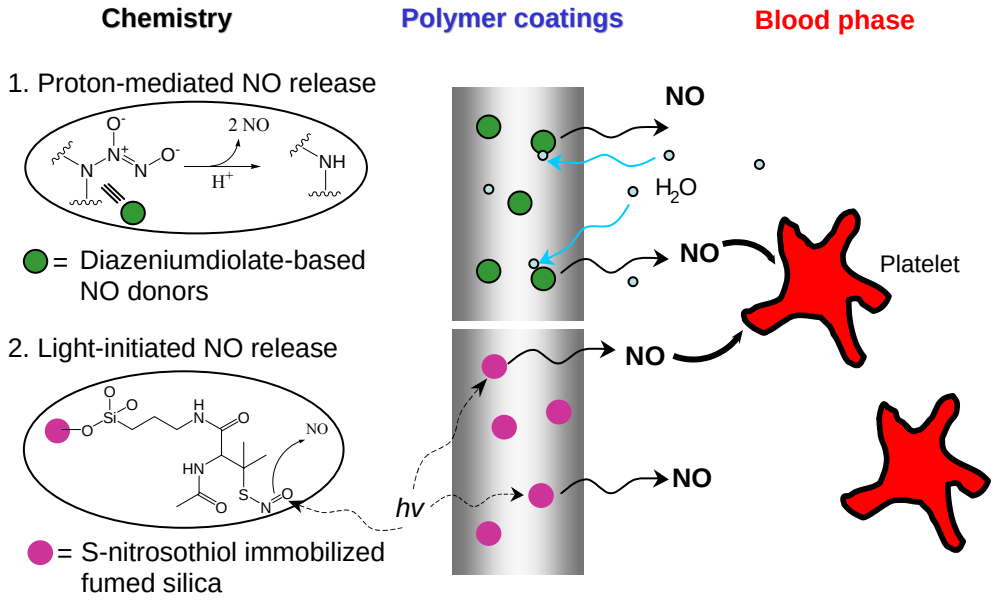

Figure 1.2 Schemes for NO releasing polymers in contact with blood: two different types of NO donors; (1) proton-mediated NO release from diazeniumdiloates and (2) light-initiated NO release from S-nitrosothiols.

A number of NO releasing polymers that release NO at the blood/polymer interface have been investigated to enhance the blood compatibility of medical devices. While they have shown to exhibit greatly reduced platelet adhesion and thrombus formation *in vitro* and *in vivo* using animal models, [19, 48] and also the potential to inhibit restenosis after angioplasty,[49-51] the ultimate biomedical applications of such materials

may be limited to short-term use (i.e., on the order of a few days) due to the relatively small reservoir of NO donors that can be loaded within thin coatings of the new polymeric materials.

One plausible way to replenish the NO reservoir of biomedical devices after implantation is to create catalytic sites within the polymeric materials, which could keep generating NO locally upon contact with blood from endogenous NO precursors and reducing agents already present in blood. Hence, such materials are termed NO generating polymers (NOGPs) (see **Figure 1.3**).

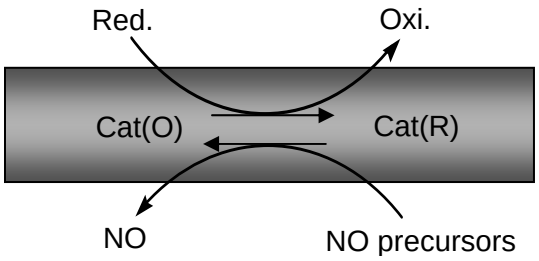

Figure 1.3 Depiction of a NO generating polymer (NOGP); an oxidized form of catalyst (Cat(O)) created in polymeric materials can be reduced by endogenous reducing agents (Red.) into a reduced form of catalyst (Cat(R)) within the polymer phase, which is now able to decompose NO precursors to NO, while returning back to the original form, Cat(O).

The combination of redox catalysts in the polymer and substrates in blood should enable such NOGPs to produce NO for long periods of time when in contact with blood provided that the catalytic activity of the polymer is maintained, and corresponding endogenous NO precursor sources and reducing equivalents remain available in the blood.

1.3. Biological NO production

In order to assess the feasibility of proposed NOGPs, it is important to examine how NO is formed within our bodies. The generation of NO by biological systems can be summarized into three pathways, depending on known NO sources and their enzymes required to produce NO as shown **Figure 1.4**.

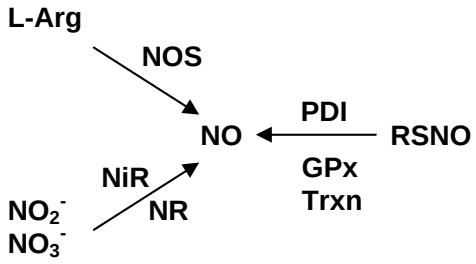

Figure 1.4 Three typical pathways of NO production in biological systems in which various enzymes such as NOS (nitric oxide synthase), NiR (nitrite reductase), NR (nitrate reductase), PDI (protein disulfide-isomerase), GPx (glutathione peroxidase), and Trxn (thioredoxin) are involved in NO synthesis from various NO sources such as L-Arg (L-arginine), NO_2^- (nitrite), NO_3^- (nitrate), and RSNO (S-nitrosothiol).

The first part of NO production involves NOS. NOS is known to exist as three isoforms, neuronal NOS (called nNOS, NOS1, or NOSI),[52] inducible NOS (called iNOS, NOS2, or NOSII),[53] and endothelial NOS (called eNOS, NOS3, or NOSIII).[54] eNOS is the primary NO producing catalyst in biological systems. Despite a homology of ~ 50 – 60 % in sequence, the three NOSs are found to differ in size, intracellular location, and regulation;[55] however, they are all members of a superfamily of heme-containing monooxgyenases including cytochrome P-450. The main substrate of NOSs to generate NO is L-arginine.

Nitrite and nitrate formed by oxidation of NO *in vivo* can also recycle back to NO via nitrite reductase (NiR) and nitrate reductase (NR) activities.[56] Indeed, deoxyhemoglobin (dHb)[57-59] and xanthine oxidase (XO)[60-62] have recently been reported as NO recycling enzymes (dHb as a NiR, and XO as both NiR and NR). Further, it is known that cytochrome cd1[63] and copper NiR[64] in certain bacteria reduce nitrite to NO. It is worth noting that the catalytic redox chemistry of copper species plays a key role in generating NO from nitrite in copper NiR. It is believed that Cu(II) is within the active site of copper NiR, which can be reduced to Cu(I) by reducing agents such as reduced adenine dinucleotide (NADH) and then the reduced Cu(I) species causes the reduction of nitrite to NO by the transfer of one electron.[64]

Finally, there is a group of endogenous S-nitrosothiols (RSNOs) found in blood including, S-nitrosoglutathione (GSNO), S-nitrosocysteine (CySNO), S-nitrosoalbumin (AlbSNO), and S-nitrosohemoglobin (HbSNO), where GSNO and CySNO are low molecular weight (LMW) RSNOs (see **Figure 1.5**), and AlbSNO and HbSNO are high molecular weight (HMW) RSNOs.

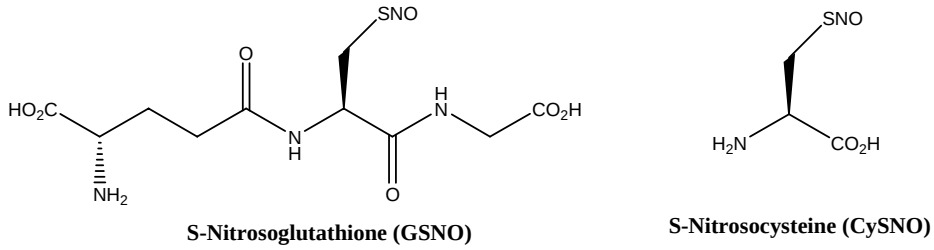

Figure 1.5 Structures of low molecular weight S-nitrosothiols (RSNOs) such as S-nitrosoglutathione (GSNO) and S-nitrosocysteine (CySNO) found in blood.

These RSNOs are known to play a pivotal role in NO biochemistry,[65-68] and are also identified as a source of biological NO. Interestingly, Mutus and co-workers recently

reported that the platelet cell-surface protein disulfide-isomerase (csPDI, a protein that catalyzes thio–disulfide exchange reactions) consumes GSNO to liberate NO, and this function reduces platelet aggregation in the presence of GSNO.[69] Thioredoxin (Trxn) that reduces disulfides and free radicals [70-72] is also known for catalytically denitrosating LMW and HMW RSNOs.[73, 74] A selenium-containing enzyme, glutathione peroxidase (GPx), known as an antioxidant enzyme that reduces lipid hydroperoxides (LOOH) to the corresponding alcohols by the oxidation of reduced glutathione (GSH, L-γ-glutamyl-L-cysteinylglycine),[75] is also recognized for its ability to decompose RSNOs` to NO.[76, 77]

1.4. Endogenous S-nitrosothiols as potential substrates for NOGPs

There are several known biological pathways for the formation of RSNOs, typically from the NO-mediated S-nitrosation of thiol-containing amino acids, peptides and proteins (see **Figure 1.6**).[78]

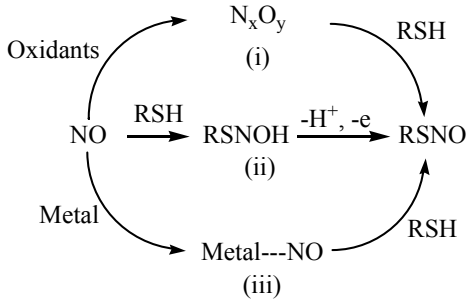

Figure 1.6 Biological pathways for the S-nitrosothiol (RSNO) formation from NO and free thiols (RSHs) through (i) oxidative products (N_xO_y) such as nitrogen dioxide (NO_2), dinitrogen trioxide (N_2O_3), and peroxynitrite $(ONOO)^{\bullet-}$; (ii) the formation of a radical intermediate, (RS-N$^{\bullet}$-OH); or (iii) nitrosylated metal centers such as copper or iron.

The first pathway to form endogenous RSNOs is via an oxidative NO intermediate such as dinitrogen trioxide (N_2O_3) followed by nitrosation of free thiol

(RSH) such as GSH or CySH (L-cysteine)[79, 80] as shown by pathway (i) in **Figure 1.6** (also see **equations (1.1) – (1.6)**). It should be noted that this pathway requires two NO molecules to form a N_2O_3 intermediate, which suggests it is likely to occur at high concentrations of NO such as that found during inflammatory conditions.[67] In contrast, the RSNOH radical intermediate[81] as well as the metal-catalyzed[82, 83] reaction (pathway (ii) and (iii), respectively) are first order with regard to NO concentration. Therefore, these pathways are considered to take place more readily under normal physiological concentrations of NO. Both the RSNOH radical and metal-catalyzed intermediate necessitate the abstraction of an electron and a proton. Hemoglobin (Hb)[82] and celuroplasmin[83] (a plasma protein with multiple copper binding sites) have been reported to catalyze RSNO formation via their metal centers.

$$NO + O_2 \rightleftharpoons NO_3 \qquad (1.1)$$

$$NO_3 + NO \longrightarrow ONOONO \qquad (1.2)$$

$$ONOONO \longrightarrow 2\,NO_2 \qquad (1.3)$$

$$NO + NO_2 \rightleftharpoons N_2O_3 \qquad (1.4)$$

$$N_2O_3 + H_2O \longrightarrow 2\,H^+ + 2\,NO_2^- \qquad (1.5)$$

$$N_2O_3 + RSH \longrightarrow H^+ + RSNO + NO_2^- \qquad (1.6)$$

It is worth noting that endogenous RSNOs are known to reallocate NO to other thiols, which is a reversible reaction as shown in **equation (1.7)**.[84]

$$RSNO + R'SH \rightleftharpoons RSH + R'SNO \qquad (1.7)$$

This transnitrosation reaction has been invoked as a method to transfer NO from species to species, and provides a potential mechanism for the modification of protein activity[85-88] as well as a signaling mechanism in which NO controls cellular processes.[89, 90]

Endogenous RSNOs have been well recognized as transfer and storage agents of physiological NO;[67, 78, 91-93] hence, they exhibit similar physiological functions of NO, such as inhibition of platelet aggregation[94] and vascular smooth muscle relaxation.[95] They are also known to participate in host defense processes such as killing tumors[96] and intracellular pathogens,[97] in addition to intracellular signaling,[98] ion channel regulation,[99,100] apoptosis,[101, 102] etc.

Endogenous RSNOs are potentially useful NO precursors for NOGPs, since the decomposition of endogenous RSNOs to NO occurs relatively easily via certain catalysts compared to the transformation of nitrite, nitrate, or L-arginine to NO. Although the exact concentrations of RSNOs in normal human blood are still in debate,[103, 104] levels of RSNOs are thought to be in the nM - μM range;[105, 106] however, very low levels of NO (< 1 nM) can be effective in maintaining a non-thrombogenic surface.[107] Therefore, even a small fractional conversion of endogenous RSNO species to NO at a polymer/blood boundary could be beneficial in reducing the risk of thrombus formation at the surface of biomedical devices.

1.5. Potential catalysts for NOGPs

There are also several known LMW chemicals that can catalytically decompose various RSNOs to NO in a beaker. These chemicals can be widely categorized into two types; metal ions (Cu^{+}, Fe^{2+}, Hg^{2+}, and Ag^{+})[16] or chalcogenide (S or Se)-containing

compounds.[77] It is very interesting that biological NO production from endogenous RSNOs is mediated by some enzymes containing metal ion centers (Cu and Fe) or chalcogenides (S or Se), as discussed above. This is in line with observations made with LMW chemicals. It is worth noting that ascorbate, air, photon, and thermal-induced RSNO decomposition to NO has also been reported.[108, 109]

Williams and co-workers reported that copper ions are the most efficient metal ion catalyst,[110] liberating NO from RSNOs in the presence of reducing agents such as free thiols (RSHs) or ascorbate.[111] The catalytic mechanism of the copper redox cycle has been suggested[112] as shown **Figure 1.7**; where Cu^{2+} can be easily reduced by a reducing

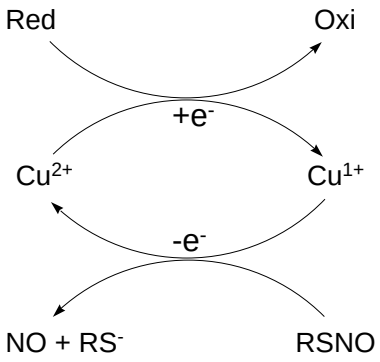

Figure 1.7 The redox chemistry of Cu(II/I) in generating NO from RSNOs. Reduction of Cu(II) to Cu(I) induced by reducing agents (Red) results in NO generation from endogenous S-nitrosothiols (RSNOs).

agent such as thiolate (RS^-) or ascorbate to afford Cu^{1+} and an oxidized form of reducing agent such as a disulfide (RSSR) or dehydroascorbate (DHA). Then, Cu^{1+} reduces RSNO to produce NO and RS^-, as well as regenerating the original Cu^{2+} catalyst. It should be noted that peptide and protein bound copper(II) ions are also known to be reduced to copper(I) by a thiol to generate NO from a RSNO.[113] Furthermore, the

Meyerhoff group has reported that poly(vinyl chloride) (PVC) films doped with Cu(II)-dibenzo[e,k]-2,3,8,9-tetrapheny-1,4,7,10-tetraaza-cyclododeca-1,3,7,9-tetraene (Cu(II)-DTTCT, see **Figure 1.8(A)**) catalytically decompose GSNO to NO at their interface in the presence of GSH.[114]

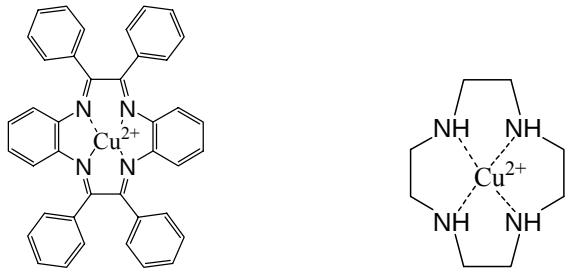

(A) Cu(II)-DTTCT (B) Cu(II)-cyclen

Figure 1.8 Examples of copper ion-complexes liberating NO from RSNOs in the presence of reducing agents (DTTCT= dibenzo[e,k]-2,3,8,9-tetrapheny-1,4,7,10-tetraaza-cyclododeca-1,3,7,9-tetraene; cyclen= 1,4,7,10-tetraazacyclododecane).

In order to develop de novo NOGPs using copper ion complexes, some key factors should be taken into account. These include:

a. A complex must have at least one open coordination site to interact with reducing agents and RSNOs (for example, square planar or pyramidal structures).

b. A complex covalently attached to the polymer backbone would be ideal to prevent its possible leaching.

c. The ligands must have strong Cu(II)/Cu(I) ion complexation constants so that little or no copper ions will be lost into the blood due to the transmetallation with a species having high affinity for copper ions.

Between the two types of copper-complexes, Cu(II)-DTTCT and Cu(II)-cyclen (cyclen= 1,4,7,10-tetraazacyclododecane, see **Figure 1.8(B)**) reported for NO generation from S-

nitrosothiols,[114, 115] the Cu(II)-cyclen complex is more beneficial for the development of NOGPs. Even though both complexes have open axial sites to react with RSNO substrates, cyclen has a high Cu(II) ion binding constant (10^{23} M^{-1})[116] comparable to that of EDTA (10^{24} M^{-1}),[117] while the DTTCT binding constant to Cu(II) is unknown; however, it is likely to be much lower [118] mainly due to the weak metal coordination of sp^2 nitrogen in DTTCT versus the strong metal ion coordination of sp^3 nitrogen in cylen. Further, the structure of cyclen is known to be more flexible than the rigid DTTCT ligand, allowing better response to a change of metal ion size after reduction.[116] That is, the change of copper ion size from Cu(II) to Cu(I) should be accommodated by this ligand. Hence it is expected that cyclen will more tightly bind copper ions during a catalytic redox cycle than DTTCT. In addition, cyclen can be easily modified to have a functional group that will allow covalent attachment to a polymer backbone.[119] Furthermore, the binding stability of Cu(II)-cyclen would not be significantly changed after the modification of cyclen unless the amine groups in cyclen are altered to other groups, such as amide bonds, which would decrease the metal ion binding constant. Therefore, Cu(II)-cyclen is an attractive potential catalyst to study in the design of new copper ion complex-based NOGPs.

Chalcogenide (S or Se) compounds have also been shown to decompose RSNOs to NO. For example, an application of transnitrosation chemistry using a free thiol compound into biomaterials has been demonstrated by Lewis and colleagues.[120, 121] They employed polymers with appended CySH groups that transfer NO from endogenous RSNO species in blood to the CySH modified polymer, followed by the subsequent release of NO to exhibit its physiological effects such as a reduced platelet adhesion.

Wang and co-workers discovered that the organodiselenides (RSeSeR) catalytically liberate NO from RSNOs in the presence of thiols.[77] Indeed, the Meyerhoff group covalently attached diselenide compounds such as selenocystamine, or dipropionic diselenide to polymeric materials, and the resulting polymers showed catalytic denitrosation of RSNOs.[122, 123] The mechanism of organodiselenide-mediated RSNO decomposition remains unclear; however, it has been suggested that a seleno-sulfide (RSeSR') is a main intermediate, and organoselenolate (RSe^-) is the active reducing species that reacts with and liberates NO from RSNOs.[77, 123, 124]

Meanwhile, the redox chemistry of organotellurium has been reported to be comparable to that of organoselenium. For example, both organodiselenides (RSeSeR)[125, 126] and organoditellurides (RTeTeR)[127-129] have GPx like activity, which catalyzes GSH oxidation to GSSG (glutathione disulfide) by reducing organic peroxides (ROOH) or hydrogen peroxide (H_2O_2) to the corresponding alcohols (ROH) or water. The mechanisms are known to be equivalent including the intermediate, chalcogeno-sulfide (RSeSR' or RTeSR'). Considering such parallel redox chemistry of the organodichalcogenides, organoditellurides are very likely to catalyze RSNO decomposition to NO as well. Therefore, it is worth investigating a novel organoditelluride-mediated catalytic RSNO decomposition to NO and its potential application to NOGPs.

It should be noted that in both copper complex-mediated and organochalcogenide-mediated reactions, endogenous RSHs are known to be common reducing agents that reduce both catalysts, and then, the reduced catalysts can liberate NO from RSNOs. Hemoglobin (Hb), albumin (Alb), glutathione (GSH or Glu), and cysteine (CySH or Cys)

which possess free thiol moieties, are the predominant reducing species in circulating blood, where their concentrations (potential reducing agents for NOGPs) are known to range from μM to mM (see **Table 1.1**).[106]

Table 1.1 Concentrations of free thiol species in plasma (P) or blood (B).

Free thiols	Concentraton (μM)	Molecular Weight (g/mole)	Plasma (P), Blood (B)
Cysteine (Cys)	10 -30	121	(P)
Glutathione (Glu)	20	307	(P)
Albumin (Alb)	500	69,000	(P)
Hemoglobin (Hb)	2.2×10^3	64,458	(B)

1.6. Statement of dissertation research

The goals of this dissertation include the design, synthesis and characterization of novel NO generating polymers (NOGPs) with covalently attached catalytic sites. Additionally, this work includes the evaluation of catalytic NO generation of various NOGPs from endogenous RSNOs and reducing equivalents *in vitro*, the assessments of the leaching of catalysts from the polymeric materials, as well as the demonstration of spontaneous NO generation of the NOGPs in fresh animal whole blood *in vitro*. These investigations are pre-requisites for developing novel NOGPs that must be optimized further before applying these materials in biomedical devices. To achieve such goals, the investigation of two types of potential NOGPs based on the NO generating catalysts is presented. One includes attaching Cu(II)-cyclen complexes to polymers (Chapters 2 and

3) and the other approach is based on attaching organoditellurides to polymers (Chapters 4 - 6).

Chapter 2 describes the synthesis and characterization of a de novo Cu(II)-cyclen-based NOGP consisting of crosslinked poly(2-hydroxyethyl methacrylate) (pHEMA) with a covalently linked Cu(II)-cyclen complex. Local NO generation of the polymer from RSNO species is demonstrated via a chemiluminescence NO analyzer (NOA). Spontaneous NO generation by the new polymer in fresh whole sheep blood *in vitro* is also observed. Most of the content of this chapter is reorganized from a 2006 publication (Hwang, S.; Cha, W.; Meyerhoff, M. E., *Angew. Chem. Int. Ed.* **2006**, *45*, 2745-2748).

Another example of a Cu(II)-cyclen based NOGP is presented in Chapter 3. In this work, a newly modified Cu(II)-cyclen is tethered to hydrophilic thermoplastic polyurethane (PU), a biomedical grade polymer. This polymeric material successfully exhibits catalytic NO production from endogenous RSNOs in animal whole blood *in vitro*. Because of the good solubility of this polymer in organic solvents, it can be readily applied as a coating material for existing medical devices or implantable sensors. This chapter is adapted from a manuscript in preparation for *Biomaterials (2007)*.

Chapter 4 describes the chemistry of organoditelluride-mediated catalytic RSNO decomposition to NO. A newly synthesized organoditelluride, 5,5'-ditelluro-2,2'-dithiophenecarboxylic acid (DTDTCA), is discovered to have such catalytic activity under ambient conditions. In addition, a suitable mechanism for this chemistry is proposed. This work is reported in a recently published paper (Hwang, S.; Meyerhoff, M. E., *J. Mater. Chem.* **2007**. *17*. 1462-1465). The focus of Chapter 4 is on the chemistry and mechanism of DTDTCA-mediated catalytic RSNO decomposition.

Chapter 5 illustrates a couple of examples of organoditelluride-based NOGPs. The first is the covalent attachment of DTDTCA to hydrophilic thermoplastic PU. The second is based on DTDTCA coupling to poly(allylamine hydrochloride) (PAH), affording a water-soluble NOGP. The third is crosslinking the DTDTCA-tethered PAH within a cellulose membrane to yield an interpenetrating polymeric network (IPN). The polymers obtained form these approaches display catalytic denitrosation of RSNO in the presence of RSH at physiological pH. Further, spontaneous NO generation of the IPN from fresh animal blood *in vitro* has been observed via amperometric NO gas sensor measurements. The research described in this chapter is taken, in part, from the manuscript published in *Journal of Materials Chemistry (2007)* as well as a manuscript to be submitted to *Advanced Materials (2007)*.

Finally, an application of the organoditelluride-tethered polymers developed in this thesis is demonstrated in Chapter 6. In this chapter, the detection of various RSNOs including GSNO, CySNO, SNAP (S-nitroso-N-acetylpenicillamine), and AlbSNO is investigated using a new RSNO sensor that employs the DTDTCA-PAH-immobilized polymer within a cellulose membrane at the surface of an amperometric NO sensor. The long-term stability and RSNO measurement in animal blood is presented as well. The data presented in this chapter is adapted from a recently submitted manuscript to *Electroanalysis* (*2007*).

Conclusions of this dissertation are summarized in Chapter 7, with further dialogue on the future directions toward the applications of the NOGPs for vascular stents, implantable glucose sensors, and amperometric RSNO sensors to demonstrate the

true effectiveness of the newly proposed NOGPs in reducing thrombus formation when such polymers are coated on biomedical devices.

1.7. References

1. Gorbet, M. B.; Sefton, M. V., Biomaterial-associated thrombosis: roles of coagulation factors, complement, platelets and leukocytes. *Biomaterials* **2004,** 25, (26), 5681-5703.
2 Sefton, M. V.; Gemmell, C. H.; Gorbet, M. B., What really is blood compatibility? *Journal of Biomaterials Science-Polymer Edition* **2000,** 11, (11), 1165-1182.
3. Courtney, J. M.; Forbes, C. D., Thrombosis on foreign surfaces. *British Medical Bulletin* **1994,** 50, (4), 966-981.
4. Courtney, J. M.; Lamba, N. M. K.; Sundaram, S.; Forbes, C. D., Biomaterials for blood-contacting applications. *Biomaterials* **1994,** 15, (10), 737-744.
5. Park, K. D.; Okano, T.; Nojiri, C.; Kim, S. W., Heparin immobilization onto degmented polyurethaneurea surfaces - Effect of hydrophilic spacers. *Journal of Biomedical Materials Research* **1988,** 22, (11), 977-992.
6. Feng, J.; Tseng, P. Y.; Faucher, K. M.; Orban, J. M.; Sun, X. L.; Chaikof, E. L., Functional reconstitution of thrombomodulin within a substrate-supported membrane-mimetic polymer film. *Langmuir* **2002,** 18, (25), 9907-9913.
7. Ebert, C. D.; Lee, E. S.; Kim, S. W., The anti-platelet activity of immobilized prostacyclin. *Journal of Biomedical Materials Research* **1982,** 16, (5), 629-638.
8. Krejcy, K.; Schmetterer, L.; Kastner, J.; Nieszpaurlos, M.; Monitzer, B.; Schutz, W.; Eichler, H. G.; Kyrle, P. A., Role of nitric-oxide in hemostatic system activation in-vivo in humans. *Arteriosclerosis Thrombosis & Vascular Biology* **1995,** 15, (11), 2063-2067.
9. Salvemini, D.; Masini, E.; Anggard, E.; Mannaioni, P. F.; Vane, J., Synthesis of a nitric oxide-like factor from L-arginine by rat serosal mast-cells - stimulation of guanylate-cyclase and inhibition of platelet-aggregation. *Biochemical and Biophysical Research Communications* **1990,** 169, (2), 596-601.
10. Samama, C. M.; Diaby, M.; Fellahi, J. L.; Mdhafar, A.; Eyraud, D.; Arock, M.; Guillosson, J. J.; Coriat, P.; Rouby, J. J., Inhibition of platelet-sggregation by inhaled nitric-oxide in patients with scute respiratory-distress syndrome. *Anesthesiology* **1995,** 83, (1), 56-65.
11. Sarkar, R.; Webb, R. C., Does nitric oxide regulate smooth muscle proliferation? A critical appraisal. *Journal of Vascular Research* **1998,** 35, (3), 135-142.
12. Mancinelli, R. L.; McKay, C. P., Effects of nitric-oxide and nitrogen-dioxide on bacterial-growth. *Applied and Environmental Microbiology* **1983,** 46, (1), 198-202.
13. Rizk, M.; Witte, M. B.; Barbul, A., Nitric oxide and wound healing. *World Journal of Surgery* **2004,** 28, (3), 301-306.
14. Witte, M. B.; Barbul, A., Role of nitric oxide in wound repair. *American Journal of Surgery* **2002,** 183, (4), 406-412.
15. Broughton, G.; Janis, J. E.; Attinger, C. E., The basic science of wound healing. *Plastic & Reconstructive Surgery* **2006,** 117, (7), 12S-34S.
16. Wang, P. G.; Xian, M.; Tang, X. P.; Wu, X. J.; Wen, Z.; Cai, T. W.; Janczuk, A. J., Nitric oxide donors: Chemical activities and biological applications. *Chemical Reviews* **2002,** 102, (4), 1091-1134.

17. Keefer, L. K., Progress toward clinical application of the nitric oxide-releasing diazeniumdiolates. *Annual Review of Pharmacology and Toxicology* **2003,** 43, 585-607.
18. Schoenfisch, M. H.; Mowery, K. A.; Rader, M. V.; Baliga, N.; Wahr, J. A.; Meyerhoff, M. E., Improving the thromboresistivity of chemical sensors via nitric oxide release: fabrication and in vivo evaluation of NO-releasing oxygen-sensing catheters. *Analytical chemistry* **2000,** 72, (6), 1119-1126.
19. Zhang, H. P.; Annich, G. M.; Miskulin, J.; Osterholzer, K.; Merz, S. I.; Bartlett, R. H.; Meyerhoff, M. E., Nitric oxide releasing silicone rubbers with improved blood compatibility: preparation, characterization, and in vivo evaluation. *Biomaterials* **2002,** 23, (6), 1485-1494.
20. Garthwaite, J.; Charles, S. L.; Chess-Williams, R., Endothelium-derived relaxing factor release on activation of NMDA receptors suggests role as intercellular messenger in the brain. *Nature* **1988,** 336, (6197), 385-388.
21. Kroncke, K. D.; Fehsel, K.; Kolb-Bachofen, V., Nitric oxide: Cytotoxicity versus cytoprotection - How, why, when, and where? *Nitric Oxide-Biology & Chemistry* **1997,** 1, (2), 107-120.
22. Rosen, G. M.; Eccles, C. U.; Pou, S., Nitric oxide in the brain: Looking at two sides of the same coin. *Neurologist* **1995,** 1, (6), 311-325.
23. Isenberg, J. S., Nitric oxide modulation of early angiogenesis. *Microsurgery* **2004,** 24, (5), 385-391.
24. Dawson, V. L.; Dawson, T. M.; London, E. D.; Bredt, D. S.; Snyder, S. H., Nitric oxide mediates glutamate neurotoxicity in primary cortical cultures. *Proceedings of the National Academy of Sciences of the United States of America* **1991,** 88, (14), 6368-6371.
25. Wink, D. A.; Kasprzak, K. S.; Maragos, C. M.; Elespuru, R. K.; Misra, M.; Dunams, T. M.; Cebula, T. A.; Koch, W. H.; Andrews, A. W.; Allen, J. S.; Keefer, L. K., Dna Deaminating Ability and genotoxicity of nitric-oxide and its progenitors. *Science* **1991,** 254, (5034), 1001-1003.
26. Cai, T. B.; Wang, P. G., Recent developments in anticancer nitric oxide donors. *Expert Opinion on Therapeutic Patents* **2004,** 14, (6), 849-857.
27. Nakane, M., Soluble guanylyl cyclase: Physiological role as an NO receptor and the potential molecular target for therapeutic application. *Clinical Chemistry & Laboratory Medicine* **2003,** 41, (7), 865-870.
28. Denninger, J. W.; Marletta, M. A., Guanylate cyclase and the (NO)-N-./cGMP signaling pathway. *Biochimica et Biophysica Acta* **1999,** 1411, (2-3), 334-350.
29. Michiels, C., Endothelial cell functions. *Journal of Cellular Physiology* **2003,** 196, (3), 430-443.
30. Grant, M. K. O.; El-Fakahany, E. E., Therapeutic interventions targeting the nitric oxide system: Current and potential uses in obstetrics, bone disease and erectile dysfunction. *Life Sciences* **2004,** 74, (14), 1701-1721.
31. Bian, K.; Murad, F., Nitric oxide (NO) - Biogeneration, regulation, and relevence to human diseases. *Frontiers in Bioscience* **2003,** 8, D264-D278.
32. Gewaltig, M. T.; Kojda, G., Vasoprotection by nitric oxide: mechanisms and therapeutic potential. *Cardiovascular Research* **2002,** 55, (2), 250-260.

33. Wu, K. K.; Thiagarajan, P., Role of endothelium in thrombosis and hemostasis. *Annual Review of Medicine* **1996,** 47, 315-331.
34. Eigenthaler, M.; Nolte, C.; Halbrugge, M.; Walter, U., Concentration and regulation of cyclic-nucleotides, cyclic-nucleotide-dependent protein-kinases and one of their major substrates in human platelets - estimating the rate of cAMP-regulated and cGMP-regulated protein-phosphorylation in intact-cells. *European Journal of Biochemistry* **1992,** 205, (2), 471-481.
35. El-Daher, S. S.; Patel, Y.; Siddiqua, A.; Hassock, S.; Edmunds, S.; Maddison, B.; Patel, G.; Goulding, D.; Lupu, F.; Wojcikiewicz, R. J. H.; Authi, K. S., Distinct localization and function of (IP3)-I-1,4,5 receptor subtypes and the (IP4)-I-1,3,4,5 receptor GAP1(IP4BP) in highly purified human platelet membranes. *Blood* **2000,** 95, (11), 3412-3422.
36. Aktas, B.; Utz, A.; Hoenig-Liedl, P.; Walter, U.; Geiger, J., Dipyridamole enhances NO/cGMP-mediated vasodilator-stimulated phosphoprotein phosphorylation and signaling in human platelets - in vitro and in vivo/ex vivo studies. *Stroke* **2003,** 34, (3), 764-769.
37. Schwarz, U. R.; Walter, U.; Eigenthaler, M., Taming platelets with cyclic nucleotides. *Biochemical Pharmacology* **2001,** 62, (9), 1153-1161.
38. Geiger, J.; Nolte, C.; Walter, U., Regulation of calcium mobilization and entry in human platelets by endothelium-derived factors. *American Journal of Physiology* **1994,** 267, (1), C236-C244.
39. Mendelsohn, M. E.; Oneill, S.; George, D.; Loscalzo, J., Inhibition of Fibrinogen Binding to Human Platelets by S-Nitroso-N-Acetylcysteine. *Journal of Biological Chemistry* **1990,** 265, (31), 19028-19034.
40. Bennett, M. R.; O'Sullivan, M., Mechanisms of angioplasty and stent restenosis: implications for design of rational therapy. *Pharmacology & Therapeutics* **2001,** 91, (2), 149-166.
41. Kavurma, M. M.; Khachigian, L. M., ERK, JNK, and p38 MAP kinases differentially regulate proliferation and migration of phenotypically distinct smooth muscle cell subtypes. *Journal of Cellular Biochemistry* **2003,** 89, (2), 289-300.
42. Cornwell, T. L.; Arnold, E.; Boerth, N. J.; Lincoln, T. M., Inhibition of smooth-muscle cell-growth by nitric-oxide and activation of cAMP-dependent protein-kinase by cGMP. *American Journal of Physiology-Cell Physiology* **1994,** 36, (5), C1405-C1413.
43. Osinski, M. T.; Rauch, B. H.; Schror, K., Antimitogenic actions of organic nitrates are potentiated by sildenafil and mediated via activation of protein kinase A. *Molecular Pharmacology* **2001,** 59, (5), 1044-1050.
44. Cook, S. J.; Mccormick, F., Inhibition by Camp of Ras-Dependent Activation of Raf. *Science* **1993,** 262, (5136), 1069-1072.
45. Wei, L. H.; Wu, G. Y.; Morris, S. M.; Ignarro, L. J., Elevated arginase I expression in rat aortic smooth muscle cells increases cell proliferation. *Proceedings of the National Academy of Sciences of the United States of America* **2001,** 98, (16), 9260-9264.

46. Parzuchowski, P. G.; Frost, M. C.; Meyerhoff, M. E., Synthesis and characterization of polymethacrylate-based nitric oxide donors. *Journal of the American Chemical Society* **2002,** 124, (41), 12182-12191.
47. Frost, M. C.; Meyerhoff, M. E., Controlled photoinitiated release of nitric oxide from polymer films containing S-nitroso-N-acetyl-DL-penicillamine derivatized fumed silica filler. *Journal of the American Chemical Society* **2004,** 126, (5), 1348-1349.
48. Smith, D. J.; Chakravarthy, D.; Pulfer, S.; Simmons, M. L.; Hrabie, J. A.; Citro, M. L.; Saavedra, J. E.; Davies, K. M.; Hutsell, T. C.; Mooradian, D. L.; Hanson, S. R.; Keefer, L. K., Nitric oxide-releasing polymers containing the [N(O)NO](-) group. *Journal of Medicinal Chemistry* **1996,** 39, (5), 1148-1156.
49. Bohl, K. S.; West, J. L., Nitric oxide-releasing hydrogels for the prevention of thrombosis and restenosis. *Circulation* **2000,** 102, (18), 734-734.
50. Kaul, S.; Cercek, B.; Rengstrom, J.; Xu, X. P.; Molloy, M. D.; Dimayuga, P.; Parikh, A. K.; Fishbein, M. C.; Nilsson, J.; Rajavashisth, T. B.; Shah, P. K., Polymeric-based perivascular delivery of a nitric oxide donor inhibits intimal thickening after balloon denudation arterial injury: Role of nuclear factor-kappaB. *Journal of the American College of Cardiology* **2000,** 35, (2), 493-501.
51. Baek, S. H.; Hrabie, J. A.; Keefer, L. K.; Hou, D. M.; Fineberg, N.; Rhoades, R.; March, K. L., Augmentation of intrapericardial nitric oxide level by a prolonged-release nitric oxide donor reduces luminal narrowing after porcine coronary angioplasty. *Circulation* **2002,** 105, (23), 2779-2784.
52. Wang, Y.; Newton, D. C.; Marsden, P. A., Neuronal NOS: Gene structure, mRNA diversity, and functional relevance. *Critical Reviews in Neurobiology* **1999,** 13, (1), 21-43.
53. Crane, B. R.; Arvai, A. S.; Ghosh, D. K.; Wu, C. Q.; Getzoff, E. D.; Stuehr, D. J.; Tainer, J. A., Structure of nitric oxide synthase oxygenase dimer with pterin and substrate. *Science* **1998,** 279, (5359), 2121-2126.
54. Huang, P. L.; Huang, Z. H.; Mashimo, H.; Bloch, K. D.; Moskowitz, M. A.; Bevan, J. A.; Fishman, M. C., Hypertension in mice lacking the gene for endothelial nitric-oxide synthase. *Nature* **1995,** 377, (6546), 239-242.
55. Porasuphatana, S.; Tsai, P.; Rosen, G. M., The generation of free radicals by nitric oxide synthase. *Comparative Biochemistry and Physiology C-Toxicology & Pharmacology* **2003,** 134, (3), 281-289.
56. Averill, B. A., Dissimilatory nitrite and nitric oxide reductases. *Chemical Reviews* **1996,** 96, (7), 2951-2964.
57. Cosby, K.; Partovi, K. S.; Crawford, J. H.; Patel, R. P.; Reiter, C. D.; Martyr, S.; Yang, B. K.; Waclawiw, M. A.; Zalos, G.; Xu, X. L.; Huang, K. T.; Shields, H.; Kim-Shapiro, D. B.; Schechter, A. N.; Cannon, R. O.; Gladwin, M. T., Nitrite reduction to nitric oxide by deoxyhemoglobin vasodilates the human circulation. *Nature Medicine* **2003,** 9, (12), 1498-1505.
58. Gladwin, M. T.; Cosby, K.; Partovi, K.; Martyr, S.; Reiter, C.; Zalos, G.; Schechter, A. N.; Cannon, R. O., Nitrite reduction to nitric oxide by deoxyhemoglobin vasodilalates the human circulation. *Circulation* **2003,** 108, (17), 20-21.

59. Gladwin, M. T.; Cosby, K.; Partovi, K. S.; Patel, R. P.; Crawford, J. H.; Kim-Shapiro, D. B.; Schechter, A. N.; Cannon, R. O., Novel function of human hemoglobin as a nitrite reductase regulates nitric oxide homeostasis and hypoxic vasodilation. *Blood* **2003,** 102, (11), 255A-255A.
60. Zweier, J. L.; Li, H. T.; Samouilov, A.; Liu, X. P., Xanthine oxidase-catalyzed nitric oxide generation in the ischemic heart. *Journal of Molecular and Cellular Cardiology* **2003,** 35, (6), A7-A7.
61. Li, H. T.; Samouilov, A.; Liu, X. Q.; Zweier, J. L., Characterization of the magnitude and kinetics of xanthine oxidase-catalyzed nitrate reduction: Evaluation of its role in nitrite and nitric oxide generation in anoxic tissues. *Biochemistry* **2003,** 42, (4), 1150-1159.
62. Zhang, Z.; Naughton, D.; Winyard, P. G.; Benjamin, N.; Blake, D. R.; Symons, M. C. R., Generation of nitric oxide by a nitrite reductase activity of xanthine oxidase: A potential pathway for nitric oxide formation in the absence of nitric oxide synthase activity. *Biochemical & Biophysical Research Communications* **1998,** 249, (3), 767-772.
63. Gordon, E. H. J.; Sjogren, T.; Lofqvist, M.; Richter, C. D.; Allen, J. W. A.; Higham, C. W.; Hajdu, J.; Fulop, V.; Ferguson, S. J., Structure and kinetic properties of paracoccus pantotrophus cytochrome cd(1) nitrite reductase with the d(1) heme active site ligand tyrosine 25 replaced by serine. *Journal of Biological Chemistry* **2003,** 278, (14), 11773-11781.
64. Cutruzzola, F., Bacterial nitric oxide synthesis. *Biochimica et Biophysica Acta* **1999,** 1411, (2-3), 231-249.
65. Stamler, J. S.; Singel, D. J.; Loscalzo, J., Biochemistry of nitric-oxide and its redox-activated forms. *Science* **1992,** 258, (5090), 1898-1902.
66. Stamler, J. S., Redox signaling - nitrosylation and related target interactions of nitric-oxide. *Cell* **1994,** 78, (6), 931-936.
67. Gow, A. J.; Farkouh, C. R.; Munson, D. A.; Posencheg, M. A.; Ischiropoulos, H., Biological significance of nitric oxide-mediated protein modifications. *American Journal of Physiology-Lung Cellular & Molecular Physiology* **2004,** 287, (2), L262-L268.
68. Stamler, J. S.; Jia, L.; Eu, J. P.; McMahon, T. J.; Demchenko, I. T.; Bonaventura, J.; Gernert, K.; Piantadosi, C. A., Blood flow regulation by S-nitrosohemoglobin in the physiological oxygen gradient. *Science* **1997,** 276, (5321), 2034-2037.
69. Root, P.; Sliskovic, I.; Mutus, B., Platelet cell-surface protein disulphide-isomerase mediated S-nitrosoglutathione consumption. *Biochemical Journal* **2004,** 382, 575-580.
70. Laurent, T. C.; Moore, E. C.; Reichard, P., Enzymatic synthesis of deoxyribonucleotides.4. Isolation + characterization of thioredoxin hydrogen donor from escherichia coli B. *Journal of Biological Chemistry* **1964,** 239, (10), 3436-3444.
71. Holmgren, A., Thioredoxin. *Annual Review of Biochemistry* **1985,** 54, 237-271.
72. Goldman, R.; Stoyanovsky, D. A.; Day, B. W.; Kagan, V. E., Reduction of phenoxyl radicals by thioredoxin results in selective oxidation of its SH-groups to disulfides - an antioxidant function of thioredoxin. *Biochemistry* **1995,** 34, (14), 4765-4772.

73. Stoyanovsky, D. A.; Tyurina, Y. Y.; Tyurin, V. A.; Anand, D.; Mandavia, D. N.; Gius, D.; Ivanova, J.; Pitt, B.; Billiar, T. R.; Kagan, V. E., Thioredoxin and lipoic acid catalyze the denitrosation of low molecular weight and protein S-nitrosothiols. *Journal of the American Chemical Society* **2005,** 127, (45), 15815-15823.
74. Nikitovic, D.; Holmgren, A., S-Nitrosoglutathione is cleaved by the thioredoxin system with liberation of glutathione and redox regulating nitric oxide. *Journal of Biological Chemistry* **1996,** 271, (32), 19180-19185.
75. Avissar, N.; Whitin, J. C.; Allen, P. Z.; Palmer, I. S.; Cohen, H. J., Antihuman plasma glutathione-peroxidase antibodies - Immunological investigations to determine plasma glutathione-peroxidase protein and selenium content in plasma. *Blood* **1989,** 73, (1), 318-323.
76. Freedman, J. E.; Frei, B.; Loscalzo, J., Glutathione-peroxidase prevents the inactivation of nitric-oxide and restores the inhibition of platelet-function by S-nitrosothiols. *Circulation* **1994,** 90, (4), 131-131.
77. Hou, Y. C.; Guo, Z. M.; Li, J.; Wang, P. G., Seleno compounds and glutathione peroxidase catalyzed decomposition of S-nitrosothiols. *Biochemical & Biophysical Research Communications* **1996,** 228, (1), 88-93.
78. Broillet, M. C., S-Nitrosylation of proteins. *Cellular and Molecular Life Sciences* **1999,** 55, (8-9), 1036-1042.
79. Kharitonov, V. G.; Sundquist, A. R.; Sharma, V. S., Kinetics of nitrosation of thiols by nitric-oxide in the presence of oxygen. *Journal of Biological Chemistry* **1995,** 270, (47), 28158-28164.
80. Wink, D. A.; Nims, R. W.; Darbyshire, J. F.; Christodoulou, D.; Hanbauer, I.; Cox, G. W.; Laval, F.; Laval, J.; Cook, J. A.; Krishna, M. C.; Degraff, W. G.; Mitchell, J. B., Reaction-kinetics for nitrosation of cysteine and glutathione in aerobic nitric-oxide solutions at neutral pH - Insights into the fate and physiological-effects of intermediates generated in the NO/O^{-2} reaction. *Chemical Research in Toxicology* **1994,** 7, (4), 519-525.
81. Gow, A. J.; Buerk, D. G.; Ischiropoulos, H., A novel reaction mechanism for the formation of S-nitrosothiol in vivo. *Journal of Biological Chemistry* **1997,** 272, (5), 2841-2845.
82. Gow, A. J.; Stamler, J. S., Reactions between nitric oxide and haemoglobin under physiological conditions. *Nature* **1998,** 391, (6663), 169-173.
83. Inoue, K.; Akaike, T.; Miyamoto, Y.; Okamoto, T.; Sawa, T.; Otagiri, M.; Suzuki, S.; Yoshimura, T.; Maeda, H., Nitrosothiol formation catalyzed by ceruloplasmin - Implication for cytoprotective mechanism in vivo. *Journal of Biological Chemistry* **1999,** 274, (38), 27069-27075.
84. Hogg, N., The kinetics of S-transnitrosation - A reversible second-order reaction. *Analytical Biochemistry* **1999,** 272, (2), 257-262.
85. Shah, C. M.; Bell, S. E.; Locke, I. C.; Chowdrey, H. S.; Gordge, M. P., Interactions between cell surface protein disulphide isomerase and S-nitrosoglutathione during nitric oxide delivery. *Nitric Oxide-Biology & Chemistry* **2007,** 16, (1), 135-142.
86. Srivastava, S.; Dixit, B. L.; Ramana, K. V.; Chandra, A.; Chandra, D.; Zacarias, A.; Petrash, J. M.; Bhatnagar, A.; Srivastava, S. K., Structural and kinetic

modifications of aldose reductase by S-nitrosothiols. *Biochemical Journal* **2001,** 358, 111-118.
87. Konorev, E. A.; Kalyanaraman, B.; Hogg, N., Modification of creatine kinase by S-nitrosothiols: S-nitrosation vs. S-thiolation. *Free Radical Biology and Medicine* **2000,** 28, (11), 1671-1678.
88. Mohr, S.; Stamler, J. S.; Brune, B., Posttranslational modification of glyceraldehyde-3-phosphate dehydrogenase by S-nitrosylation and subsequent NADH attachment. *Journal of Biological Chemistry* **1996,** 271, (8), 4209-4214.
89. Stamler, J. S.; Lamas, S.; Fang, F. C., Nitrosylation: The prototypic redox-based signaling mechanism. *Cell* **2001,** 106, (6), 675-683.
90. Mannick, J. B.; Hausladen, A.; Liu, L. M.; Hess, D. T.; Zeng, M.; Miao, Q. X.; Kane, L. S.; Gow, A. J.; Stamler, J. S., Fas-induced caspase denitrosylation. *Science* **1999,** 284, (5414), 651-654.
91. Giustarini, D.; Milzani, A.; Colombo, R.; Dalle-Donne, I.; Rossi, R., Nitric oxide, S-nitrosothiols and hemoglobin: is methodology the key? *Trends in Pharmacological Sciences* **2004,** 25, (6), 311-316.
92. Zhang, Y. H.; Hogg, N., S-Nitrosothiols: cellular formation and transport. *Free Radical Biology & Medicine* **2005,** 38, (7), 831-838.
93. Butler, A. R.; Rhodes, P., Chemistry, analysis, and biological roles of S-nitrosothiols. *Analytical Biochemistry* **1997,** 249, (1), 1-9.
94. Pawloski, J. R.; Swaminathan, R. V.; Stamler, J. S., Cell-free and erythrocytic S-nitrosohemoglobin inhibits human platelet aggregation. *Circulation* **1998,** 97, (3), 263-267.
95. Ignarro, L. J.; Lippton, H.; Edwards, J. C.; Baricos, W. H.; Hyman, A. L.; Kadowitz, P. J.; Gruetter, C. A., Mechanism of vascular smooth-muscle relaxation by organic nitrates, nitrites, nitroprusside and nitric-oxide - evidence for the involvement of S-nitrosothiols as sctive intermediates. *Journal of Pharmacology & Experimental Therapeutics* **1981,** 218, (3), 739-749.
96. Gobert, A. P.; Semballa, S.; Daulouede, S.; Lesthelle, S.; Taxile, M.; Veyret, B.; Vincendeau, P., Murine macrophages use oxygen- and nitric oxide-dependent mechanisms to synthesize S-nitroso-albumin and to kill extracellular trypanosomes. *Infection & Immunity* **1998,** 66, (9), 4068-4072.
97. Persichini, T.; Colasanti, M.; Lauro, G. M.; Ascenzi, P., Cysteine nitrosylation inactivates the HIV-1 protease. *Biochemical and Biophysical Research Communications* **1998,** 250, (3), 575-576.
98. DelaTorre, A.; Schroeder, R. A.; Bartlett, S. T.; Kuo, P. C., Differential effects of nitric oxide-mediated S-nitrosylation on p50 and c-jun DNA binding. *Surgery* **1998,** 124, (2), 137-141.
99. Broillet, M. C.; Firestein, S., Direct activation of the olfactory cyclic nucleotide-gated channel through modification of sulfhydryl groups by NO compounds. *Neuron* **1996,** 16, (2), 377-385.
100. Broillet, M. C.; Firestein, S., beta subunits of the olfactory cyclic nucleotide-gated channel form a nitric oxide activated Ca^{2+} channel. *Neuron* **1997,** 18, (6), 951-958.
101. Tenneti, L.; DEmilia, D. M.; Lipton, S. A., Suppression of neuronal apoptosis by S-nitrosylation of caspases. *Neuroscience Letters* **1997,** 236, (3), 139-142.

102. Li, J. R.; Billiar, T. R.; Talanian, R. V.; Kim, Y. M., Nitric oxide reversibly inhibits seven members of the caspase family via S-nitrosylation. *Biochemical and Biophysical Research Communications* **1997,** 240, (2), 419-424.
103. Rossi, R.; Giustarini, D.; Milzani, A.; Colombo, R.; Dalle-Donne, I.; Di Simplicio, P., Physiological levels of S-nitrosothiols in human plasma. *Circulation Research* **2001,** 89, (12).
104. Stamler, J. S., S-Nitrosothiols in the blood - Roles, amounts, and methods of analysis. *Circulation Research* **2004,** 94, (4), 414-417.
105. Rassaf, T.; Bryan, N. S.; Kelm, M.; Feelisch, M., Concomitant presence of N-nitroso and S-nitroso proteins in human plasma. *Free Radical Biology And Medicine* **2002,** 33, (11), 1590-1596.
106. Kelm, M., Nitric oxide metabolism and breakdown. *Biochimica et Biophysica Acta* **1999,** 1411, (2-3), 273-289.
107. Vaughn, M. W.; Kuo, L.; Liao, J. C., Estimation of nitric oxide production and reaction rates in tissue by use of a mathematical model. *the American Journal of Physiology* **1998,** 274, (6 Pt 2), H2163-2176.
108. Stamler, J. S.; Toone, E. J., The decomposition of thionitrites. *Current Opinion In Chemical Biology* **2002,** 6, (6), 779-785.
109. Szacilowski, K.; Stasicka, Z., S-Nitrosothiols: Materials, reactivity and mechanisms. *Progress in Reaction Kinetics & Mechanism* **2001,** 26, (1), 1-58.
110. Williams, D. L. H., The chemistry of S-nitrosothiols. *Accounts of Chemical Research* **1999,** 32, (10), 869-876.
111. Mcaninly, J.; Williams, D. L. H.; Askew, S. C.; Butler, A. R.; Russell, C., Metal-ion catalysis in nitrosothiol (RSNO) decomposition. *Journal of the Chemical Society-Chemical Communications* **1993**, (23), 1758-1759.
112. Dicks, A. P.; Swift, H. R.; Williams, D. L. H.; Butler, A. R.; AlSadoni, H. H.; Cox, B. G., Identification of Cu^{+} as the effective reagent in nitric oxide formation from S-nitrosothiols (RSNO). *Journal of the Chemical Society-Perkin Transactions 2* **1996**, (4), 481-487.
113. Dicks, A. P.; Williams, D. L. H., Generation of nitric oxide from S-nitrosothiols using protein-bound Cu^{2+} sources. *Chemistry & Biology* **1996,** 3, (8), 655-659.
114. Oh, B. K.; Meyerhoff, M. E., Spontaneous catalytic generation of nitric oxide from S-nitrosothiols at the surface of polymer films doped with lipophilic copper(II) complex. *Journal of the American Chemical Society* **2003,** 125, (32), 9552-9553.
115. Oh, B. K.; Meyerhoff, M. E., Catalytic generation of nitric oxide from nitrite at the interface of polymeric films doped with lipophilic Cu(Il)-complex: a potential route to the preparation of thromboresistant coatings. *Biomaterials* **2004,** 25, (2), 283-293.
116. Thom, V. J.; Hosken, G. D.; Hancock, R. D., Anomalous Metal-ion size selectivity of tetraaza macrocycles. *Inorganic Chemistry* **1985,** 24, (21), 3378-3381.
117. Juang, R. S.; Lin, S. H.; Wang, T. Y., Removal of metal ions from the complexed solutions in fixed bed using a strong-acid ion exchange resin. *Chemosphere* **2003,** 53, (10), 1221-1228.

118. Aqra, F. M. A. M., Encapsulation of nickel(II) and copper(II) by a tetraazamacrocyclic ligand. *Transition Metal Chemistry* **2003,** 28, (2), 224-228.
119. Kimura, E.; Aoki, S.; Koike, T.; Shiro, M., A tris(Zn-II-1,4,7,10-tetraazacyclododecane) complex as a new receptor for phosphate dianions in aqueous solution. *Journal of the American Chemical Society* **1997,** 119, (13), 3068-3076.
120. Gappa-Fahlenkamp, H.; Lewis, R. S., Improved hemocompatibility of poly(ethylene terephthalate) modified with various thiol-containing groups. *Biomaterials* **2005,** 26, (17), 3479-3485.
121. Duan, X. B.; Lewis, R. S., Improved haemocompatibility of cysteine-modified polymers via endogenous nitric oxide. *Biomaterials* **2002,** 23, (4), 1197-1203.
122. Cha, W.; Meyerhoff, M. E., S-Nitrosothiol detection via amperometric nitric oxide sensor with surface modified hydrogel layer containing immobilized organoselenium catalyst. *Langmuir* **2006,** 22, (25), 10830-10836.
123. Cha, W.; Meyerhoff, M. E., Catalytic generation of nitric oxide from S-nitrosothiols using immobilized organoselenium species. *Biomaterials* **2007,** 28, (1), 19-27.
124. Wismach, C.; du Mont, W. W.; Jones, P. G.; Ernst, L.; Papke, U.; Mugesh, G.; Kaim, W.; Wanner, M.; Becker, K. D., Selenol nitrosation and Se-nitrososelenol homolysis: A reaction path with possible biochemical implications. *Angewandte Chemie-International Edition* **2004,** 43, (30), 3970-3974.
125. Mugesh, G.; Panda, A.; Singh, H. B.; Punekar, N. S.; Butcher, R. J., Glutathione peroxidase-like antioxidant activity of diaryl diselenides: A mechanistic study. *Journal of the American Chemical Society* **2001,** 123, (5), 839-850.
126. Wilson, S. R.; Zucker, P. A.; Huang, R. R. C.; Spector, A., Development of synthetic compounds with glutathione-peroxidase activity. *Journal of the American Chemical Society* **1989,** 111, (15), 5936-5939.
127. Engman, L.; Stern, D.; Cotgreave, I. A.; Andersson, C. M., Thiol peroxidase-activity of diaryl ditellurides as determined by a H^1-NMR method. *Journal of the American Chemical Society* **1992,** 114, (25), 9737-9743.
128. Dong, Z.; Liu, J.; Mao, S.; Huang, X.; Yang, B.; Ren, X.; Luo, G.; Shen, J., Aryl thiol substrate 3-carboxy-4-nitrobenzenethiol strongly stimulating thiol peroxidase activity of glutathione peroxidase mimic 2, 2'-ditellurobis(2-deoxy-b-cyclodextrin). *Journal of the American Chemical Society* **2004,** 126, (50), 16395-16404.
129. Mugesh, G.; Panda, A.; Kumar, S.; Apte, S. D.; Singh, H. B.; Butcher, R. J., Intramolecularly coordinated diorganyl ditellurides: Thiol peroxidase-like antioxidants. *Organometallics* **2002,** 21, (5), 884-892.
130. Cha, W.; Lee, Y.; Oh, B. K.; Meyerhoff, M. E., Direct detection of S-nitrosothiols using planar amperometric nitric oxide sensor modified with polymeric films containing catalytic copper species. *Analytical Chemistry* **2005,** 77, (11), 3516-3524.

CHAPTER 2

Polymethacrylates with Covalently Linked Copper(II)-Cyclen Complex for In Situ Generation of Nitric Oxide from Nitrosothiols in Blood

2.1. Introduction

To develop the first nitric oxide generating polymer (NOGP) containing a metal ion complex as the catalytic site, the Cu(II)-cyclen (cyclen = 1,4,7,10-tetraazacyclododecane) complex is evaluated as a potential pendant catalyst attached to a polymer as proposed in Chapter 1. Cuprous ion (Cu^{+1}) is known as the most efficient reactant for S-nitrosothiol (RSNO) decomposition.[1] In order to maximize the NO generating efficacy of the Cu(II)-cyclen tethered polymer, where the polymeric matrix serves as the reaction environment for the catalyst to generate NO within the bulk phase of the polymer, the catalyst must be distributed throughout the polymeric matrix. Then, potential NO generation by the NOGP could take place not only at the polymer/blood interface, but also within the bulk phase of the polymer because low molecular weight (LMW) biomolecules such as free thiols (cysteine (CySH), glutathione (GSH), ascorbate, etc.) and LMW RSNOs (S-nitrosocysteine (CySNO) and S-nitrosoglutathione (GSNO)) are likely to penetrate into the polymeric matrix.

Based on the above comments, hydrogels, polymeric materials that can imbibe water up to a thousand times their dried weight without dissolution, are the most

desirable polymeric material for creating the new NOGPs. Indeed, hydrogels have been of great interest to biomaterial scientists due to their unique characteristics including water swelling, permeation, and mechanics similar to the extracellular matrix (ECM).[2, 3] Because of the hydrophilicity of hydrogels, they have a low contact angle and low protein absorption on the surface as well.[4] Owing to these features, hydrogels have been applied into a wide variety biomedical applications including tissue engineering,[5, 6] drug delivery,[7, 8] and contact lenses,[12, 13] etc. Hydrogels can be classified by the following three types:[2] i) natural polymers and their derivatives (hyaluronate, alginate, dextran, chitosan, polylysine, collagen and gelatin, fibrin, agarose, etc.); ii) synthetic polymers (PAAc [poly(acrylic acid)], PEG [poly(ethylene glycol)], PEO [poly(ethylene oxide)], pHEMA [poly(2-hydroxyethyl methacrylate)], PLA [poly(lactic acid)], PNIPAAm [poly(N-isopropyl acrylamide)], PNVP [poly(N-vinyl pyrrolidone)], PVA [poly(vinyl alcohol)], etc.); and iii) combinations of synthetic and natural polymers (P (PEG-*co*-peptides), collagen-acrylate, alginate-acrylate, hyaluronate-*g*-PNIPAAm, etc.).

Poly(2-hydroxyethyl methacrylate) (pHEMA) has been the most widely investigated of all hydrogels for use in biomedical applications,[9-11] especially after its use revolutionized the contact lens industry.[12, 13] Since the first synthesis reported by Wichterle and Lim in 1960,[14] the chemical and physical properties of pHEMA have been well characterized, including diffusion studies as a fully hydrated material.[11, 15-19] An extra benefit of pHEMA is that the pore size of the crosslinked network can be controlled by adjusting amounts of various crosslinking agents and by altering the curing process.[2,20-22] A tunable network of pHEMA allows a size selective permeation so that LMW blood components can diffuse into the polymeric matrix, but high molecular

weight (HMW) proteins and blood cells can not. Therefore, pHEMA offers an excellent platform to initially evaluate as a matrix for development of novel NOGPs.

In this chapter, the synthesis of a modified Cu(II)-cyclen complex covalently attached to a crosslinked pHEMA is reported (see **Scheme 2.1**). The ability of this polymeric material to mediate catalytic decomposition of endogenous RSNOs to NO at physiological pH is demonstrated. Various soaking experiments using this new material were also conducted to study its potential for copper leaching. Further, it will be shown that spontaneous NO generation from RSNOs that exist in fresh sheep blood can be achieved with this novel material.

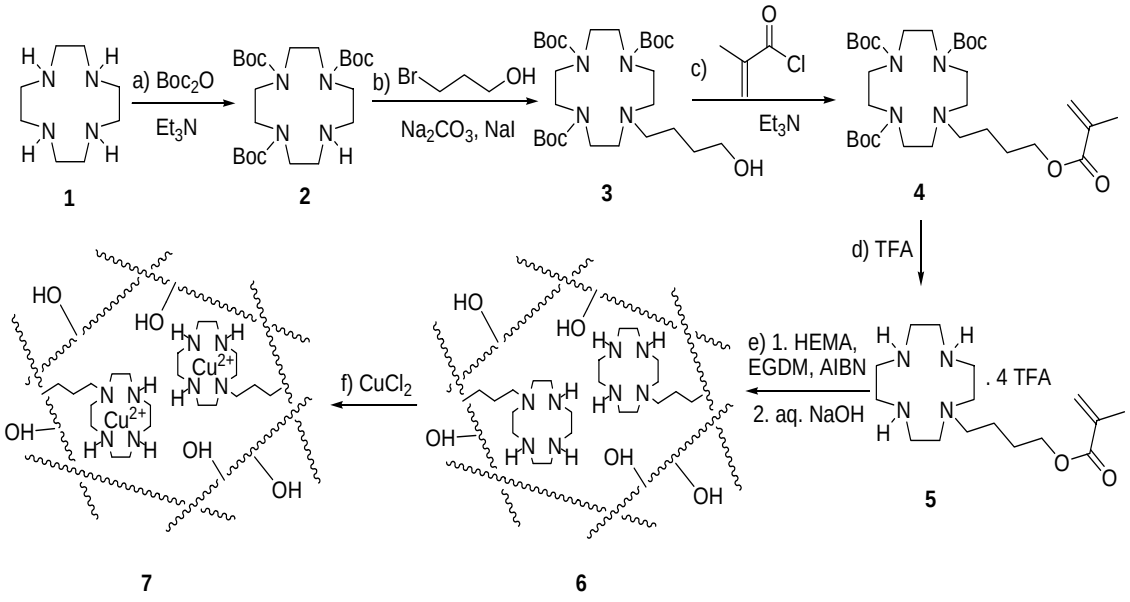

Scheme 2.1 The synthetic scheme for preparing a crosslinked hydrogel, Cu(II)-cyclen-pHEMA **7**. a) Boc_2O (3 eq.), Et_3N (3 eq.), $CHCl_3$, RT, 12h (y= 76%); b) 3-Bromopropanol (3.4 eq.), Na_2CO_3 (1.2 eq.), NaI (1.3 eq.), CH_3CN, 80 °C, 12h (y= 88%); c) Methacryloyl chloride (5.4 eq.), Et_3N (9.5 eq.), THF, -20 °C, RT, 1h (y= 59%); d) TFA, CH_2Cl_2, 0 °C, RT, 12h (y= quantitative); e) 1. 2-Hydroxyethyl methacrylate (HEMA; 66.0 wt %), ethyleneglycol dimethacrylate (EGDM; 2.1 wt %), AIBN (0.4 wt %), 65 °C, 12h; 2. soaked and washed with the solution of aq. NaOH / EtOH (1 / 10, v / v, pH 11-12); f) $CuCl_2.2H_2O$ (1 eq. vs. 5) in EtOH, 65 °C, 4h.

2.2. Experimental

2.2.1. Materials

Cyclen was purchased from Aldrich (Milwaukee, WI) or Strem Chemicals Co (Newburyport, MA). $CuCl_2 \cdot 2H_2O$ was a product of Sigma (St. Louis, MO). Hydrophilic polyurethane (HPU; Tecophilic, SP-93A-100) was a gift from Thermedics Inc. (Wilmington, MA). The other reagents from Aldrich and all solvents from Fisher Scientific were used without further purification unless otherwise noted. Distillation was used for the purification of Et_3N, THF, CH_3CN, and 2-hydroxyethyl methacrylate (HEMA) prior to use. DI water was prepared by a Milli-Q filter system (18 MΩ cm^{-1}: Millipore Corp., Billerica, MA, USA).

2.2.2. Measurements

^{1}H and ^{13}C NMR spectra were obtained on a Varian 400 MHz spectrometer. High-resolution (HR) mass spectra were obtained via a Waters Autospec Ultima Magnetic Sector mass spectrometer with electrospray interface. FTIR spectra were collected with a Perkin-Elmer spectrum BX FT-IR system. UV spectra were recorded by a Perkin-Elmer Lambda 35 UV/VIS spectrometer. EPR spectra were taken by a Bruker EMX (Center field, 3300 G; Sweep Width, 2000 G; Frequency, 9.248 GHz). Copper content of the polymers was measured by atomic absorption spectrophotometry (AA) or inductively coupled plasma emission-mass spectrometry (ICP-MS). All NO generation measurements were made using a Sievers nitric oxide analyzer (NOA), model 280. The current signals of the amperometric sensor were monitored by a microchemical sensor analyzer (Diamond General, Ann Arbor, MI).

2.2.3. Synthesis (see **Scheme 2.1**)

1,4,7-Tris(tert-butyloxycarbonyl)-1,4,7,10-tetraazacyclododecane, **2**:

The synthetic method followed a reported procedure.[23] To a solution of cyclen (0.22 g, 1.28 mmol) and Et_3N (0.55 mL, 3.95 mL) in $CHCl_3$ (12 mL) was added very slowly a solution of di-*tert*-butyl dicarbonate (0.79 g, 3.62 mmol) in chloroform (10 mL) over 3 h. The reaction mixture was stirred overnight at RT and the solvent was evaporated under reduced pressure. Then, the residue was purified by a column chromatography using silica gel (AcOEt/Hexanes=10/7) to yield the desired product, white solid (0.45 g, 76 % yield)

m.p. 64 - 68 °C; ^{1}H NMR (400 MHz, $CDCl_3$, 25 °C, TMS): δ=3.53-3.75 (m, 4H; 2 NCH_2), 3.14-3.48 (m, 8H; 4 NCH_2), 2.73-2.84 (m, 4H; 2 NCH_2), 1.47 (s, 9H; 3 CH_3), 1.45 (s, 18H; 6 CH_3); ^{13}C NMR (100 MHz, $CDCl_3$, 25 °C, TMS): δ=155.67, 79.33, 79.12, 50.87, 49.50, 45.97, 45.41, 28.63, 28.46.

1-(3-Hydroxypropyl)-4,7,10-tris(tert-butyloxycarbonyl)-1,4,7,10-tetraazacyclododecane, **3**:

To a solution of compound **2** (30 mg, 63 mmol), Na_2CO_3 (8.0 mg, 76 mmol), and NaI (12 mg, 80 mmol) in CH_3CN (1.0 mL), 3-bromopropanol (30 mg, 216 mmol) was added at RT. The reaction mixture was stirred at 80 °C under a nitrogen atmosphere overnight. The mixture was then concentrated under reduced pressure and the residue was purified by a column chromatography with silica gel (AcOEt/Hexanes=1/1) to afford **3** as a white amorphous solid (30 mg, 88 % yield).

m.p. 63 - 67 °C; ^{1}H NMR (400 MHz, $CDCl_3$, 25 °C, TMS): δ=3.62 (t, J= 5.6 Hz, 2H; OCH_2), 3.21-3.59 (m, 12H; 6 NCH_2), 2.85 (bs, 1H; OH), 2.51-2.73 (m, 6H; 3 NCH_2),

1.70 (m, 2H; CH_2), 1.47 (s, 9H; 3 CH_3), 1.45 (s, 18H; 6 CH_3); ^{13}C NMR (100 MHz, $CDCl_3$, 25 °C, TMS): δ=155.41, 79.75, 79.46, 59.97 55.17, 54.63, 49.90, 49.23, 48.06, 28.61, 28.46; MS (HR-ESI): m/z: [M+Na]+ calcd for $C_{26}H_{50}N_4O_7$, 553.3577: found 553.3560.

1-(3-Methacryloxypropyl)-4,7,10-tris(tert-butyloxycarbonyl)-1,4,7,10-tetraazacyclododecane, **4**:

To a stirred solution of compound **3** (30 mg, 0.057 mmol) and Et_3N (55 mg, 0.54 mmol) in THF (1.0 mL), methacryloyl chloride (30 μL, 0.31 mmol) was slowly added at -20 °C under the nitrogen atmosphere over 10 min, and then the reaction temperature was slowly raised to RT. After 1 h, the reaction solvent was evaporated. Then, the residue was diluted with Et_2O and washed two times with DI water. The separated organic layer was dried with anhydrous Na_2SO_4, filtered, and washed with Et_2O. After the collected filtrate was concentrated under reduced pressure, the residue was purified by column chromatography on silica gel (AcOEt/Hexanes=1/3) to afford **4** as a white amorphous solid (20 mg, 59 % yield).

m.p. 65 - 70 °C; ^1H NMR (400 MHz, $CDCl_3$, 25 °C, TMS): δ=6.11 (d, J = 0.8 Hz, 1H; CHH=), 5.57 (m, 1H; CHH=), 4.16 (t, J=6.2 Hz, 2H; OCH_2), 3.19-3.65 (m, 12H; 6 NCH_2), 2.54-2.79 (m, 6H; 3 NCH_2), 1.95 (d, J = 0.8 Hz, 3H; $C(CH_2)CH_3$), 1.86 (m, 2H; $(NCH_2)CH_2(CH_2O)$), 1.47 (s, 9H; 3 CH_3), 1.45 (s,18H; 6 CH_3); ^{13}C NMR (100 MHz, $CDCl_3$, 25 °C, TMS): δ=167.26, 155.69, 155.37, 136.19, 125.48, 79.58, 79.34, 63.03, 54.56, 53.39, 49.96, 48.75, 47.85, 28.61, 28.43, 24.41, 18.25; MS (HR-ESI): m/z: [M+Na]+ calcd for $C_{30}H_{54}N_4O_8$, 599.4020: found 599.4023.

1-(3-Methacryloxypropyl)-1,4,7,10-tetraazacyclododecane TFA salt, **5**:

To a solution of compound **4** (20 mg, 0.033 mmol) in CH_2Cl_2 (1 mL), in a water-ice bath, TFA (0.1 mL) was added. The reaction mixture was stirred at RT overnight. The reaction mixture was then concentrated under reduced pressure and the residue was diluted with CH_2Cl_2 and again concentrated in the same manner. Several repetitive cycles were performed to remove the excess of TFA from the residue. Extensive drying of the residue under vacuum pump afforded the desired product as an off-white amorphous solid (quantitative yield) (this compound was very unstable even in the refrigerator, so it is recommended to be used immediately after preparation).

m.p. 105 – 110 °C; ^{1}H NMR (400 MHz, CD_3OD, 25 °C): δ=5.92 (s, 1H; CHH=), 5.45 (s, 1H; CHH=), 4.02 (t, J = 6.6 Hz, 2H; OCH_2), 2.47–3.17 (m, 18H; 9 NCH_2), 1.75 (s, 3H; CH_3); ^{13}C NMR (100 MHz, CD_3OD, 25 °C): δ=168.83, 163.80, 137.65, 126.42, 115.71, 63.82, 50.69, 45.62, 43.35, 43.23, 24.63, 18.37; MS (HR-ESI): m/z: [M+H]+ calcd for $C_{15}H_{30}N_4O_2$, 299.2447: found 299.2442.

Crosslinked polymer, **6**:

2-Hydroxyethyl methacrylate (HEMA; 154 mg, 1.18 mmol), ethyleneglycol dimethacrylate (EGDM; 5.0 mg, 25 μmol), and compound **5** (73.5 mg, 97 μmol) were dissolved in methanol (2 mL) and purged with nitrogen gas. After AIBN (1 mg, 6 μmol) was dissolved in the mixture, the solution was poured onto the two glass slides, and then cured at 65 °C overnight. The formed film was soaked and shaken in ethanol/THF (1/1, v/v) at RT for 1 d. After washing with the same solvents, the film was immersed and shaken in ethanol/aq. NaOH (10/1, v/v; pH 11-12) for 1 d. The film was then soaked and washed with DI water until the rinsing water was pH 7. The film was further washed in

DI water for 1 d, followed by washing in EtOH for 1 d. Finally, the film was washed again with ethanol and dried by vacuum pump for 3 d to give a colorless cosslinked polymer **6**.

IR (KBr)= 3443 cm^{-1} (-OH), 2951 cm^{-1} ($-CH_3$), 2886 cm^{-1} ($-CH_2$), 1729 cm^{-1} (C=O), 1274 cm^{-1} (C-O).

Cu(II)-cyclen-pHEMA, **7**:

The crosslinked polymer **6** was added to a solution of $CuCl_2.2H_2O$ (15 mg, 88 μmol) in ethanol (20 mL) and warmed to 65 °C for 3 h. The film was washed a few times with ethanol, placed into fresh ethanol and shaken at RT for 1 d. The film was thoroughly washed with ethanol and dried by vacuum pump for 4 d to afford a green colored Cu(II)-cyclen-pHEMA **7**. The color of film was changed to a blue when it was soaked in DI water or PBS buffer, pH 7.4 (The swelling ratio, q= 1.6).

IR=3439 cm^{-1} (-OH), 2952 cm^{-1} ($-CH_3$), 2887 cm^{-1} ($-CH_2$), 1730 cm^{-1} (C=O), 1273 cm^{-1} (C-O); UV/Vis (the film itself hydrated with DI water or PBS buffer, pH 7.4): λ_{max}= 621 - 644 nm.

2.2.4. Preparation of RSNO solutions

CySNO and GSNO solutions were prepared by a modification of a previously reported method.[24] A solution of 10 mM L-cysteine or L-glutathione in DI water containing 110 mM H_2SO_4 was well mixed with an equal volume of a 10 mM $NaNO_2$ solution in DI water for 5 – 10 min to give the corresponding 5 mM RSNO solution. The reaction vial was completely wrapped with aluminum foil to avoid the light-induced decomposition.[25] Because a tiny amount of NO (below pmole) naturally released from the original RSNO can be detected by the NOA, every RSNO solution was freshly

prepared from its corresponding stock solutions (10 mM of $NaNO_2$ and acidified GSH) for each experiment. Stock solutions were prepared daily as needed.

2.2.5. General procedure for the NO measurements using a nitric oxide analyzer (NOA)

A nitrogen flow (positive pressure, 50 mL/min) continuously bubbles into a sample solution (usually 2 mL of 10 mM PBS buffer, pH 7.4; the same PBS buffer used unless otherwise noted) in a brown-colored amber cell, and flows into the NOA detector by an equipped vacuum pump (negative pressure, 200 mL/min). Hence, any tiny amount of NO, if generated in the solution, flows into the chamber of the NOA, where NO reacts with ozone produced by an ozone generator built in the instrument to yield a chemiluminescence signal, which is converted to a NO concentration equivalent (ppb·sec) continuously (see **Figure 2.1**).

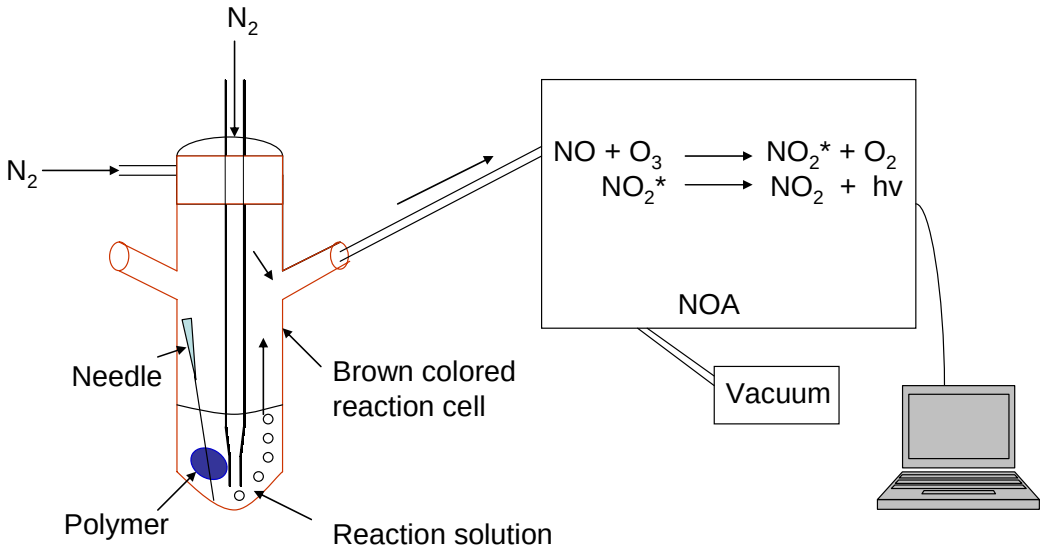

Figure 2.1 A general experimental configuration for NO measurements via a chemiluminescence NO analyzer (NOA).

A conversion constant for the mole number of NO (mol/ppb·sec) can be pre-calibrated by injecting a known amount of $NaNO_2$ into a solution of excess KI in a diluted sulfuric acid solution. Prior to the experiment, each measurement is also calibrated by an internal two-point calibration (the nitrogen flow as zero gas and 45 ppm NO gas). Therefore, the number of moles of NO evolved during the experiment can be calculated by multiplying the peak area (ppb·sec) and the pre-calibrated conversion constant (mol/ppb·sec). This data is further corrected by the basal NO signal that appears when measuring NO released from RSNO in solution phase before any NO generating species is added. The baseline of NO for every experiment varies depending on the specific reaction conditions (usually up to 5 ppb); however, the baseline of given GSNO solutions do not change significantly over 12 h in the presence of EDTA (the μM concentration of EDTA is necessary to prevent any innate RSNO decomposition to NO by tiny amount of metal ion impurities present elsewhere). Thus, the initial steady-state NO amounts already present in the absence of the catalytic species, which are the basal NO values, are subtracted to obtain the NO levels produced by the presence of the given catalyst. In order to demonstrate the catalytic activity of a given polymer, a piece of polymer is pierced by a stainless steel needle (which does not affect RSNO decomposition). Then, the polymer portion is fully immersed into an RSNO reaction solution in the cell. After a newly increased steady-state of NO signal is observed, pulling the needle out from the reaction cell results in decrease in the NO level back to the original baseline signal.

2.2.6. Sample preparation for the analysis of copper content in the polymer

The typical procedure used for measuring the copper content in a polymer was as follows. In brief, a given small piece of polymer (a few mg) was dissolved in conc.

sulfuric acid (0.5 mL) overnight at RT and then diluted with DI water (4.5 mL). The resultant clear mixture was passed through a syringe filter (0.45 μm PTFE, a National Scientific Company product), and then the copper content in the filtrate solution was analyzed by AA or ICP-MS.

2.2.7. Preparation of a interpenetrating polymer network (IPN) of Cu(II)-cyclen-pHEMA 7 and HPU

A modified procedure for the synthesis of Cu(II)-cyclen-pHEMA **7** was employed for the synthesis of an IPN of Cu(II)-cyclen-pHEMA **7** and HPU. In brief, a thin film ($\leq$ 10 μm) of hydrophilic polyurethane (HPU; Tecophilic, SP-93A-100) was coated on one side of a glass slide. Then, compound **5** was polymerized on the HPU coated glass slide, using the same reaction process employed for the synthesis of polymer **6** (refer to section 2.2.3), resulting in a new IPN consisting of polymer **6** and HPU. Finally, the incorporation of copper ions into this new IPN by the same method described for the synthesis of Cu(II)-cyclen-pHEMA **7** yielded the IPN of Cu(II)-cyclen-pHEMA **7** and HPU.

2.2.8. Amperometric NO detection in blood

Fresh sheep blood (obtained from Extracorporeal Membrane Oxygenation (ECMO) laboratory at the University of Michigan Medical School) was heparinized (to achieve 250 s of activated clotting time (ACT) post-heparin) and protected from ambient light by wrapping with aluminum foil. The blood sample was kept at 37 °C before and during the experiments. A control amperometic NO sensor mounted with a bare HPU film and a RSNO sensor prepared with a IPN of Cu(II)-cyclen-pHEMA **7** and HPU were assembled according to reported methods (see **Figure 2.2**).[26] The sensors were pre-

calibrated to obtain their intrinsic NO response in the stirred PBS buffer, pH 7.4, at 37 °C. Both the NO and RSNO sensors were immersed into a new PBS buffer (30 mL) prior to use. The amperometric signal of each sensor was monitored after adding the fresh sheep blood (6 mL) into the solution. The current signals of both sensors were converted into the NO equivalent concentration based on the prior NO calibration of each sensor.

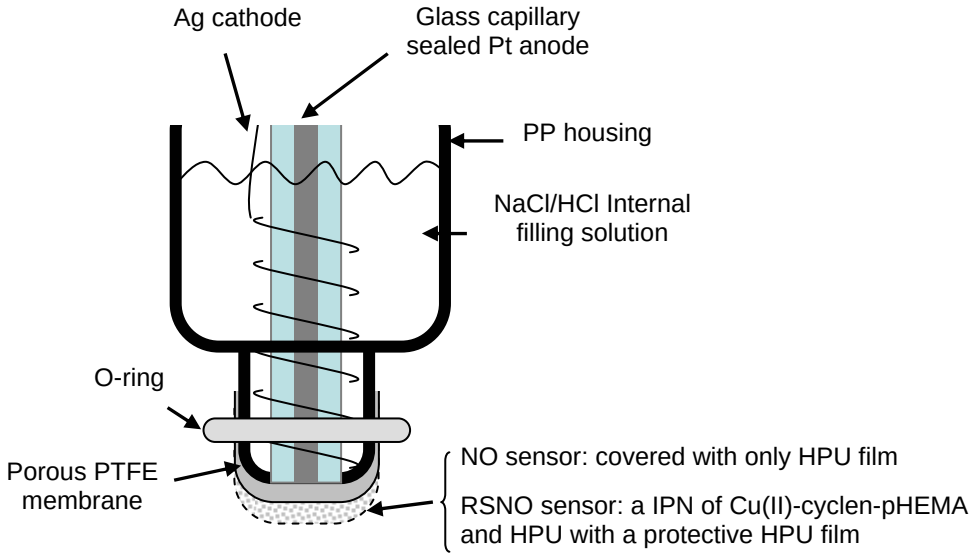

Figure 2.2 The configuration of amperometric NO sensor used for the direct detection of RSNOs in fresh sheep blood.

2.3. Results and discussion

2.3.1. Synthesis and characterization

In brief (see **Scheme 2.1**), to synthesize the pHEMA material with appended Cu(II)-cyclen sites, three amines of cyclen were protected with Boc groups,[23] and a hydroxyl propyl group was introduced on the remaining nitrogen via a substitution reaction with 3-bromopropanol. Reaction of this derivative with methacryloyl chloride

yielded compound **4**, possessing a polymerizable group. Deprotecting the Boc groups of the compound **4** using trifluoroacetic acid (TFA) afforded a modified cyclen monomer **5** (this compound is very unstable even in the refrigerator, so it is recommended to be used immediately after preparation). Co-polymerization of the modified cyclen monomer **5**, 2-hydroxyethyl methacrylate (HEMA) and the crosslinking agent, ethylene glycol dimethacrylate (EGDM) was achieved using AIBN as the initiator. This reaction was carried out using the reactants sandwiched as a thin liquid film layer between two glass plates. The resulting crosslinked film **6** was soaked overnight and washed with various solvents including NaOH, DI water, THF, and ethanol to remove any residual TFA and small molecules. The crosslinked film **6** was then reacted with $CuCl_2$ in hot ethanol solution to form the Cu(II)-cyclen complexes within the polymeric matrix. Again, extensive washing with various solvents to remove free copper ions non-specifically bound to the polymer backbone afforded the hydrogel, Cu(II)-cyclen-pHEMA **7** (see section 2.2 for details).

It has been suggested that square-pyramidal copper(II) complexes have an absorption band in the region 550–670 nm in the visible region of the spectrum.[27] While the λ_{max} of $Cu(cyclen)Cl_2$ is known to be 594 nm in water[27] and 608 nm in 10 mM PBS buffer, pH 7.4 (the concentration and pH of the PBS buffers used here are the same unless otherwise noted), the film of Cu(II)-cyclen-pHEMA **7** displayed a λ_{max} in the range of 621-644 nm after being fully hydrated with DI water or PBS buffer. The bathochromic shift in λ_{max} may be attributed to the substitution of hydroxide ions for chloride ions since Cu(II)-cyclen-pHEMA **7** was treated with aq. NaOH during preparation. In addition, the surrounding polymer matrix as well as possible structural

distortion of the Cu(II)-cyclen complex in Cu(II)-cyclen-pHEMA **7** could also influence the visible absorption spectrum.

Both frozen aqueous and PBS buffered EPR spectra of the Cu(II)-cyclen-pHEMA **7** material exhibited the typical four-line patterns expected for a Cu(II)-cyclen complex (see **Figure 2.3**).[28] Moreover, the extent of visible blue color of the Cu(II)-cyclen-pHEMA **7** and the corresponding copper content determined by atomic absorption spectrophotometry (AA) after dissolving a given mass of film in sulfuric acid solution, correlated very closely with mole ratios of the modified cyclen monomer **5** to HEMA used in the polymerization reaction, as well as with the theoretical amount of copper expected (see **Table 2.1** and **Figure 2.4**). Taken together, the data suggest that most of cyclen sites covalently linked to the polymer are complexed with copper(II) ions in the final crosslinked pHEMA films.

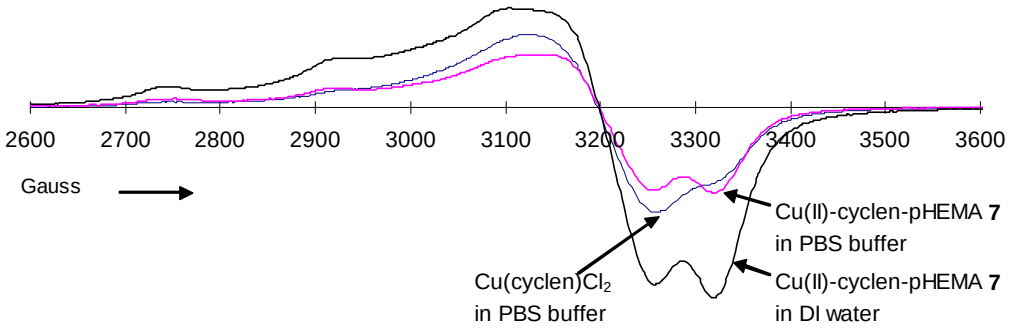

Figure 2.3 EPR spectra of Cu(cyclen)Cl_2 and Cu(II)-cyclen-pHEMA **7** in DI water or PBS buffer, pH 7.4 at 77K: Center field, 3300 G; Sweep Width, 2000 G; Frequency, 9.248 GHz.

Table 2.1 The correlation between the modified cyclen monomer **5** used in the polymerization reactions and the theoretical and measured copper content of films (Cu(II)-cyclen-pHEMA **7**) as determined by atomic absorption spectrophotometer (AA) (see **Figure 2.4**).

Samples	A	B	C	D
The modified cyclen monomer **5** applied to the polymerization (mol %)	0	0.07	0.5	3.8
Theoretical copper content in the films (wt %)	0	0.03	0.21	1.7
Copper content in the films (wt %)	N.A.	0.04	0.28	1.4

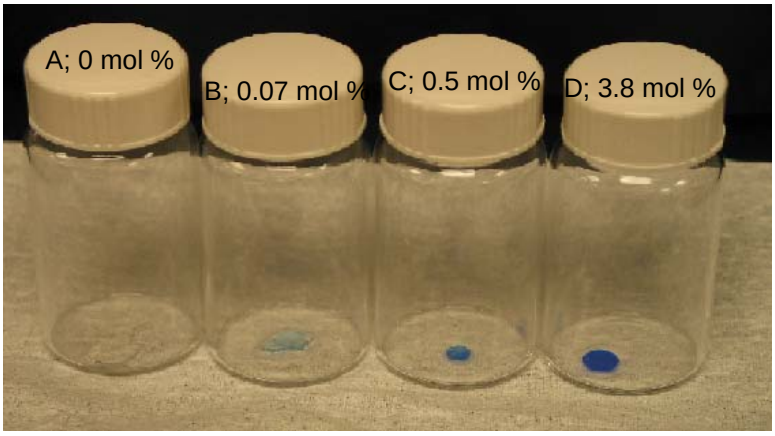

Figure 2.4 The pictures of crosslinked pHEMA and Cu(II)-cyclen-pHMEAs **7** with various copper content after being hydrated in DI water; the extent of blue color of films correlates well with the amount of the modified cyclen monomer **5** used in the polymerization, and therefore with copper content (see **Table 2.1**).

2.3.2. Catalytic S-nitrosothiol decomposition to nitric oxide

Figure 2.5 illustrates the NO generation that is achieved when a small piece of the film (Cu(II)-cyclen-pHEMA **7**) is placed in and then removed from a solution of GSNO (or CysNO) and GSH (or CySH) in deoxygenated PBS buffer. The NO generated is monitored continuously using a chemiluminescence NO analyzer (NOA). As shown in **Figure 2.5-a**, a blank experiment in which a hydrogel film **6** (not reacted with copper) was placed in the test solution did not generate any detectable NO. This demonstrates

that, as expected, copper ions are the key element for NO generation. In a second blank experiment, the same size of a crosslinked pHEMA film, prepared by the reaction of HEMA, EGDM, and AIBN but without co-polymerization of the cyclen monomer **5**, and further reacted with copper ions using the same method employed for the preparation of Cu(II)-cyclen-pHEMA **7**, yielded only a small NO flux upon the very first immersion in the GSNO solution.

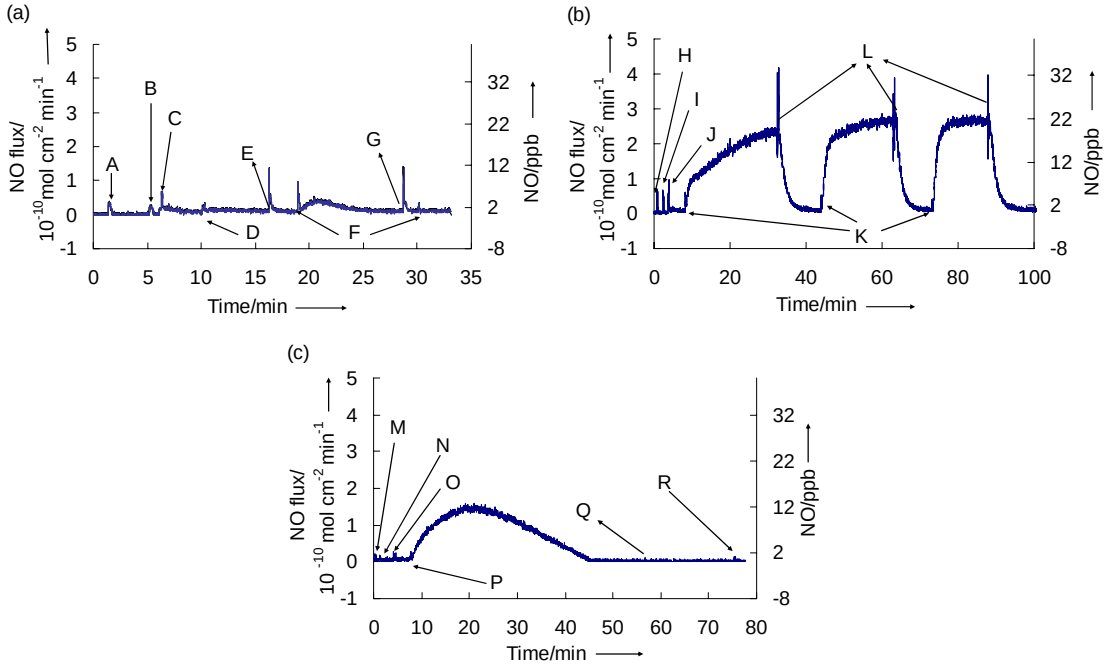

Figure 2.5 The profiles of NO generation for the following disk polymers (thickness, 0.3 mm; radius, 2.0 mm) in 2 mL of 10 mM deoxgenated PBS buffer, pH=7.4, monitored with a chemiluminescence NO analyzer (NOA) at RT after the following steps: (a) A, adding 10 μM EDTA; B, adding 30 μM GSH; C, adding 10 μM GSNO ; D, putting the crosslinked film **6** in; E, taking the crosslinked film **6** out; F, putting pHEMA in; G, taking pHEMA out, (b) H, adding 10 μM EDTA; I, adding 5 μM GSH; J, adding 5 μM GSNO; K, inserting Cu(II)-cyclen-pHEMA **7** in; L, removing Cu(II)-cyclen-pHEMA **7** out, (c) M, adding 10 μM EDTA; N, adding 0.5 μM CySH; O, adding 0.5 μM CySNO; P, immersing Cu(II)-cyclen-pHEMA **7** in; Q, taking Cu(II)-cyclen-pHEMA **7** out; R, adding excess amount of free copper ion.

This is due to non-specifically adsorbed Cu(II) ions adhered to the pHEMA matrix. Indeed, little or no NO generation was observed for subsequent immersions of the same blank films (see **Figure 2.5(a)**). In contrast, the first immersion of the same size of a Cu(II)-cyclen-pHEMA **7** film into the GSNO solution provides a slow increase in the NO flux that reaches a steady-state (see **Figure 2.5(b)**). After this film was removed from the reaction cell, the NO flux decreased to the baseline quickly. Subsequent immersion/removal cycles of the same film showed that the Cu(II)-cyclen-pHEMA **7** material could reversibly achieve nearly the same steady-state NO flux on sequential immersions into fresh GSNO/GSH solutions.

When CySNO at 10 times lower concentration than GSNO was examined as the RSNO substrate for the films, nearly equivalent fluxes of NO generation was achieved over a relatively short time periods (see **Figure 2.5(c)**), but the NO generation decreased quickly, as the bulk CySNO substrate was consumed by the more rapid catalytic reaction (any further NO signal was not detected when an excess of free copper ions was added into the solution right after removing the film). The relatively higher short-term NO flux achieved in the case of CySNO compared to the behavior of GSNO (data not shown here) probably relates to their relative reaction rates with Cu(II)-cyclen-pHEMA **7**. The concentration of CySNO in blood is known to be higher than GSNO;[29] hence, CySNO is more likely to contribute toward a larger fraction of the potential NO generating capability by the new Cu(II)-cyclen-pHEMA polymers when they are in contact with fresh blood.

2.3.3. Stability tests

To be effective as a thromboresistant coating for biomedical applications, the Cu(II)-cyclen-pHEMA material must be chemically stable and also maintain catalytic activity under physiological conditions for an extended time period. Although pHEMA and its copolymers are known to be suitable biomaterials,[30-32] the Cu(II)-cyclen complex attached to the pHEMA could potentially demetalate, and/or be deactivated by other ligands such as free thiols, proteins, and other blood components that have high binding affinities with the copper(II) sites of the complex. To investigate the potential of copper ion leaching and deactivation of Cu(II)-cyclen-pHEMA **7**, several soaking experiments with the new polymeric films were conducted. First, copper leaching was examined by soaking the same size circular films (radius, 1.9 mm; thickness, 0.3 mm; initial average copper content, 0.64 μmol) in 10 mL of 2 μM EDTA in 10 mM phosphate buffer, pH 7.7 (solution A), and also in 10 mL of solution containing 2 μM EDTA, 6 μM GSH, and 2 μM GSNO in 10 mM phosphate buffer, pH 7.7 (solution B), at 37.5 °C. The solutions were shaken continuously, and replaced with fresh solution daily. After a fixed time period, the amount of copper remaining in the films was determined by AA. Films soaked in solution A retained 73 % of their original copper content after 15 d, while films soaked in solution B had 64 % of the original copper levels after the same period of soaking (see **Figure 2.6**). This data suggests that the copper ions are bound quite tightly to the cyclen on the pHEMA structure, since even the presence of a very strong copper(II) chelator such as EDTA in the soaking solution had a relatively small effect on the total copper remaining in the films.

To determine whether the NO generating catalytic activity Cu(II)-cyclen-pHEMA **7** films can be deactivated by free thiols, such as GSH (a reducing agent), as well as disulfides (such as glutathione disulfide (GSSG), a by-product of the NO generation reaction), both strong ligands for copper ions,[33, 34] a small piece of Cu(II)-cyclen-pHEMA **7** (initial copper content, 0.26 μmol) was immersed and shaken in a solution containing 0.25 μmol GSH and 0.25 μmol GSNO in 10 ml PBS buffer at RT for 8 d. Such a solution will generate GSSG if the catalytic reaction takes place.

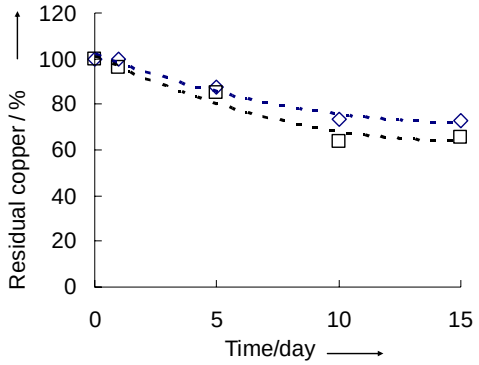

Figure 2.6 Copper leaching from Cu(II)-cyclen-pHEMA **7** after soaking experiments: the films (radius, 1.9 mm; thickness, 0.3 mm; copper content, average 0.64 μmol) were soaked and shaken in a 10 ml solution of 2 μM EDTA in 10 mM phosphate buffer, pH 7.7 (solution A; ◊) and in a 10 ml solution of 2 μM EDTA, 6 μM GSH, and 2μM GSNO in 10 mM phosphate buffer, pH 7.7 (solution B; □) at 37.5 ˚C. The solutions were replaced with fresh one everyday, and a sample film at a given time interval was dissolved in sulfuric acid to measure the residual copper content by AA at that time point.

The solution was replaced daily with fresh solution (except on day 6 of the 8 day experiment). It was found that there was an approx. 50% decrease in the apparent NO flux (using 5 μM GSH/GSNO reaction solution) for the film soaked in the solution (after 8 d) compared to a control of the same film (not soaked in GSH/GSNO solution) that was tested for NO generation prior to soaking. Inductively coupled plasma-mass

spectrometric (ICP-MS) data confirmed that a 20 mol % of total copper was removed from the polymer after 8 d of soaking. In a second experiment, a small piece of a new Cu(II)-cyclen-pHEMA **7** (initial copper content, 0.46 μmol) film was placed into a solution containing a large concentration of GSH only (50 μmol GSH in 10 ml of PBS buffer) and incubated overnight at RT. The goal was to determine whether such higher levels of GSH alone, inhibit catalytic activity over shorter time periods. In this case, there was approx. a 25% decrease in the apparent NO flux under the normal conditions use to test NO generation after this one day incubation. In addition, the UV-Vis λ_{max} of the film did not change in location before and after such soaking in the excess of GSH, suggesting that GSH does not bind irreversibly as a ligand to the complex. These data suggest that the loss of NO flux most likely results from leaching of copper ions from the polymer rather than deactivation by GSH and/or GSSG.

A more critical test is to examine the NO generation of films of the new Cu(II)-cyclen-pHEMA **7** material (radius, 2.8 mm; thickness, 0.2 mm; disk type) from GSNO before and after the exposure to animal blood for a finite period. It was found that NO generation from GSNO is maintained after soaking such films in 10 mL of the sheep plasma for 3 d at 4 °C, or whole blood for 1 day at 4 °C (see **Figure 2.7**). These results indicate the deactivation of Cu(II)-cyclen-pHEMA **7** caused by endogenous free thiols, proteins, and other blood components may not be a significant issue with these new hydrogel materials. Clearly, a large number of *in vivo* studies over varying time periods will be required to fully assess the true NO generation ability and resultant thromboresistance under physiological conditions.

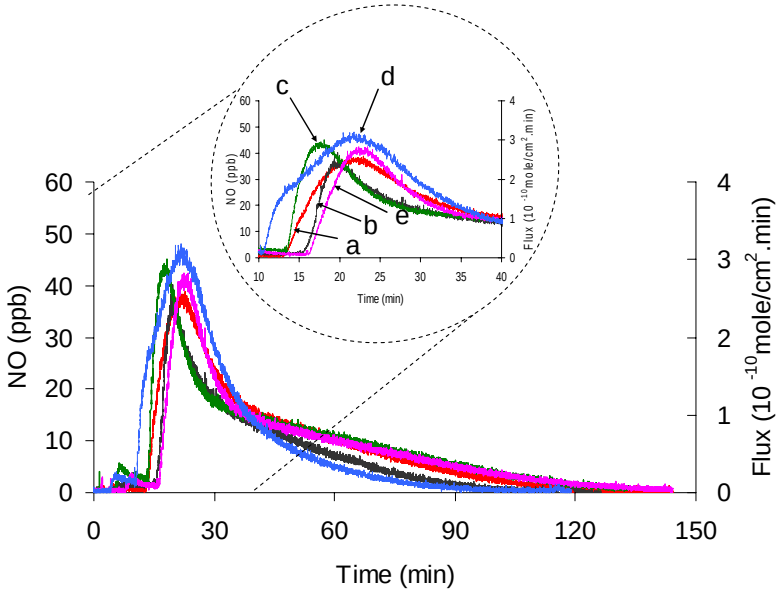

Figure 2.7 The NO generation profiles of Cu(II)-cyclen-pHEMA **7** before and after soaking in the sheep plasma or whole blood over the various time periods were recorded by the NOA: the films (radius, 2.8 mm; thickness, 0.2 mm; disk type) were tested in a solution of 2 μM GSNO and 75 μM GSH in 2 mL PBS buffer, pH=7.4, in the presence of 5 μM EDTA, before and after soaking in 10 ml of the sheep plasma or whole blood at 4 °C under various time intervals; a, unsoaked film; b, after 3 h in plasma; c, after 1 d in plasma; d, after 3 d in plasma; e, after 1 d in whole blood.

2.3.4. Spontaneous NO generation in contact with blood *in vitro*

To further demonstrate that the Cu(II)-cyclen-pHEMA polymer can generate NO spontaneously in fresh whole blood, an amperometric RSNO sensor was constructed using an interpenetrating network (IPN) film of Cu(II)-cyclen-pHEMA **7** and hydrophilic polyurethane (HPU, Tecophilic, SP-93A-100) as an outer film on a NO selective electrochemical sensor (see **Figure 2.2**). The response of a control NO sensor without the polymer containing Cu(II)-cyclen (but with an HPU outer membrane) was also monitored in the same blood samples. Each sensor was pre-calibrated for intrinsic direct amperometric response to NO (see **Figure 2.8**), and then respectively measured NO and RSNO levels in the fresh sheep blood diluted with PBS buffer at 37 °C.

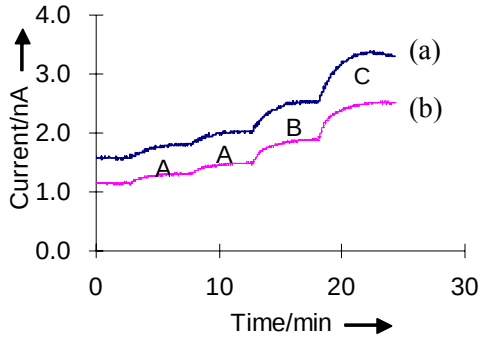

Figure 2.8 Calibration responses for RSNO sensor (a) and NO sensor (b) toward the different NO levels: Current levels of both sensors were plotted for the intrinsic direct amperometric response upon the addition of standard NO solution (A, 20 nM; B, 40 nM; C, 80 nM).

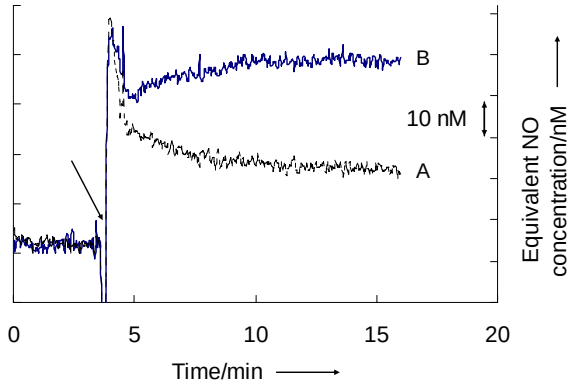

Figure 2.9 The direct amperometric detection of endogenous RSNOs in fresh sheep blood using a NO sensor (A) as a control and a RSNO sensor (B) upon injection of 6 mL of fresh sheep blood (→) into 30 mL of 10 mM PBS buffer, pH 7.4, at 37 ˚C under nitrogen stream.

Figure 2.9 shows that the NO sensor without the catalytic Cu(II)-cyclen-pHEMA polymer site in the outer membrane has relatively little amperometric response when placed in the blood sample, whereas the difference of NO responses between RSNO and

NO sensor (equivalent to ~25 nM NO calculated from calibration curves) was due to the decomposition of RSNO species in the sheep blood via the IPN film of Cu(II)-cyclen-pHEMA **7** and HPU. Therefore, Cu(II)-cyclen complex covalently attached to pHEMA generates NO from endogenous substrates in the sheep blood *in vitro*.

2.4. Conclusions

The aim of this work was to create and evaluate a novel NOGP containing an immobilized Cu(II)-cyclen complex as NO generating catalytic sites in a polymeric material. To maximize the catalytic efficiency of the NOGP, pHEMA that can highly swell in water was used as the polymeric matrix to covalently attach the catalyst. In this study, Cu(II)-cyclen was successfully linked with a crosslinked pHEMA and the resulting material was found to be capable of generating NO from naturally occurring RSNO species, both in buffer and also directly when in contact with fresh whole blood. The presence of endogenous reducing equivalents is required to observe such catalytic chemistry. Assessment of the stability of the new Cu(II)-cyclen-pHEMA **7** material suggests that the slow leaching of copper ions from the polymer film may cause a measurable decrease of NO generation with time, but copper deactivation is not a significant problem. Although fundamental questions with respect to the exact mechanism by which Cu(II)-cyclen-pHEMA **7** generates NO remain, the data presented herein suggest that this new material may prove beneficial as a potentially new thromboresistant blood contacting polymer for biomedical applications with contact times of hours to several days.

2.5. References

1. Williams, D. L. H., The chemistry of S-nitrosothiols. *Accounts of Chemical Research* **1999,** 32, (10), 869-876.
2. Hoffman, A. S., Hydrogels for biomedical applications. *Advanced Drug Delivery Reviews* **2002,** 54, (1), 3-12.
3. Roy, I.; Gupta, M. N., Smart polymeric materials: Emerging biochemical applications. *Chemistry & Biology* **2003,** 10, (12), 1161-1171.
4. Elbert, D. L.; Hubbell, J. A., Surface treatments of polymers for biocompatibility. *Annual Review of Materials Science* **1996,** 26, 365-394.
5. Lee, K. Y.; Mooney, D. J., Hydrogels for tissue engineering. *Chemical Reviews* **2001,** 101, (7), 1869-1879.
6. Weinberg, C. B.; Bell, E., A Blood-vessel model constructed from collagen and cultured vascular cells. *Science* **1986,** 231, (4736), 397-400.
7. Park, H.; Park, K., Biocompatibility issues of implantable drug delivery systems. *Pharmaceutical Research* **1996,** 13, (12), 1770-1776.
8. Peppas, N. A.; Bures, P.; Leobandung, W.; Ichikawa, H., Hydrogels in pharmaceutical formulations. *European Journal of Pharmaceutics and Biopharmaceutics* **2000,** 50, (1), 27-46.
9. Ramakrishna, S.; Mayer, J.; Wintermantel, E.; Leong, K. W., Biomedical applications of polymer-composite materials: a review. *Composites Science and Technology* **2001,** 61, (9), 1189-1224.
10. Midha, R.; Munro, C. A.; Dalton, P. D.; Tator, C. H.; Shoichet, M. S., Growth factor enhancement of peripheral nerve regeneration through a novel synthetic hydrogel tube. *Journal of Neurosurgery* **2003,** 99, (3), 555-565.
11. Montheard, J. P.; Chatzopoulos, M.; Chappard, D., 2-Hydroxyethyl methacrylate (HEMA) - Chemical-properties and applications in biomedical fields. *Journal of Macromolecular Science-Reviews in Macromolecular Chemistry and Physics* **1992,** C32, (1), 1-34.
12. Goda, T.; Ishihara, K., Soft contact lens biomaterials from bioinspired phospholipid polymers. *Expert Review of Medical Devices* **2006,** 3, (2), 167-174.
13. Wu, S. N.; Li, H.; Chen, J. P., Modeling investigation of volume variation kinetics of fast response hydrogels. *Journal of Macromolecular Science-Polymer Reviews* **2004,** C44, (2), 113-130.
14. Wichterle, O.; Lim, D., Hydrophilic gels for biological use. *Nature* **1960,** 185, (4706), 117-118.
15. Rosso, F.; Barbarisi, A.; Barbarisi, M.; Giordano, A.; Ambrosio, L., Synthesis and characterisation of poly(2-hydroxyethyl methacrylate) polyelectrolyte complexes. *Journal of Materials Science-Materials in Medicine* **2004,** 15, (6), 679-686.
16. Horak, D., Preparation and properties of poly (2-hydroxyethyl methacrylates). *Chemicke Listy* **1992,** 86, (5), 359-374.
17. Slomkowski, S., Polyacrolein containing microspheres: Synthesis, properties and possible medical applications. *Progress in Polymer Science* **1998,** 23, (5), 815-874.

18. Young, C. D.; Wu, J. R.; Tsou, T. L., Fabrication and characteristics of polyHEMA artificial skin with improved tensile properties. *Journal of Membrane Science* **1998,** 146, (1), 83-93.
19. Fornasiero, F.; Krull, F.; Radke, C. J.; Prausnitz, J. M., Diffusivity of water through a HEMA-based soft contact lens. *Fluid Phase Equilibria* **2005,** 228, 269-273.
20. Huang, C. W.; Sun, Y. M.; Huang, W. F., Curing kinetics of the synthesis of poly(2-hydroxyethyl methacrylate) (PHEMA) with ethylene glycol dimethacrylate (EGDMA) as a crosslinking agent. *Journal of Polymer Science Part A-Polymer Chemistry* **1997,** 35, (10), 1873-1889.
21. Hermitte, L.; Thomas, F.; Bougaran, R.; Martelet, C., Contribution of the comonomers to the bulk and surface properties of methacrylate copolymers. *Journal of Colloid and Interface Science* **2004,** 272, (1), 82-89.
22. Hennink, W. E.; van Nostrum, C. F., Novel crosslinking methods to design hydrogels. *Advanced Drug Delivery Reviews* **2002,** 54, (1), 13-36.
23. Kimura, E.; Aoki, S.; Koike, T.; Shiro, M., A tris(Zn-II-1,4,7,10-tetraazacyclododecane) complex as a new receptor for phosphate dianions in aqueous solution. *Journal of the American Chemical Society* **1997,** 119, (13), 3068-3076.
24. Stamler, J. S.; Loscalzo, J., Capillary zone electrophoretic detection of biological thiols and their S-nitrosated derivatives. *Analytical Chemistry* **1992,** 64, (7), 779-785.
25. Szacilowski, K.; Stasicka, Z., S-Nitrosothiols: Materials, reactivity and mechanisms. *Progress in Reaction Kinetics and Mechanism* **2001,** 26, (1), 1-58.
26. Cha, W.; Lee, Y.; Oh, B. K.; Meyerhoff, M. E., Direct detection of S-nitrosothiols using planar amperometric nitric oxide sensor modified with polymeric films containing catalytic copper species. *Analytical Chemistry* **2005,** 77, (11), 3516-3524.
27. Styka, M. C.; Smierciak, R. C.; Blinn, E. L.; Desimone, R. E.; Passariello, J. V., Copper(II) complexes containing a 12-membered macrocyclic ligand. *Inorganic Chemistry* **1978,** 17, (1), 82-86.
28. Soibinet, M.; Dechamps-Olivier, I.; Guillon, E.; Barbier, J. P.; Aplincourt, M.; Chuburu, F.; Le Baccon, M.; Handel, H., XAS, ESR and potentiometric studies of three dinuclear N,N '-para-xylylenebis(tetraazamacrocycle)copper(II) complexes - X-ray crystal structure of [N,N '-p-xylylenebis(cyclen)]copper(II). *European Journal of Inorganic Chemistry* **2003**, (10), 1984-1994.
29. Kelm, M., Nitric oxide metabolism and breakdown. *Biochimica et Biophysica Acta* **1999,** 1411, (2-3), 273-289.
30. Bajpai, A. K.; Mishra, D. D., Adsorption of a blood protein on to hydrophilic sponges based on poly(2-hydroxyethyl methacrylate). *Journal of Materials Science-Materials in Medicine* **2004,** 15, (5), 583-592.
31. Mabilleau, G.; Moreau, M. F.; Filmon, R.; Basle, M. F.; Chappard, D., Biodegradability of poly (2-hydroxyethyl methacrylate) in the presence of the J774.2 macrophage cell line. *Biomaterials* **2004,** 25, (21), 5155-5162.

32. Belkas, J. S.; Munro, C. A.; Shoichet, M. S.; Midha, R., Peripheral nerve regeneration through a synthetic hydrogel nerve tube. *Restorative Neurology and Neuroscience* **2005,** 23, (1), 19-29.
33. Baek, H. K.; Cooper, R. L.; Holwerda, R. A., Stability of the Cu(II)-S bond in mercapto amino-acid complexes of [2,2',2''-tris(dimethylamino)triethylamine]copper(II) and [tris(2-pyridylmethyl)amine]copper(II). *Inorganic Chemistry* **1985,** 24, (7), 1077-1081.
34. Gilbert, B. C.; Silvester, S.; Walton, P. H., Spectroscopic, kinetic and mechanistic studies of the influence of ligand and substrate concentration on the activation by peroxides of Cu-I-thiolate and other Cu-I complexes. *Journal of the Chemical Society-Perkin Transactions 2* **1999**, (6), 1115-1121.

Chapter 3

Polyurethanes with a Tethered Copper(II)-Cyclen Complex: Synthesis and Catalytic Generation of Nitric Oxide From S-Nitrosothiols

3.1. Introduction

Thermoplastic polyurethanes (PUs) are considered to offer relatively good hemocompatibility and mechanical properties when compared to the other synthetic materials for biomedical applications (e.g., poly(vinyl chloride) and silicone rubber).[1-3] Hence, they have been used to prepare a variety of medical devices including blood bags, catheters, vascular grafts, and portions of artificial hearts.[2, 4, 5] However, PUs are not free from biocompatibility problems such as platelet adhesion/activation and thrombus formation when in contact with blood and used for extended periods of time.[2, 6-8]

Thermoplastic PUs are block copolymers composed of a hard segment (A) and soft segment (B) blocks arranged in an $(AB)_n$ type structure (see **Scheme 3.1**).[1] The hard segment (HS) block is composed of a diisocyanate (aromatic diisocyanate such as 4,4'-methlyenediphenyl diisocyanate (MDI) or aliphatic diisocyanate such as hydrogenated MDI (HMDI)) and a chain extender (usually a low molecular diol such as 1,4-butanediol (BDO) or diamine such as ethylene diamine (ED)). The soft segment (SS) is usually a macrodiol (M.W. 600 – 2000) such as poly(tetramethyleneoxide) (PTMO), the one

mostly employed in recent medical-grade PUs (see **Scheme 3.1**).[2] Utilizing a variety of chemical compositions of PUs (the diisocyanates, the chain extenders, and the macrodiols), synthetic polymer chemists are now able to tailor their structures to meet specific property requirements ranging from engineering polymers to medical grade polymers.

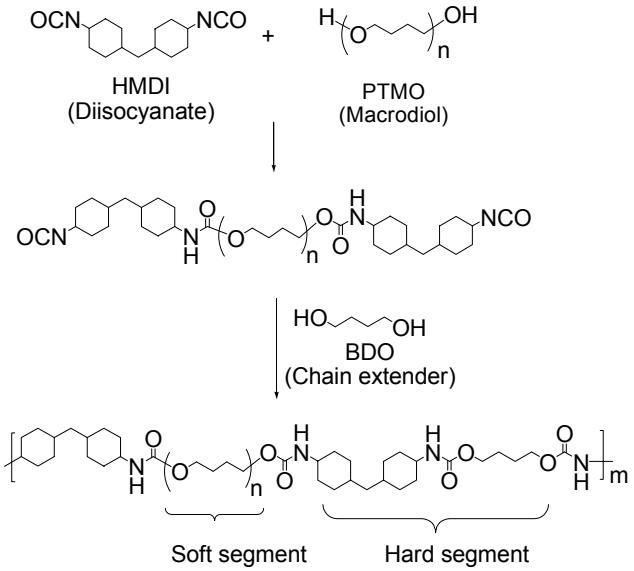

Scheme 3.1 The typical synthetic scheme for preparing a thermoplastic polyurethane (PU) using HMDI (hydrogenated 4,4'-methlyenediphenyl diisocyanate) as the diisocyanate agent, PTMO (poly(tetramethyleneoxide)) as the macrodiol, and BDO (1,4-butanediol) as the chain extender, where the soft segment (HS) is composed of the macrodiol and the hard segment (SS) is composed of the diisocyanate and chain extender.

We recently introduced a new hydrogel (pHEMA with appended Cu(II)-cyclen catalytic sites) polymeric material that can catalytically generate nitric oxide (NO) from S-nitrosothiols (RSNOs) known to exist in blood (see Chapter 2). Owing to the well known biological activities of NO, such as the inhibition of platelet activation/adhesion as well as smooth cell proliferation,[9-12] such NO generating polymers (NOGPs) that can produce locally elevated NO levels at the blood/polymer interface may be useful to

enhance the hemocompatibility of various biomedical devices. However, the NO generating catalyst in any NOGP occupies a very small portion of the total volume (or surface) of the polymer. Thus, the polymeric matrix used to prepare the NOGP will dictate the physical properties of this polymeric material, which are also critical factors to be considered for any implanted biomaterial. Given this circumstance, research on ways to tailor a medical grade PU to exhibit NO generating activity seems warranted. That is, PU materials with covalently linked sites that can generate NO from endogenous blood components will incorporate the combined benefits of the base PU's mechanical properties with NO's biological activities, yielding a new biomaterial with, hopefully, enhanced hemocompatibility.

Therefore, we now report a new NOGP, in which a medical-grade hydrophilic thermoplastic PU (Tecophilic, SP-93A-100, see **Scheme 3.1** for its structure) is covalently linked with a NO generating catalyst, Cu(II)-cyclen complex. In this chapter, the synthesis and characterization of this new NOGP, Cu(II)-cyclen-PU (**5**) are presented (see **Scheme 3.2**). Similar to the previous work described in Chapter 2, the catalytic NO generation activities of this new polymeric material are examined using RSNOs and RSHs as substrates at physiological pH. This study also includes examination of the potential copper(II) ion leaching from the polymer under various soaking conditions. Furthermore, the spontaneous NO generation using this polymer in animal whole blood is demonstrated via use of the polymer to construct an amperometric RSNO sensor. Hence, based on the data presented herein, this new PU material is likely to provide an attractive and practically useful coating for a number of medical devices.

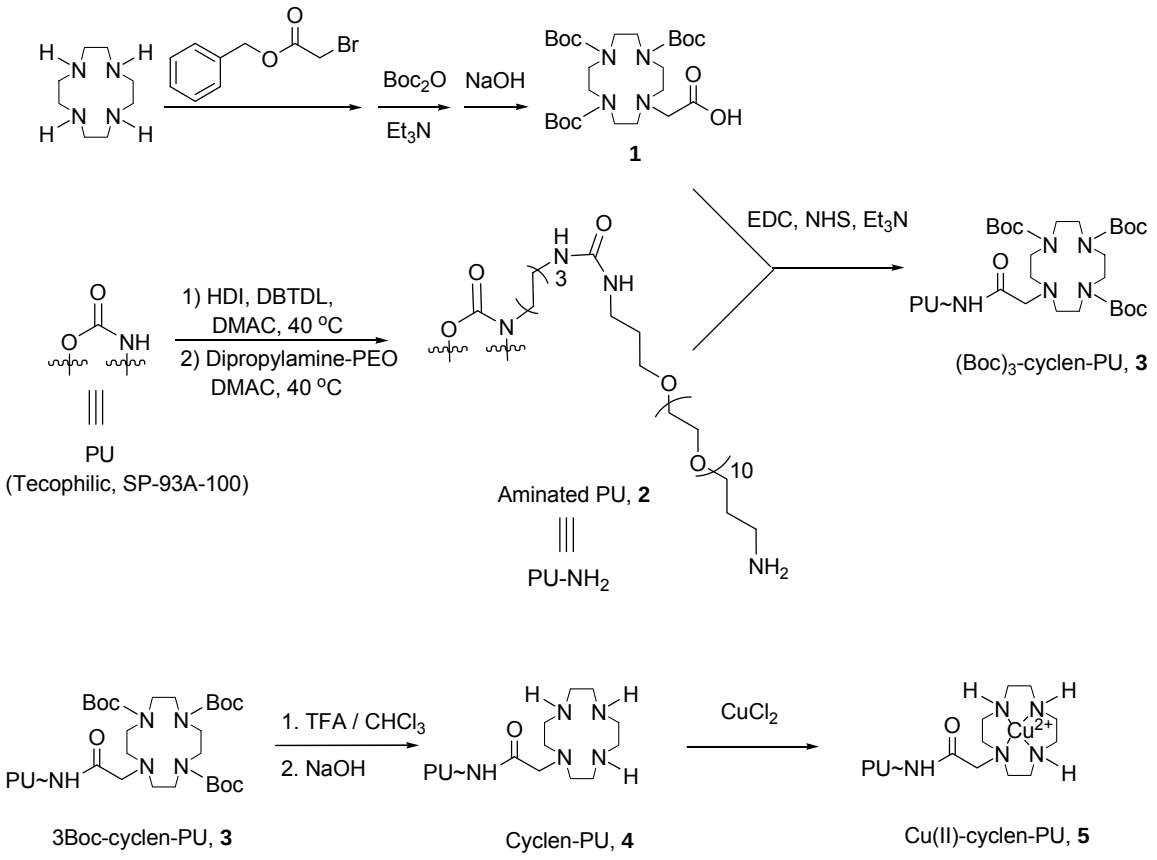

Scheme 3.2 The synthesis of a polyurethane possessing covalently appended Cu(II)-cyclen complex (Cu(II)-cyclen-PU (**5**)) from a modified cyclen derivative (**1**) and aminated PU (**2**) (see **Experimental** for details).

3.2. Experimental

3.2.1. Materials

1,4,7,10-Tetraazacyclododecane (cyclen) was purchased from Strem Chemicals (Newburyport, MA). N-(3-dimethylaminopropyl)-N'-ethylcarbodiimide hydrochloride (EDC), N-hydroxysuccinimide (NHS), glutathione (GSH) and cysteine (CySH) were products of Sigma (St. Louis, MO). Theromplastic polyurethane (Tecophilic, SP-93A-100) was a gift from Lubrizol Advanced Materials, Inc. (formerly Noveon Inc.)

(Cleveland, OH). Dipropylamine-PEO (DPA-400E, F.W.= 573.73) was donated from Tomah products (Milton, WI). Other chemical reagents from Aldrich (Milwaukee, WI), all solvents from Fisher Scientific (Fair Lawn, NJ), and NMR reagents from Cambridge Isotope Laboratories, Inc. (Andover, MA) were used without further purification unless otherwise noted. Distillation was employed for the purification of hexamethylene diisocyanate (HDI), N,N'-dimethyl acetamide (DMAC), triethylamine (Et_3N), acetonitrile (CH_3CN) and tetrahydrofuran (THF) prior to use. DI water was prepared by a Milli-Q filter system (18 MΩ cm^{-1}; Millipore Corp., Billerica, MA, USA).

3.2.2. Measurements

^{1}H and ^{13}C NMR spectra were recorded using either a Varian 400 or 500 MHz spectrometer. High-resolution (HR) mass spectra were obtained on a Waters Autospec Ultima Magnetic Sector mass spectrometer with an electrospray interface. FTIR spectra were collected with a Perkin-Elmer spectrum BX FT-IR system. EPR spectra were taken with a Bruker EMX (Center field, 3300 G; Sweep Width, 2000 G; Frequency, 9.248 GHz). The copper content of the polymers was analyzed by inductively coupled plasma-high resolution mass spectrometry (ICP-HRMS), using a Thermo Finnigan Element. NO generation measurements were made using a Sievers Nitric Oxide Analyzer (NOA), model 280. The current signals of amperometric NO/RSNO sensors were monitored by a microchemical sensor analyzer (Diamond General, Ann Arbor, MI).

3.2.3. Synthesis

*$(Boc)_3$-cyclen-N-acetic acid (**1**)*:

$(Boc)_3$-cyclen-N-acetic acid (**1**) (see **Scheme 3.2**), was synthesized by modifying a reported procedure.[13] In brief, to a stirred solution of cyclen (3.0 g, 17.4 mmol) in

anhydrous CH_3CN (40 mL) was slowly added a solution of benzyl 2-bromoacetate (1.5 mL, 9.2 mmol) in anhydrous CH_3CN (50 mL) over 6.5 h at 85 °C under a nitrogen atmosphere. After additional stirring for 1 h, the mixture was cooled down to RT. Without further purification, an excess amount of Et_3N (10 mL) was poured into the mixture at 0 °C, followed by the addition of di-*tert*-butyl-dicarbonate (Boc_2O, 14.8 g, 65.8 mmol), and then the mixture was stirred overnight at RT. The mixture was then concentrated, and the residue was extracted with Et_2O/water. The separated organic layer was washed with diluted HCl, water, sat'd $NaHCO_3$, and water sequentially. The organic layer was dried with anhydrous Na_2SO_4, filtered, and washed with Et_2O. After the filtrate was concentrated, the crude material was dissolved in MeOH (20 mL) and stirred at RT, and then a solution of 2 N NaOH (10 mL) was dropped into the solution over a 2 h period. The solvent was evaporated under a reduced pressure, and then the residue was extracted with Et_2O/water. The separated water layer was acidified with citric acid to adjust it to between pH 3 – 4. After the extraction with ethyl acetate (EA) 3 times, the combined organic layers were dried with Na_2SO_4, filtered, and washed with EA. After the filtrate was concentrated, the crude product was purified by a column chromatography using silica gel (EA, then MeOH/CH_2Cl_2 = 1/8) to afford the desired product, an amorphous white solid (1.4 g, overall yield = 15%).

^{1}H NMR (500 MHz, $CDCl_3$): δ=3.90 ~ 3.06 (m, 14H; 7 NCH_2), 2.86 (bs, 4H; $(CH_2)NCH_2CO_2$), 1.40 (s, 9H; 3 CH_3), 1.37 (s, 18H; 6 CH_3); ^{13}C NMR (125 MHz, $CDCl_3$): δ=155.92, 155.34, 79.77, 79.43, 53.77, 51.34, 49.68, 47.30, 28.59, 28.39; HRMS(EI): *m*/*z*: $[M + Na]^+$ calcd. for $C_{25}H_{46}N_4O_8Na$, 553.3213, found 553.3207.

*Aminated PU (**2**)*:

A procedure adopted from previous reports[14, 15] was employed to prepare the aminated PU polymer. Thermoplastic PU (Tecophilic, SP-93A-100) was purified by soxhlet extraction with methyl *tert*-butyl ether (MTBE) for 3 d prior to use. A dried PU (20 g, ca. 80 mmole of urethane group) was dissolved in anhydrous DMAC (400 mL). This solution was slowly dropped into a stirred solution of HMDI (39 mL, 241 mmole) and DBTDL (0.72 mL, 1.2 mmole) in DMAC (40 mL) at 40 °C over a 3.5 h period, and then stirred for 1.5 d. The mixture was cooled to RT and slowly added into anhydrous Et_2O (4 L) under a nitrogen atmosphere. The resultant solid was filtered and washed with anhydrous Et_2O (600 mL). After the filter cake was dried by blowing N_2, it was further vacuum dried to give a colorless polymer. This polymer (19.3 g) was again dissolved in anhydrous DMAC (400 mL) and slowly added into a stirred solution of dipropylamine-PEO (15.5 g) in anhydrous DMAC (40 mL) at 40 °C over 3 h. The mixture was stirred for 4 d at 40 °C, and then slowly added into Et_2O (4 L) to form a solid, which was filtered and washed with Et_2O (600 mL). The filter cake was soxhlet extracted with MTBE for 3 d, and then cooled to RT. The remaining polymer was dried under a vacuum pump for 4 d to yield an aminated PU (**2**) (19.4 g, see **Scheme 3.2**). The amount of free amine sites created in the aminated PU (**2**) was analyzed by a colorimetric method to vary depending on the reaction scale and time used (see section 3.2.4). The given method described above afforded ca. 80 μmole of amine sites per one gram of the polymer.

IR (neat) = 3323 cm^{-1} (N-H), 2916, 2857 cm^{-1} (CH_2), 1715 cm^{-1} (C=O), 1614 cm^{-1} (HNCONH), 1529 cm^{-1} (C-N, N-H), 1102 cm^{-1} (CH_2-O-CH_2).

*Cu(II)-cyclen-PU (**5**)*:

EDC (0.4 g, 2.1 mmole), Et_3N (0.8 mL, 5.7 mmole), and NHS (0.26 g, 2.3 mmole) were sequentially added into a stirred solution of $(Boc)_3$-cyclen-N-acetic acid (**1**) (0.8 g, 1.5 mmol), in THF/water (10 mL/10 mL). After 30 min, this mixture was poured into a clear solution of aminated PU (**2**) (19.1 g, ca. 1.53 mmole of amine sites) in THF (500 mL). The reaction mixture was stirred for 5 d at 30 °C, and then concentrated to one-fifth volume under a reduced pressure. The gradual addition of the residue into stirred solvents of DI water/Et_2O (0.25 L/3.75 L) yielded a solid polymer. The polymer was sieved and washed with DI water. The residual polymer was immersed and stirred in Et_2O (1 L) for 1 d at RT. The resulting polymer was filtered and washed with Et_2O, and then dried by a vacuum pump to give a polymer, $(Boc)_3$-cyclen-PU (**3**) (18.5 g, see **Scheme 3.2**).

To remove the Boc groups from the appended cyclen moieties, without further purification, TFA (10 mL) was added into the polymer (17 g) solution in $CHCl_3$ (500 mL) at 0 °C, and the mixture was stirred for 3 d at RT. The reaction mixture was then concentrated using a rotary evaporator and the residue was diluted with $CHCl_3$. The same procedure was repeated 3 times to remove any remaining TFA. The solid polymer formed in Et_2O was filtered and washed with Et_2O. The filtercake was soaked in diluted NaOH (pH ~12) for 6 h at RT, and then filtered and washed with DI water until the pH of the filtrate reached pH 7. The polymer was washed with Et_2O and MTBE and then soxhlet extracted with MTBE for 3 d to afford a slightly yellowish polymer, cyclen-PU (**4**) (16 g, see **Scheme 3.2**), after drying via a vacuum pump.

In order to incorporate Cu(II) into the deprotected cylen-PU, to a stirred solution of cyclen-PU (**4**) (15 g) in THF (500 mL) was added a clear solution of cupric chloride dihydrate (2.9 g) in EtOH (100 mL) at 50 °C. The mixture was stirred overnight and cooled to RT. The solvents of the mixture were evaporated to one-third the original volume under reduced pressure, and then the residue was slowly added into a mixed solvent of EtOH/Et_2O (0.5 L/2 L) to form a green-colored solid polymer. After this polymer was filtered and washed with EtOH/Et_2O (0.5 L/2 L), the filtercake was fully immersed and stirred in EtOH and then filtered and washed with EtOH/Et_2O (0.5 L/2 L). The filtercake was soaked and stirred in DI water for 1 d, and the residual solid was filtered and washed with DI water and MTBE sequentially. Finally, the polymer was purified by soxhlet extraction with MTBE, and dried via a vacuum pump for 3 d to give a slightly blue-tinted polymer, Cu(II)-cyclen-PU, **5** (10 g, see **Scheme 3.2**).

IR (neat) = 3325 cm^{-1} (N-H), 2919, 2863 cm^{-1} (CH_2), 1715 cm^{-1} (C=O), 1530 cm^{-1} (C-N, N-H), 1109 cm^{-1} (CH_2-O-CH_2).

3.2.4. Determination of free amine equivalents in the aminated PU (2)

Amine equivalents in the aminated PU (**2**) were determined by a conventional colorimetric titration. Three different solutions were prepared as follows; i) colorimetric indicator: 0.1 N NaOH solution was slowly dropped into a solution of bromophenol blue (0.1 g) in MeOH (100 mL) until the solution color changed from pale purple to blue; ii) samples: three solutions of aminated PU (**2**) (73.1, 73.6, and 71.6 mg, respectively) dissolved in DMAC (5 mL), and a blank solution having only the solvent; iii) titrating agent: 1.0 mM p-toluenesulfonic acid monohydrate dissolved in isopropanol. Each sample solution (including the blank sample) was diluted with isopropanol (5 mL) and

mixed with one drop of the indicator solution. Finally, this mixture was titrated by a solution of p-toluenesulfonic acid until the color disappeared. The average value of free amine sites in the polymer was obtained after correction for the endpoint of the blank solution.

3.2.5. Measurements of copper content in polymers

To assess the copper content of the various PU-Cu(II)-cyclen polymers, the same method described in Chapter 2 was followed.

3.2.6. NO measurements via a chemiluminescence NO analyzer (NOA)

All NO generation measurements from RSNO species for the new PU-based NOGP were carried out using the NOA via the same methodology presented in Chapter 2.

3.2.7. Pre-conditioning of NOGP by soaking in a GSH/GSNO solution

Prior to soaking, the NO generation flux of a small disk-shaped film of Cu(II)-cyclen-PU (**5**) (r= 3.2 mm, Θ= 65 μm) was determined in presence of 10 μM GSH/GSNO solution dissolved in 2 mL of 10 mM PBS buffer, pH 7.4, containing 3 μM EDTA at RT via the NOA. This film was then fully bathed and shaken under relatively harsh conditions with high concentration of GSH/GSNO (0.1 mM) and low pH solution in 2 mL of PBS buffer, pH 6.6, overnight at RT. The film was removed from the mixture and placed into 10 mL of a fresh PBS buffer, pH 7.4. Then, the same procedure to wash the film was carried out a couple of times using fresh PBS buffer. The resulting film was stored in fresh PBS buffer to ensure that the film was in a hydrated state immediately before use in the NOA experiments. Finally, this film was retested to assess whether this soaking treatment changed the levels of NO generation that could be achieved (compared

to the initial test, before extensive conditioning) using the same test reaction conditions (10 μM GSH/GSNO).

3.2.8. Soaking in sheep plasma

The NO generation from a small disk of the Cu(II)-cyclen-PU (**5**) (r= 2.6 mm, Θ= 30 μm) was also monitored in a solution of 0.5 μM CySH/CySNO in 2 mL of 10 mM PBS buffer, pH 7.4, containing 3 μM EDTA. Simultaneously, several same-sized films were separately immersed in platelet-rich sheep plasma obtained by centrifuging (1300 rpm for 18 min at 4 °C) whole blood from sheep (purchased from Lampire Biological Lab; Pipersville, PA), and then stored at 4 °C. After a given time interval, the typical washing procedure (see section 2.9) was carried out. Then, the NO generation ability of each film was examined under the same reaction conditions (0.5 μM CySH/CySNO) as the film that had not been soaked in sheep plasma.

3.2.9. Fabrication of amperometric NO/RSNO sensors

Each amperometric sensor was constructed in a manner analogous to that reported in Chapter 2. In brief, a platinized Pt working electrode (Pt disk with 250 μm o.d.) sealed in glass wall tubing was surrounded by a coiled Ag/AgCl wire reference/counter electrode, and these two electrodes were integrated behind a PTFE gas-permeable membrane (GPM) treated with 0.5 μL of 1 % Teflon AF solution (Dupont Fluoroproducts, Wilmington, DE).[16] A thermoplastic PU film (Tecophilic®, SP-93A-100) was used as a control layer for one sensor (control sensor with no NO generation) by mounting it on the GPM of a NO sensor using an O-ring. To make the RSNO sensor, a piece of the Cu(II)-cyclen-HPU (**5**) was mounted over the GPM of the NO sensor.

Finally, both sensors were polarized at +0.75 V vs Ag/AgCl for at least 12 h prior to use. All amperometric measurements were performed using the same applied potential.

3.2.10. Amperometric NO detection in blood

The amperometric NO measurements in blood using both the NO and RSNO sensors were carried out using the procedures described in Chpater 2. In these experiments, 70 mL of PBS buffer, pH 7.4, containing 5 μM EDTA and 10 μM GSH was used to dilute 30 mL of whole sheep blood.

3.3. Results and Discussion

3.3.1. Synthesis and characterization

In order to conjugate the Cu(II)-cyclen complex to an existing medical grade hydrophilic thermoplastic PU (Tecophilic, SP-93A-100), the two key precursors, $(Boc)_3$-cyclen-N-acetic acid (**1**) and aminated PU (**2**) were prepared by methods analogous to those reported elsewhere[13-15] (see **scheme 3.2**). Since the strong Cu(II) complexation ability of the cyclen ligand needs to be maintained after covalent linkage to the polymer (without any loss of basicity in the cyclen compound), a carboxylic group was introduced via N-alkylation of the $(Boc)_3$-protected cyclen using 2-bromoacetic acid to yield $(Boc)_3$-cyclen-N-acetic acid (**1**) (see section 3.2.3 for details).

To link this species to the polymer, free amine sites were created in the thermoplastic PU by an isocyanation reaction, followed by amination in dilute conditions to form the aminated PU (**2**). The total amount of free amines in the resultant aminated PU (**2**) was 80 μmole per g of the polymer, as determined by the colorimetric titration

method. It should be noted that the amount of amine sites created in the polymer can be varied by controlling the reaction conditions (i.e., such as scales, reagent equivalents and times) and ranged from 80 – 200 μmole per g. IR spectra of the polymers clearly showed the expected characteristic absorption band patterns as reported elsewhere,[17] in which the newly formed isocyanate and urea bands appeared in the isocyanated PU-intermediate. The isocyanate band disappeared after free amine sites were formed in the final aminated PU (**2**) while the urea group still remained (see **Figure 3.1**).

After the conjugation of $(Boc)_3$-cyclen-N-acetic acid (**1**) with the aminated PU **(2)** using EDC coupling chemistry, the Boc-groups were deprotected with TFA and the mixture was treated with dilute NaOH to remove TFA. Copper ions were then incorporated into the polymer. The extensive washing procedures with various solvents to remove the non-specifically bound copper ions in the polymer backbone ultimately afforded the desired polymer, Cu(II)-cyclen-PU (**5**) (see section 3.2.3 for details).

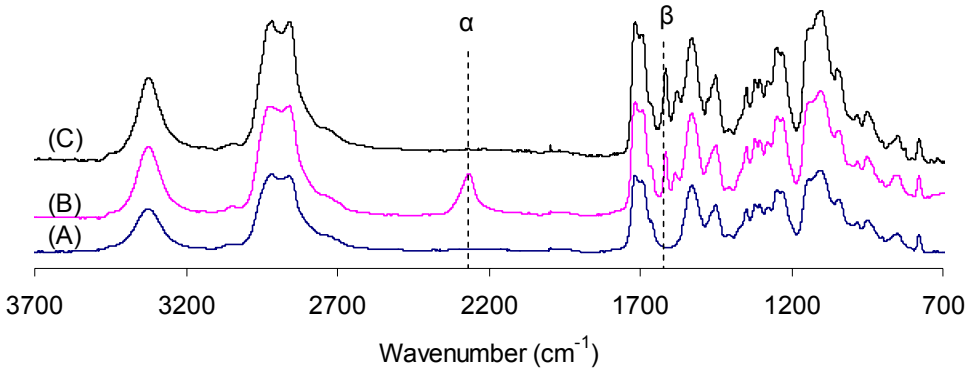

Figure 3.1 IR spectra of (A) thermoplastic PU (Tecophilic, SP-93A-100); (B) isocyanated intermediate; and (C) aminated PU (**2**), where two distinguishable peaks corresponding to the newly formed (α) isocyanate group and (β) urea group appeared in the (B) spectrum, while the (α) peak disappeared in the (C) spectrum; these spectra were recorded for the polymer containing the highest amine sites (200 μmole per g poymer).

Generally, when an aminated polymer (**2**) containing higher free amine sites was employed in the reaction**,** the resulting polymer **5** had higher copper content, as determined by ICP-HRMS, to range from 0.08 to 0.4 wt %, depending on the specific reaction conditions. This low copper content in all polymer **5** formulations suggested that only a very low percentage of cyclen was actually covalently attached to the polymer. Consequently, identifying the cyclen groups within the isolated polymers using NMR or IR was difficult. However, the UV and EPR spectra, as well as the NOA experiments (see below), support the fact that Cu(II)-cyclen complexes are linked to the hydrophilic thermoplastic PU. Indeed, the Cu(II)-cyclen complex is known to have a square pyramidal structure with an absorption band in the region 550–670 nm in the visible region of the spectrum.[18] While the λ_{max} of Cu(II)(cyclen)Cl_2 has been reported to be 594 nm in water,[18] a film of Cu(II)-cyclen-PU (**5**) was found to have an absorption maximum at 617 nm when in a fully hydrated state (see **Figure 3.2**).

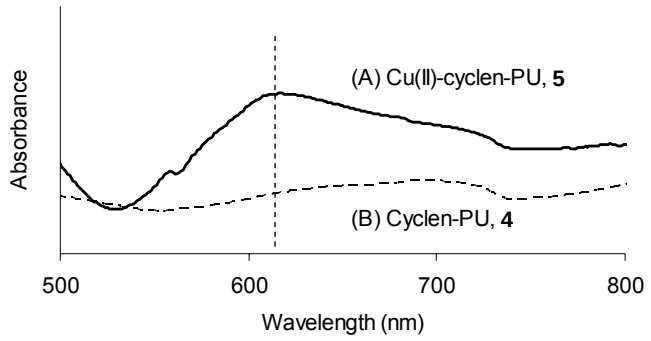

Figure 3.2 UV spectra of two films in fully hydrated states: (A) Cu(II)-cyclen-PU (**5**), and (B) cyclen-PU (**4**); Although the two spectra have a high background absorbance, Cu(II)-cyclen-PU (**5**), shows the higher absorption at λ_{max}= 617 nm.

Such a bathochromic shift in λ_{max} was also observed in the previous study (Chapter 2) where the Cu(II)-cyclen complex was covalently attached within a crosslinked poly(2-hydroxyethyl methacrylate) (pHEMA) film. This change of UV-Vis absorption may be influenced by the surrounding polymer matrix, a possible structural distortion of the Cu(II)-cyclen complex in the polymer matrix, as well as the substitution of chloride ion for hydroxide ion as a ligand for the Cu(II)-cyclen-PU (**5**) during the preparation process. Nonetheless, the EPR spectrum of Cu(II)-cyclen-PU (**5**) was quite similar to that of the small molecule Cu(II)-cyclen complex (see **Figure 3.3)**, suggesting successful copper ion complexation with the cyclen moieties appended to the polymer. Again, any non-specifically bound copper ions within the polymer backbone are not likely to yield a significant contribution to the NO generating ability of the new polymer, and this was indirectly proven by subsequent NOA experiments using a blank film (copper ion-treated $(Boc)_3$-cyclen-PU (**4**) ; see below).

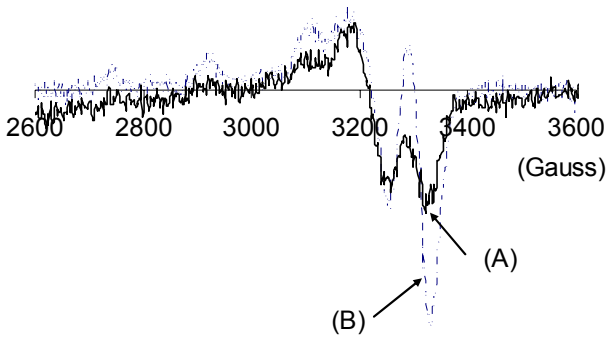

Figure 3.3 EPR spectra of (A) the polymer of Cu(II)-cyclen-PU (**5**), and (B) the solution of Cu(II)-cyclen complex, both in PBS buffer, pH, 7.4, at 77K: Center field, 3300 G; Sweep Width, 2000 G; Frequency, 9.248 GHz.

3.3.2. Catalytic NO generation from S-nitrosothiols via Cu(II)-cyclen-PU (5)

The estimated NO flux of healthy endothelium cells that line in all blood vessels is approximately 10^{-10} mole/cm^2·min. In fact, only a very low concentration of NO (< 1 nM) is known to be effective in reducing thrombus formation on the surface of a foreign material.[19-22] Endogenous RSNOs are known to exist in blood in the range of nM to μM levels, although their exact concentrations are still in question.[23, 24] Low molecular weight (LMW) endogenous RSHs such as CySH and GSH are also present at 10 – 30 μM concentrations in human plasma.[24] Therefore, even a small fractional decomposition of endogenous RSNOs to locally produce the biologically relevant NO levels at the polymer/blood boundary should be effective to improve a polymer's hemocompatibility.

Indeed, a small piece of PU material containing a low percentage of the Cu(II)-cyclen complex (Cu(II)-cyclen-PU, **5**) was able to catalytically produce a biological relevant NO flux in the presence of μM concentrations of RSNO/RSH at physiological pH (see **Figure 3.4**). The amount of NO produced from a given reaction solution by the Cu(II)-cyclen-PU (**5**) was continuously monitored by the NOA. First, a small disk shaped polymer film of **5** (radius= 2.5 mm, thickness= 30 μm, copper content= 13 nmole (0.14 wt %)) was placed into a solution of 10 μM GSNO/GSH in 2 mL of a phosphate buffered saline (PBS), pH 7.4, containing 3 μM EDTA. A burst of NO signal was initially detected (see **Figure 3.4**) and then the NO flux slowly decreased to reach a steady-state NO level (approximately 1 x 10^{-10} mole/cm^2.min). When the film was removed from the solution, the NO signal returned to the original baseline, implying that the presence of this polymer initiated the NO liberation from GSNO. The continual insertion/removal of the film demonstrated that the polymer could generate a comparable

steady-state NO flux after each immersion and removal from the test solution (see **Figure 3.4(A)**). The same film **5** was also tested in a solution of 0.5 μM CySNO/CySH in PBS buffer. Upon addition of the film into the reaction solution, the NO signal increased to reach given NO flux (approximately 1 x 10^{-10} mole/cm^2.min), and then gradually decreased to the baseline until all CysNO was completely consumed (see **Figure 3.4(B)**).

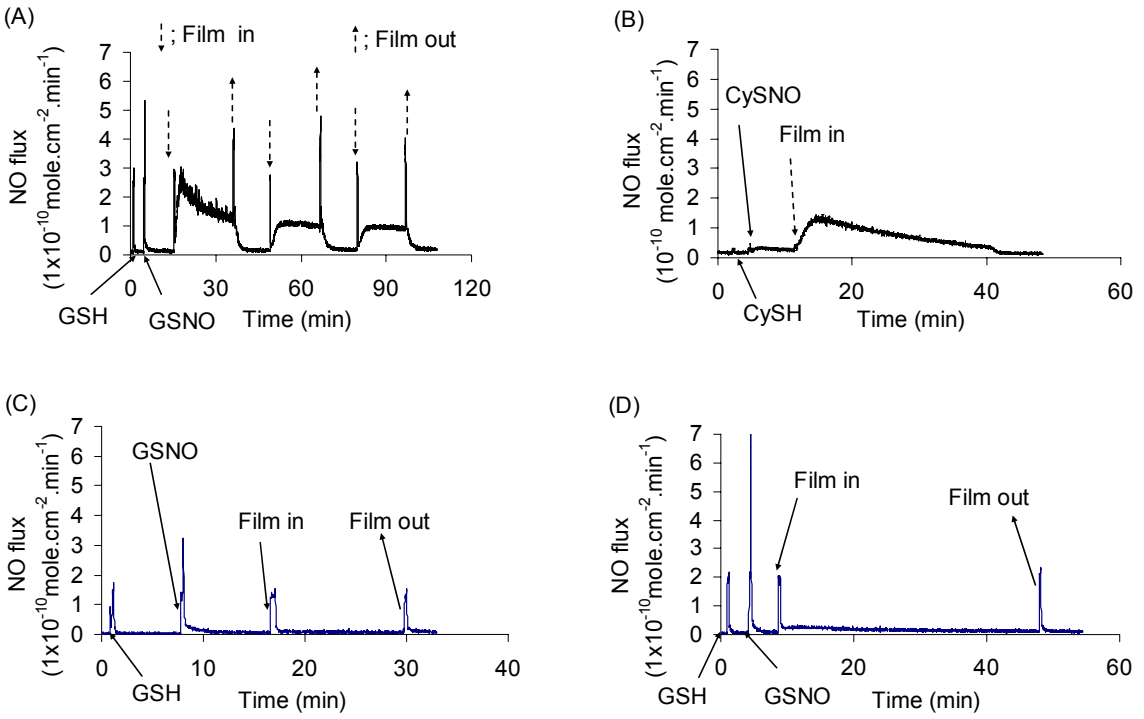

Figure 3.4 The NOA measurement of catalytic NO production by a small disk film of Cu(II)-cyclen-PU (**5**) (radius= 2.6 mm, thickness= 30 μm, W_d (weight at a dried state) = 0.6 mg, Cu content= 0.15 wt %), in the solution of (A) 10 μM GSNO/GSH, and (B) 0.5 μM CySNO/CySH in PBS buffer, pH 7.4, containing 3 μM EDTA; a similar sized film of (C) cyclen-PU (**4**) and (D) copper ion-treated 3Boc-cyclen-PU (**3**) in 10 μM GSNO/GSH solution in PBS buffer, pH 7.4, containing 3 μM EDTA; Arrows indicate the moment when a given species is added or removed.

To demonstrate that copper ions are the key active species to denitrosate the RSNO species, as a control experiment, a similar sized film of cyclen-PU (**4**) that was not treated with copper ions was tested for its NO generation ability. When this blank film

was soaked in a solution of 20 μM GSNO/GSH in the PBS buffer, the NO baseline was slightly increased and soon decreased to essentially the original baseline (see **Figure 3.4(C)**). To prove whether free copper ion can non-specifically bind to the polymeric backbone, a same sized film of 3-Boc-cyclen-PU (**3**), which was treated with copper ions by the same method employed to prepare the polymer **5,** was immersed into the 20 μM GSNO/GSH solution. Similar to the previous control film, the baseline was initially elevated, but then quickly returned to the original baseline (see **Figure 3.4(D)**). Therefore, this data supports the fact that the copper ions complexed with the cyclen moieties in Cu(II)-cyclen-PU are responsible for the NO generation observed with this polymeric material.

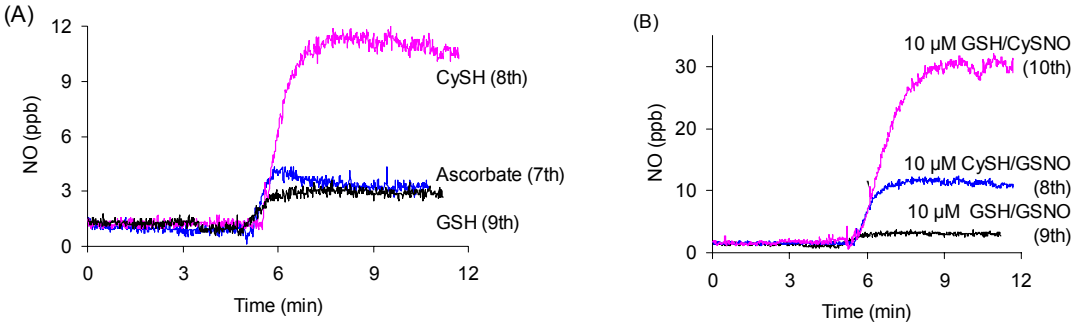

Figure 3.5 Substrate dependency on the NO generation from the same film (Cu(II)-cyclen-PU (**5**)) used in the experiments as shown **Figure 3.4**, where the parenthesis in the graph indicates the number of times when the same polymer film was sequentially used; (A) reducing agent dependency (10 μM) at a 10 μM GSNO solution, (B) RSH/RSNO variation with both at 10 μM concentrations in the PBS buffer.

Ascorbate has previously been identified as a good reducing agent for the copper ion-mediated RSNO decomposition.[25] As shown in **Figure 3.5(A)** the reducing ability of ascorbate using this NOGP (Cu(II)-cyclen-PU (**5**)**)** is clearly observed to be equivalent to GSH. When the different species at equal concentrations were tested as the reducing

agent for NO generation by polymer **5**, the highest NO flux was achieved in the presence of CySH. In addition, the reaction of CySNO with this NOGP was greater than GSNO at the same concentration of GSH and/or CysH (GSNO/GSH < GSNO/CySH < CySNO/GSH, see **Figure 3.5 (B)**). This confirms why the lower concentration of CyNO/CySH (0.5 μM) could achieve a similar NO flux as higher concentrations of GSNO/GSH (10 μM) (see **Figure 3.4 (A) and (B))**. Thus, CySNO and CySH are apparently better substrates for the new NOGP in terms of catalytic NO generation efficiency.

3.3.3. Copper leaching studies

Ideally, a useful NOGP must be designed to generate NO for long periods of time once implanted. To achieve this goal, the catalytic NO generation activity of the Cu(II)-cyclen-PU should be maintained under the physiological conditions for an extended period of time. The stability of Cu(II)-cyclen complex within the polymer is the primary concern in this type of NOGP because any blood components such as free thiols and proteins that have high binding affinities with copper ions may facilitate demetalation and/or deactivation of the complex. For example, low molecular weight endogenous RSHs as well as their oxidized forms (disulfides, RSSRs) are known to bind tightly with copper ions.[26, 27] In fact, the previous work presented in Chapter 2 proposed that free thiols such as GSH can influence the copper ion leaching from the Cu(II)-cyclen complex immobilized in the crosslinked poly(2-hydroxyethyl methacrylate), but does not deactivate the copper sites of Cu(II)-cyclen complex in the polymer.

Although the new NOGP developed here (Cu(II)-cyclen-PU (**5**)) has a different polymer matrix, thermoplastic PU, the potential leaching of copper ion from the polymer

remains. Thus, this possibility has been examined using the same metholology described in Chapter 2. First, the film of Cu(II)-cyclen-PU was repeatedly tested for its NO generation using the RSH/RSNO solutions under typical test conditions, showing that the maximum steady-state NO level was continuously decreased with every trial until it reached a certain NO level after 12 sequential uses (ca. 50 % reduction compared to the original NO flux (see **Figure 3.6(A)**). Further experiments examined whether the Cu(II)-cyclen-PU polymer was still able to liberate NO from GSNO even after soaking in harsher conditions. For example, a new piece of polymer **5** was fully bathed and shaken in a high concentration of GSH/GSNO solution (0.1 mM) and a low pH (pH= 6.6) overnight at RT (see section 3.2.7 for details), conditions that are expected to accelerate the demetalation and/or deactivation reactions. However, after such soaking and subsequent washing, the polymer is still able to generate NO from GSNO, albeit at a reduced flux (see **Figure 3.6(B)**). Taken together, the demetalation of Cu(II)-cyclen-PU, **5,** may occur under physiological conditions; however, the deactivation of the new NOGP caused by the strong coordination of small molecular RSH and/or RSSR species onto the metal center may not be a serious issue.

To evaluate how the NO generation profiles of the Cu(II)-cyclen-PU in a given RSNO/RSH solution can be changed before and after contact with sheep plasma for a finite time period, the same sized films of Cu(II)-cyclen-PU were separately immersed into the platelet-rich sheep plasma for a given time interval at 4 °C. Then, the NO production profiles mediated by these films from CySNO/CySH solution were measured by the NOA (see section 3.2.8 for details). The NO generation by these test films exhibited very similar behavior regardless of the exposure time to sheep plasma (see

Figure 3.6(C)). This result suggests that the blood components do not have a significant influence on copper ion leaching and/or deactivation of the Cu(II)-cyclen sites in polymer **5**.

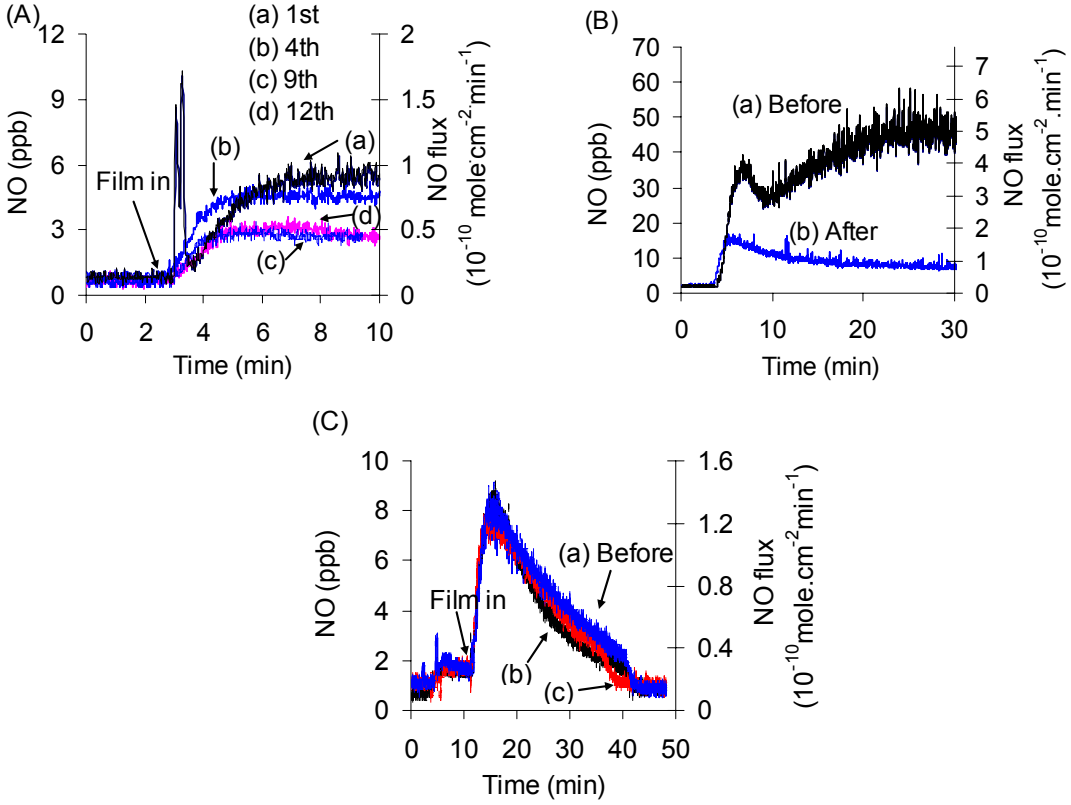

Figure 3.6 (A) A disk type of film (Cu(II)-cyclen-PU (**5**) radius= 2.6 mm, thickness= 30 μm, W_d= 0.6 mg, Cu content= 0.15 wt %) was continuously used with various substrates, where the parenthesis in the graph indicates the number of times the polymer film was sequentially used, then its NO flux at a steady-state was monitored in a solution of 10 μM GSNO/GSH in PBS buffer, pH 7.4, containing 3 μM EDTA; (B) a new film (Cu(II)-cyclen-PU (**5**) radius= 3.2 mm, thickness= 65 μm, Cu content= 0.4 wt %)-mediated NO generation was compared in the same reaction condition (10 μM GSNO/GSH in the PBS buffer) before (a) and after (b) this film was soaked in the solution of 0.1 mM GSNO/GSH in PBS buffer, pH 6.6; (C) The comparisons of new films of Cu(II)-cyclen-PU (**5**) (radius= 2.6 mm, thickness= 30 μm, Wd= 0.6 mg, Cu content= 0.15 wt %) for the NO generation profiles in a solution of 0.5 μM CySNO/CySH in the PBS buffer before (a) and after soaked in a platelet-rich sheep plasma at 4 °C for 1 d (b) and 3 d (c); all NO measurements were monitored via the NOA.

The various soaking experimental results carried out here with polymer **5** are consistent with the prior study (Chapter 2) where Cu(II)-cyclen was appended to pHEMA, and indicates that the demetalation and/or deactivation of the Cu(II)-cyclen complex in the polymeric matrix by various blood components may not be a serious concern, although LMW endogenous RSH and/or RSSR species likely can affect the rate of copper ion demetalation in this new polymer. More intensive *in vivo* studies for the various time periods are required to fully assess whether copper leaching from the new NOGP (Cu(II)-cyclen-PU, **5**) will be a problem for practical biomedical applications of this new material.

3.3.4. Spontaneous nitric oxide generation by polymer 5 when in contact with fresh blood

To further assess the potential biomedical utility of new Cu(II)-cyclen-PU, it is essential to prove that the polymer can generate NO in the presence of fresh whole blood. One experimental strategy to demonstrate this NO generation is to measure the additional NO levels produced by the Cu(II)-cyclen-PU in blood when a polymer film of this material is coated over the distal end of an amperometric NO sensor. This approach was utilized in Chapter 2 to prove that the Cu(II)-cyclen-pHEMA material can generate NO in fresh blood. In brief, two sensors need to be constructed for this experiment. One is a control NO sensor where a thin film of the bare thermoplastic PU (Tecophilic, SP-93A-100) is used as an outer membrane of the electrochemical NO selective sensor. The other sensor is an RSNO sensor where a similar sized film of Cu(II)-cyclen-PU (**5**) is employed as an outer membrane of the NO sensor (see section 3.2.9 for details). Prior to

experiments, the inherent amperometric responses of both sensors toward NO are determined using pure NO gas standard solution (see **Figure 3.7**).

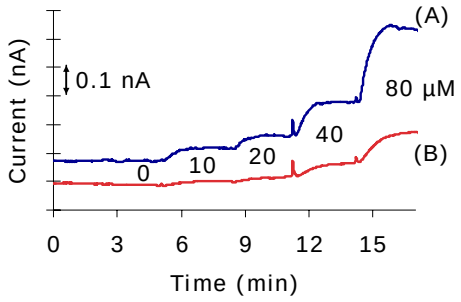

Figure 3.7 The calibration curves of both sensors ((A) NO and (B) RSNO) were plotted for their intrinsic direct amperometric responses to NO upon the addition of standard NO solution into 100 mL of 10 mM PBS buffer, pH 7.4, at 36 ^{o}C; the numbers in the graph indicate the accumulated NO concentrations after aliquots of the stock NO solution was added.

Two sensors were simultaneously placed into the fresh sheep whole blood diluted with the PBS buffer at 36 °C, and their amperometric responses (see section 3.2.10) were recorded. While the control NO sensor showed a small background signal in the fresh whole blood, the RSNO sensor exhibited a significantly higher NO signal (see **Fig. 3.8**), indicating that the Cu(II)-cyclen-PU rendered the NO levels locally elevated at the membrane phase by contact with the fresh blood. As the experiment continued, the addition of a standard GSNO solution into the same fresh blood sample clearly confirmed that the RSNO sensor (with the Cu(II)-cyclen-PU polymer on the surface) responded to the exogenous RSNO while the NO sensor did not (see **Figure 3.8**). Consequently, *in situ* NO generation in the fresh sheep whole blood by the Cu(II)-cyclen complex tethered PU (Cu(II)-cyclen-PU) was successfully demonstrated via these amperometric RSNO sensor measurements.

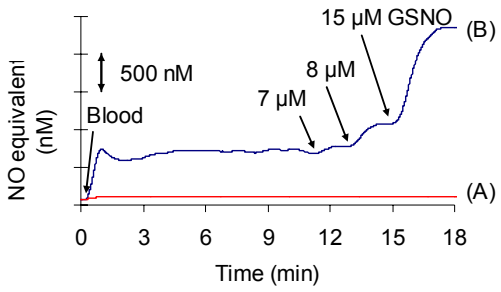

Figure 3.8 The direct detection of endogenous RSNOs in fresh sheep blood using the amperometric (A) NO sensor and (B) RSNO sensor by injecting 30 mL of fresh sheep blood into 70 mL of 10 mM PBS buffer, pH 7.4, at 36 ˚C; the intrinsic amperometric responses of two sensors toward the exogenous RSNO were demonstrated by adding the GSNO solution into the same blood sample; arrows indicate when a given species was added.

3.4. Conclusions

In summary, a biomedical grade thermoplastic PU (Tecophilic, SP-93A-100) has been utilized as a polymeric matrix to prepare an NOGP by covalently linking a Cu(II)-cyclen complex to the backbone. A combination of typical synthetic procedures, including the modification of a small molecule and a polymer, the chemistry of protection, coupling, and deprotection, as well as copper ion complexation were applied to the synthesis of Cu(II)-cyclen-PU (**5**)(see **Scheme 3.2**). The copper content was measured via ICP-HRMS to be a relatively low concentration, ranging from 0.08 to 0.4 wt %, that can be varied by the reaction conditions. The new NOGP (Cu(II)-cyclen-PU (**5**)) exhibited the catalytic denitrosation of LMW RSNOs in the presence of LMW RSHs or ascorbate at physiological pH, while two control films (cyclen-PU (**4)** and the copper treated $(Boc)_3$-cyclen-PU (**3**)) did not yield any significant NO generation in the same test

solutions of RSNOs/RSHs. In addition, the potential demetalation and/or deactivation of the Cu(II)-cyclen-PU was evaluated by various soaking experiments using excess amounts of GSNO/GSH or the platelet-rich sheep plasma, and results indicate that the presence of blood components do not significantly influence the demetalation and/or deactivation of this NOGP, although high levels of LMW endogenous RSHs and/or RSSRs are likely to accelerate the copper ion leaching from the polymeric film. Most importantly, it was shown that the new Cu(II)-cyclen-PU material can generate significant levels of NO when in contact with fresh animal whole blood, as determined via use of the polymer to construct an amperometric RSNO sensor. Hence, this new polymer is a potential candidate for *in vivo* animal testing as a coating material for a wide range of blood contacting biomedical devices.

3.5. References

1. Zdrahala, R. J.; Zdrahala, I. J., Biomedical applications of polyurethanes: A review of past promises, present realities, and a vibrant future. *Journal of Biomaterials Applications* **1999,** 14, (1), 67-90.
2. Gunatillake, P. A.; Martin, D. J.; Meijs, G. F.; McCarthy, S. J.; Adhikari, R., Designing biostable polyurethane elastomers for biomedical implants. *Australian Journal of Chemistry* **2003,** 56, (6), 545-557.
3. Francois, P.; Vaudaux, P.; Nurdin, N.; Mathieu, H. J.; Descouts, P.; Lew, D. P., Physical and biological effects of a surface coating procedure on polyurethane catheters. *Biomaterials* **1996,** 17, (7), 667-678.
4. Ajili, S. H.; Ebrahimi, N. G.; Khorasani, M. T., Study on thermoplastic polyurethane/polypropylene (TPU/PP) blend as a blood bag material. *Journal of Applied Polymer Science* **2003,** 89, (9), 2496-2501.
5. Xue, L.; Greisler, H. P., Biomaterials in the development and future of vascular grafts. *Journal of Vascular Surgery* **2003,** 37, (2), 472-480.
6. D'arrigo, P.; Giordano, C.; Macchi, P.; Malpezzi, L.; Pedrocchi-Fantoni, G.; Servi, S., Synthesis, platelet adhesion and cytotoxicity studies of new glycerophosphoryl-containing polyurethanes. *International Journal of Artificial Organs* **2007,** 30, (2), 133-143.
7. Korematsu, A.; Li, Y. J.; Murakami, T.; Sakurai, I.; Kodama, M.; Nakaya, T., Synthesis, characterization and blood compatibilities of novel segmented polyurethanes containing poly(butadiene) soft segments and phosphatidylcholine analogues in the main chains and long-chain alkyl groups in the side chains. *Journal of Materials Chemistry* **1999,** 9, (3), 647-653.
8. Chen, K. Y.; Kuo, J. F.; Chen, C. Y., Synthesis, characterization and platelet adhesion studies of novel ion-containing aliphatic polyurethanes. *Biomaterials* **2000,** 21, (2), 161-171.
9. Krejcy, K.; Schmetterer, L.; Kastner, J.; Nieszpaurlos, M.; Monitzer, B.; Schutz, W.; Eichler, H. G.; Kyrle, P. A., Role of nitric-oxide in hemostatic system activation in-vivo in humans. *Arteriosclerosis Thrombosis and Vascular Biology* **1995,** 15, (11), 2063-2067.
10. Salvemini, D.; Masini, E.; Anggard, E.; Mannaioni, P. F.; Vane, J., Synthesis of a nitric oxide-like factor from L-arginine by rat serosal mast-cells - Stimulation of guanylate-cyclase and inhibition of platelet-aggregation. *Biochemical and Biophysical Research Communications* **1990,** 169, (2), 596-601.
11. Samama, C. M.; Diaby, M.; Fellahi, J. L.; Mdhafar, A.; Eyraud, D.; Arock, M.; Guillosson, J. J.; Coriat, P.; Rouby, J. J., Inhibition of platelet-aggregation by inhaled nitric-oxide in patients with acute respiratory-distress syndrome. *Anesthesiology* **1995,** 83, (1), 56-65.
12. Sarkar, R.; Webb, R. C., Does nitric oxide regulate smooth muscle proliferation? A critical appraisal. *Journal of Vascular Research* **1998,** 35, (3), 135-142.
13. Jeon, J. W.; Son, S. J.; Yoo, C. E.; Hong, I. S.; Song, J. B.; Suh, J., Protein-cleaving catalyst selective for protein substrate. *Organic Letters* **2002,** 4, (23), 4155-4158.

14. Park, K. D.; Okano, T.; Nojiri, C.; Kim, S. W., Heparin immobilization onto segmented polyurethaneurea surfaces - effect of hydrophilic spacers. *Journal of Biomedical Materials Research* **1988,** 22, (11), 977-992.
15. Archambault, J. G.; Brash, J. L., Protein resistant polyurethane surfaces by chemical grafting of PEO: amino-terminated PEO as grafting reagent. *Colloids and Surfaces B-Biointerfaces* **2004,** 39, (1-2), 9-16.
16. Cha, W.; Meyerhoff, M. E., Enhancing the selectivity of amperometric nitric oxide sensor over ammonia and nitrite by modifying gas-permeable membrane with Teflon AF (R). *Chemia Analityczna* **2006,** 51, (6), 949-961.
17. Zhou, Z. R.; Meyerhoff, M. E., Preparation and characterization of polymeric coatings with combined nitric oxide release and immobilized active heparin. *Biomaterials* **2005,** 26, (33), 6506-6517.
18. Styka, M. C.; Smierciak, R. C.; Blinn, E. L.; Desimone, R. E.; Passariello, J. V., Copper(II) complexes containing a 12-membered macrocyclic ligand. *Inorganic Chemistry* **1978,** 17, (1), 82-86.
19. Siney, L.; Lewis, M. J., Endothelium-derived relaxing factor inhibits platelet-adhesion to cultured porcine endocardial endothelium. *European Journal of Pharmacology* **1992,** 229, (2-3), 223-226.
20. Radomski, M. W.; Palmer, R. M. J.; Moncada, S., The anti-aggregating properties of vascular endothelium - interactions between prostacyclin and nitric-oxide. *British Journal of Pharmacology* **1987,** 92, (3), 639-646.
21. Radomski, M. W.; Palmer, R. M. J.; Moncada, S., The role of nitric-oxide and cGMP in platelet-adhesion to vascular endothelium. *Biochemical and Biophysical Research Communications* **1987,** 148, (3), 1482-1489.
22. Sneddon, J. M.; Vane, J. R., Endothelium-derived relaxing factor reduces platelet-adhesion to bovine endothelial-cells. *Proceedings of the National Academy of Sciences of the United States of America* **1988,** 85, (8), 2800-2804.
23. Rassaf, T.; Bryan, N. S.; Kelm, M.; Feelisch, M., Concomitant presence of N-nitroso and S-nitroso proteins in human plasma. *Free Radical Biology and Medicine* **2002,** 33, (11), 1590-1596.
24. Kelm, M., Nitric oxide metabolism and breakdown. *Biochimica et Biophysica Acta* **1999,** 1411, (2-3), 273-289.
25. Oh, B. K.; Meyerhoff, M. E., Catalytic generation of nitric oxide from nitrite at the interface of polymeric films doped with lipophilic Cu(Il)-complex: a potential route to the preparation of thromboresistant coatings. *Biomaterials* **2004,** 25, (2), 283-293.
26. Baek, H. K.; Cooper, R. L.; Holwerda, R. A., Stability of the Cu(II)-S bond in mercapto amino-acid complexes of [2,2',2''-tris(dimethylamino)triethylamine]copper(II) and [tris(2-pyridylmethyl)amine]copper(II). *Inorganic Chemistry* **1985,** 24, (7), 1077-1081.
27. Gilbert, B. C.; Silvester, S.; Walton, P. H., Spectroscopic, kinetic and mechanistic studies of the influence of ligand and substrate concentration on the activation by peroxides of Cu-I-thiolate and other Cu-I complexes. *Journal of the Chemical Society-Perkin Transactions 2* **1999**, (6), 1115-1121.

CHAPTER 4

Organoditelluride-Mediated Catalytic S-Nitrosothiol Decomposition to Nitric Oxide

4.1. Introduction

Hou et al. first reported the organodiselenide (RSeSeR)-mediated catalytic decomposition of S-nitrosothiols (RSNOs) to nitric oxide (NO) in the presence of free thiols (RSHs) as a reducing agent.[1] More recently Meyerhoff and co-workers have applied this chemistry to polymeric materials in order to develop a new type of nitric oxide generating polymer (NOGP), and successfully demonstrated that catalytic activity comparable to solution phase is possible using organodiselenide linked polymers. Although the mechanism of organodiselenide-mediated RSNO decomposition remains unclear, it has been suggested that seleno-sulfide (RSeSR) is a key intermediate, and organoselenolate (RSe^-) is the active reducing species that reacts and liberates NO from RSNOs[1-3] via the proposed oxidized form of the catalyst (RSeNO).[4] This suggests that the redox chemistry of organoselenium species plays a key role in the catalytic cycle.

The redox chemistry of organoditellurides (RTeTeR) has been reported to be analogous to that of RSeSeR. For example, both RSeSeR[5, 6] and RTeTeR[7-9] have shown thiol peroxidase activity as a glutathione peroxidase (GPx) mimic (see **Figure 4.1** for the proposed mechanism of RTeTeR-mediated thiol peroxidase activity[8]), which catalytically

reduces organic peroxides (ROOH) to the corresponding alcohols (ROH) by the oxidation of reduced glutathione (GSH) to glutathione disulfide (GSSG). In this reaction, chalcogeno-sulfide (RSeSR or RTeSR) and chalcogenic acid (RSeOH or RTeOH) are the main intermediates, while chalcogenols (RSeH or RTeH) are the active reducing species.

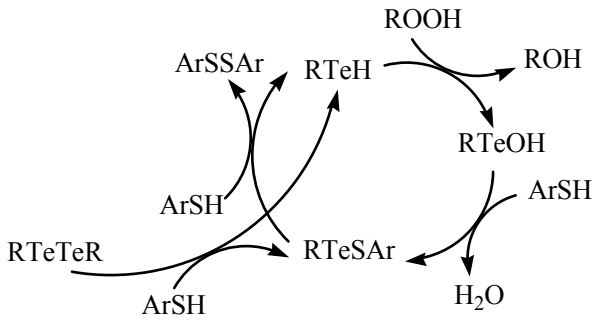

Figure 4.1 The proposed mechanism for thiol peroxidase acivity (glutathione peroxidase mimic) of organoditelluride (RTeTeR).[8]

When comparing the RSeSeR-mediated catalytic RSNO denitrosation with the RSeSeR (or RTeTeR)-mediated thiol peroxidase activity, the redox chemistry is quite analogous where the catalyst (RSeSeR), the reducing agent (RSH), the key intermediate (RSeSR), and the active reduced form of the catalyst (RSeH) are all equivalent in function. Additionally, the oxidized substrates used (RSNO or H_2O_2) are similar; hence, the oxidized form of the catalyst is proposed to be $RSeNO^4$ or RSeOH.[5, 6] This coincidence strongly supports the idea that RTeTeR is expected to catalyze the NO liberation from RSNOs as well. In this chapter, this possibility will be evaluated by studying the reaction of RSNOs with a newly synthesized RTeTeR species.

Herein, is reported the synthesis of 5,5'-ditelluro-2,2'-dithiophenecarboxylic acid **1** (see **Scheme 4.1**), and it is demonstrated that this compound catalyzes RSNO decomposition to NO in the presence of endogenous reducing agents such as glutathione

(GSH) or cysteine (CySH) at physiological pH. Based on the various studies and the known chemistry of RTeTeR, the mechanism of RTeTeR-mediated catalytic RSNOs decomposition to NO is also proposed (see **Figure 4.2**).

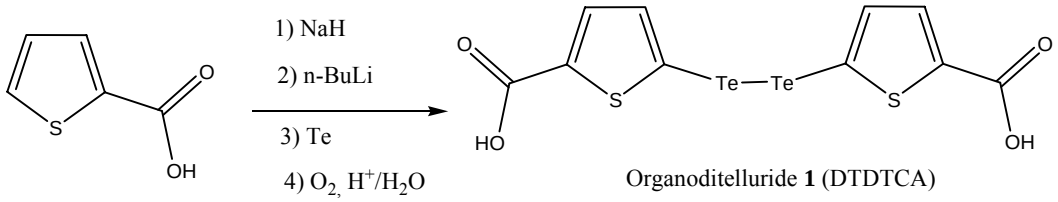

Scheme 4.1 The synthetic scheme of organoditelluride (**1**), 5,5'-ditelluro-2,2'-dithiophenecarboxylic acid (DTDTCA) using 2-thiophene carboxylic acid.

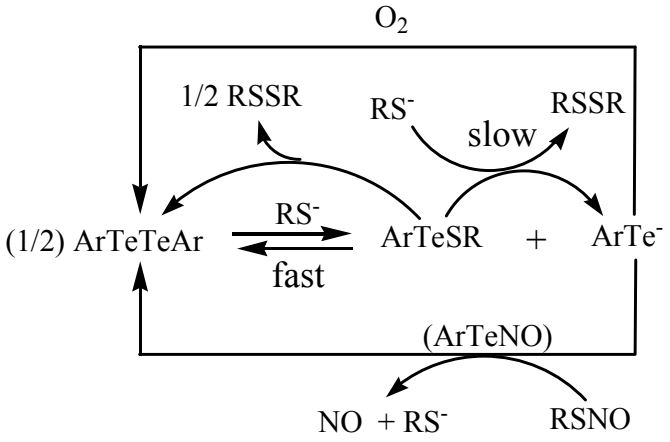

Figure 4.2 The proposed mechanism for organoditelluride-mediated catalytic RSNO decomposition to NO (ArTeTeAr, organoditelluride; RS^-, thiolate; ArTeSR, tellurosulfide; $ArTe^-$, tellurolate; RSSR, disulfide; RSNO, S-nitrosothiol; ArTeNO, nitrosotellurol; NO, nitric oxide; O_2, oxygen).

It is expected that this research can expand the redox chemistry of organotellurium, and further provide a new type of NO generating catalyst that can be widely applied to a variety of biomedical areas such as RSNO sensors,[14] anti-cancer agents,[17] and medical devices.[16]

4.2. Experimental

4.2.1. Materials

Glutathione (GSH) and cysteine (CySH) were products of Sigma (St. Louis, MO). Other reagents from Aldrich, solvents from Fisher Scientific, and NMR reagents from Cambridge Isotope Laboratories, Inc. (Andover, MA) were used without further purification unless otherwise noted. Distillation was employed for the purification of THF prior to use. DI water was prepared by a Milli-Q filter system (18 MΩ cm^{-1}: Millipore Corp., Billerica, MA, USA).

4.2.2. Measurements

^{1}H and ^{13}C NMR spectra were obtained on a Varian 400 or 500 MHz spectrometer. High-resolution (HR) mass spectra were recorded using a Waters Autospec Ultima Magnetic Sector mass spectrometer with an electrospray interface. FTIR spectra were collected with a Perkin-Elmer spectrum BX FT-IR system. UV spectra were recorded by a Perkin-Elmer Lambda 35 UV/VIS spectrometer. Tellurium content of the polymers was measured by inductively coupled plasma emission-mass spectrometry (ICP-MS). Melting points were determined by Mel-Tempo® Laboratory Devices Inc. (USA). All NO measurements were made using a Sievers nitric oxide analyzer (NOA), model 280, and the instrument was calibrated as reported in Chapter 2.

4.2.3. Synthesis of 5,5'-ditelluro-2,2'-dithiophenecarboxylic acid (DTDTCA, organoditelluride 1)

To a stirred solution of 2-thiophencarboxylic acid (2.0 g, 15.6 mmol) in THF (200 mL) was added NaH (95 %, 0.66 g, 15.7 mmol) at 0 °C. After 10 min, n-BuLi (2.5 M solution in hexanes, 6.3 mL, 15.7 mmol) was slowly dropped into the above solution and

stirred for 10 min. The reaction mixture was warmed to RT and stirred for 50 min. Tellurium (1.9 g, 14.9 mmol) was quickly added into the reaction mixture under a strong stream of nitrogen. After stirring for 2 h, the mixture was concentrated under reduced pressure to yield about 20 mL of reddish brown slurry. The slurry was poured into a solution of DI water (300 mL) and CH_2Cl_2 (200 mL) at 0 °C while adjusting the pH of solution to approx. 1 using 1.5 N HCl. The entire mixture was vigorously mixed by blowing air through it at 0 °C. The mixture was filtered to remove an undissolved solid and the filter cake was washed with CH_2Cl_2. The separated water layer was extracted 2 times more with CH_2Cl_2. The combined organic layers were dried with anhydrous Na_2SO_4, filtered and washed with CH_2Cl_2. The filtrate was concentrated to give a dark reddish solid under a reduced pressure. The crude residue was triturated with CH_2Cl_2 (50 mL), then filtered and washed with CH_2Cl_2 to give a reddish brown solid (0.93 g, 25 % yield).

Decomposition temperature 168 - 172 °C; ^{1}H NMR (500 MHz, DMSO-d_6, 25 °C): δ=13.17 (bs, 2H; 2 COOH), 7.54 (d, J= 4.5 Hz, 2H; 2 CCH), 7.43 (d, J= 4.5 Hz, 2H; 2 TeCCH); ^{13}C NMR (125 MHz, DMSO-d_6, 25 °C): δ=162.28, 142.13, 140.12, 134.53, 106.19.; ^{125}Te NMR (MHz, DMSO-d_6, 25 °C): δ=497.60; IR (KBr)= 3426 cm^{-1} (COO-H), 2959, 2554 cm^{-1} (=C-H), 1667 cm^{-1} (C=O), 1516 cm^{-1} (C=C), 1422 cm^{-1} (=C-H); HRMS(EI): *m*/*z*: $[M]^+$ calcd. for $C_{10}H_6O_4S_2Te_2$, 513.7832: found 513.7835.; EA. calcd for $C_{10}H_6O_4S_2Te_2$; C, 23.57; H, 1.19; O, 12.56; S, 12.59: found C, 23.25; H, 1.23; S, 12.28.

4.2.4. 5-Deuteriated 2-thiophene carboxylic acid; Identification of the regioisomer of organoditelluride 1

The product of organoditelluride **1** (50 mg) was put into a NaOD solution (1 mL, 40 %, w/w in D_2O) and stirred at 60 °C overnight. The solution color changed into a dark brown and then yellow color. After cooling to RT, the mixture was diluted with DI water. The product was extracted three times with $CHCl_3$ after the pH of the solution was adjusted to 1 by adding diluted HCl at 0 °C. The combined organic layer was dried with anhydrous Na_2SO_4, filtered and washed with $CHCl_3$. The filtrate was concentrated under reduced pressure, then, dried with vacuum pump to give a partially deuterium-substituted product (see **Figure 4.3**).

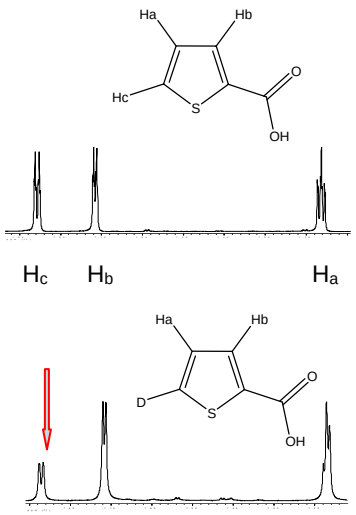

Figure 4.3 The NMR identification for the regioisomer of organoditelluride **1** via the partial substitution of Te with a deuterium using NaOD.

4.2.5. Preparation of RSNO solutions

S-Nitrosocysteine (CySNO) and s-nitosoglutathione (GSNO) solutions were prepared according to a reported procedure[10] as described in brief in Chapter 2.

4.3. Results and discussion

4.3.1. Design, synthesis and characterization of 5,5'-ditelluro-2,2'-dithiophenecarboxylic acid (DTDTCA, organoditelluride 1)

For the development of a new organoditelluride catalyst that can be incorporated into NOGPs, this molecule requires a functional group (such as carboxylic acid, free amine, etc) that can easily be covalently linked to a polymeric backbone. Good stability during a catalytic cycle at physiological pH is also a necessity that has already shown in the thiol peroxidase catalytic activity of diaryl dicalcogenides (ArSeSeAr or ArTeTeAr).[5-9]

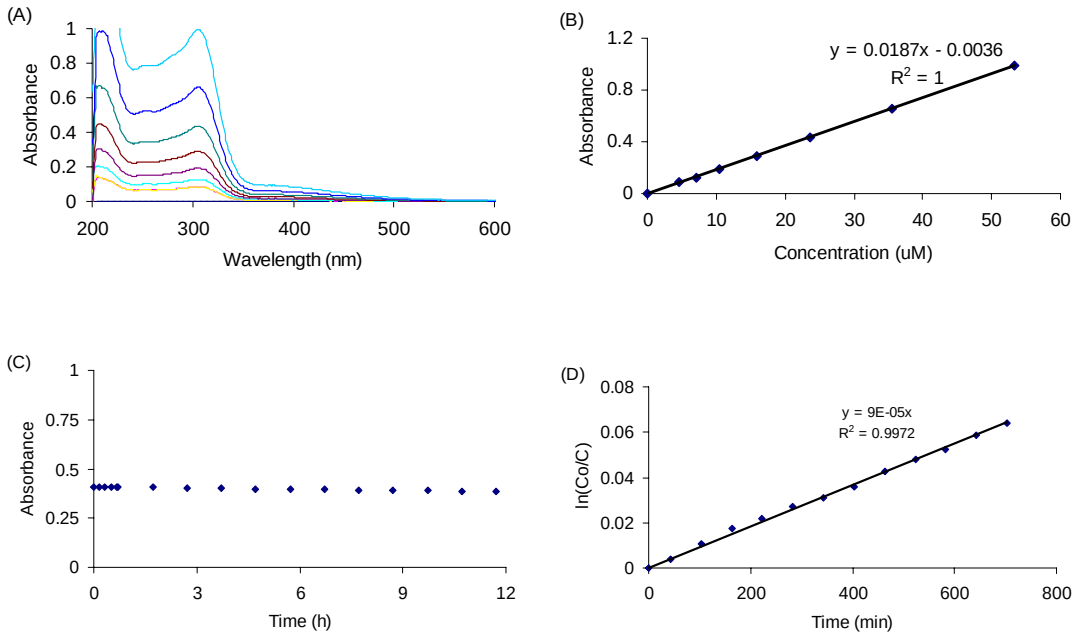

Figure 4.4 (A) UV spectroscopy of 5,5'-ditelluro-2,2'-dithiophenecarboxylic acid (DTDTCA, organoditelluride **1**) at different concentrations from 0 - 53.3 µM in 10 mM PBS buffer, pH 7.4, containing 0.5 mM EDTA under ambient condition; (B) calibration curve at maximum absorbance (306 nm); (C) the stability test of 22 µM organoditelluride **1** in the same PBS buffer at RT; the change of absorbance at 306 nm is recorded as a function of time; (D) the calculated decomposition rate of organoditelluride **1** in the same PBS buffer (first order, $k= 9 \times 10^{-5}$ min^{-1}).

Hence, the designed molecule, 5,5'-ditelluro-2,2'-dithiophenecarboxylic acid (DTDTCA, organoditelluride **1**, see **Scheme 4.1**) possessing carboxylic acid groups and aryl groups, likely satisfies these requirements. Indeed, organoditelluride **1** was synthesized from a commercially available 2-thiophene carboxylic acid by modifying a previously reported procedure (see **Scheme 4.1**).[12] The 5, 5'-positioned regioisomer was isolated as the major product, as identified by NMR through the substitution of a deuterium on the Te site using NaOD (see **4.2.4** and **Figure 4.3**). Organoditelluride **1** is fairly stable (first order decomposition, $k = 9.0 \times 10^{-5}$ min^{-1}; see **Figure 4.4**) and soluble in 10 mM phosphate-buffered saline (PBS) buffer, pH 7.4, as designed.

4.3.2. The measurements of catalytic NO generation by the organoditelluride 1 via a chemiluminescence NO analyzer (NOA)

The NO generated from a reaction solution containing RSNO, free thiol (RSH), and the catalytic amount of organoditelluride **1** was continuously monitored using a chemiluminescence NO analyzer (NOA). As shown in **Figure 4.5 (A),** a relatively large signal appears quickly upon adding organoditelluride **1** (2.5 μM) into a solution containing GSNO (25 μM) and GSH (100 μM) in deoxygenated PBS buffer. However, the rate of NO generation slowly decreases with time to reach a near steady-state level that lasts until all of the GSNO is consumed. It was found that organoditelluride **1** also decomposes GSNO to NO without adding GSH to the reaction mixture (see **Figure 4.5 (B)**).

Upon the addition of organoditelluride **1** (2.5 μM) into a solution of GSNO (50 μM) in deoxygenated PBS buffer without GSH, approximately 1.5 equivalents (after

baseline correction) of NO relative to the catalyst are quickly evolved. The NO generation then returns to baseline.

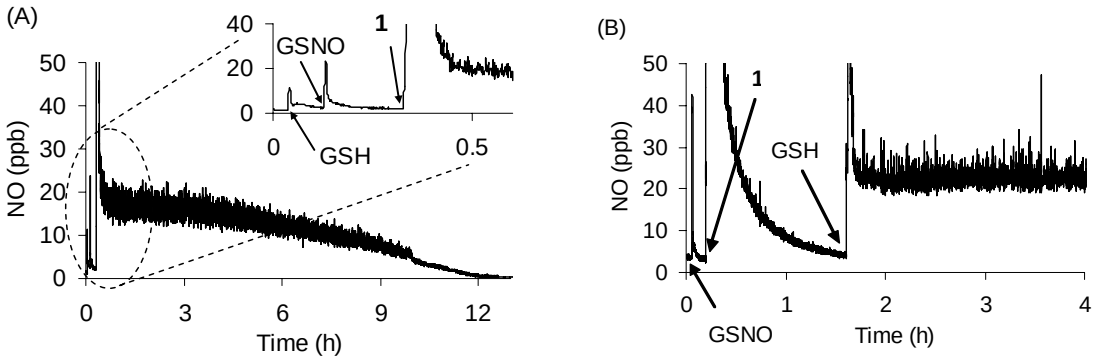

Figure 4.5 The measurements of catalytic NO generation by 2.5 μM 5,5'-ditelluro-2,2'-dithiophenecarboxylic acid (DTDTCA, organoditelluride **1**) in a solution of (A) 25 μM GSNO and 100 μM GSH, and (B) 50 μM GSNO and 100 μM GSH in PBS buffer, pH 7.4 (0.5 mM EDTA) via chemiluminescence NO analyzer (NOA). Arrow indicates addition of given species into the mixture.

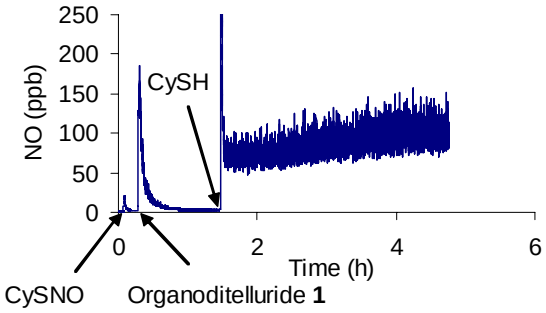

Figure 4.6 The measurements of catalytic NO generation by 2.5 μM 5,5'-ditelluro-2,2'-dithiophenecarboxylic acid (DTDTCA, organoditelluride **1**) in a solution of 50 μM CySNO and 100 μM CySH in 2 mL of 10 mM PBS buffer, pH 7.4, containing 0.5 mM EDTA, via chemiluminescence NO analyzer (NOA). Arrow indicates addition of each species into the test mixture.

The exact number of moles of NO initially liberated is variable depending on the reaction conditions employed; however, the amount produced always ranges from 1 to 2 equivalents of the initial organoditelluride level when a reducing agent is not added. Upon

addition of GSH (100 μM) to the mixture, NO generation resumes and reaches a relatively low steady-state level. Similar patterns were observed using catalytic amounts of organoditelluride **1** and CySNO/CySH substrate solution (see **Figure 4.6**).

4.3.3. Mechanistic considerations

This behavior is quite similar to that observed in a previous report regarding organodiselenide-mediated RSNO decomposition.[3] Although the mechanism is still under study, the work of Cha[3] suggested that organodiselenides could directly decompose GSNO without GSH at pH 7.4. However, another report demonstrated that organodiselenides do not directly decompose S-nitroso-N-acetyl-D-penicillamine (SNAP) or GSNO in the absence of N-acetyl-D-penicillamine or GSH at the same pH.[1] Even though organoditellurides could display a different chemistry for RSNO decomposition, it appears unlikely that such an oxidized form of the organoditelluride species could directly react with RSNO.

$$RSH + HNO_2 \overset{H^+}{\rightleftharpoons} RSNO + H_2O \qquad (4.1)$$

$$RSH \rightleftharpoons RS^- + H^+ \qquad (4.2)$$

$$ArTeTeAr + RS^- \rightleftharpoons ArTeSR + ArTe^- \qquad (4.3)$$

$$ArTeSR + RS^- \rightleftharpoons RSSR + ArTe^- \qquad (4.4)$$

Since there is always a low concentration of thiolate (RS^-) present in RSNO solutions at pH 7.4 (see **rxns 4.1** and **4.2**),[13] and the thiol form (RSH) is much less nucleophilic than the corresponding thiolate (RS^-), it is probable that the exchange reaction of RS^- and organoditelluride (ArTeTeAr) can rapidly occur as follows (**rxns 4.3**

and **4.4**),[8] yielding tellurolate ($ArTe^-$), a highly reactive and reduced form of the original ditelluride. This species is more likely to be responsible for RSNO decomposition rather than the direct reaction of oxidized organoditelluride **1** (ArTeTeAr) with RSNO.

This pathway is supported by several experiments. First, as shown **Figure 4.7**, UV measurements reveal that the absorption band (λ_{max} = 306 nm) of organoditelluride **1** (32 μM) in the presence of GSH (320 μM) in PBS buffer rapidly decreases (over 10 min period); however the absorption band of organoditelluride **1** (32 μM) in the presence of GSNO (320 μM) (λ_{max} = 311 nm; the wavelength slightly shifted because of the interference with the significant GSNO absorption band at λ_{max} = 335 nm) decreases very slowly (over 24 h period) under the same conditions.

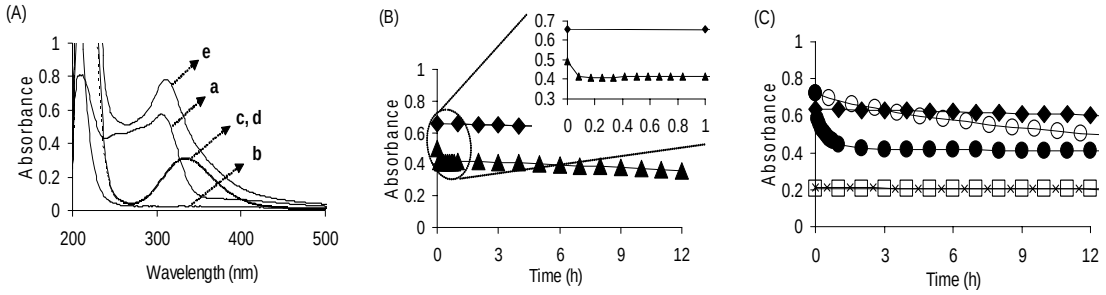

Figure 4.7 (A) UV-Vis spectrophotometric data for (a) 32 μM 5,5'-ditelluro-2,2'-dithiophenecarboxylic acid (organoditelluride **1**; λ_{max}= 306 nm), (b) 320 μM GSH, (c) 320 μM GSNO (λ_{max}= 335 nm), (d) 320 μM GSH/GSNO (λ_{max}= 335 nm), and (e) 32 μM organoditelluride **1**, 320 μM GSH/GSNO (λ_{max}= 311 nm) in 2.35 mL PBS buffer, pH 7.4, containing 0.5 mM EDTA. (B) Their absorbance changes (at 306 nm) as a function of time; (f) 80 μM organoditelluride **1,** ◆; (g) a solution of 32 μM organoditelluride **1** and 320 μM GSH**,** ▲. (C) Absorbance changes (at 311 nm) of each solution; (f), ◆; (c), □; (d), x; (h) 32 μM organoditelluride **1** and 320 μM GSNO, O; (e), ●.

In addition, in both UV experiments, a new absorption band (272 or 279 nm) increases as the 306 or 311 nm bands decrease. This new species is likely the ArTeSR

intermediate species.[8] In fact, the formation of the ArTeSR species was confirmed by mass spectrometry in the mixture of organoditelluride **1**/GSH (see **Figure 4.8**).

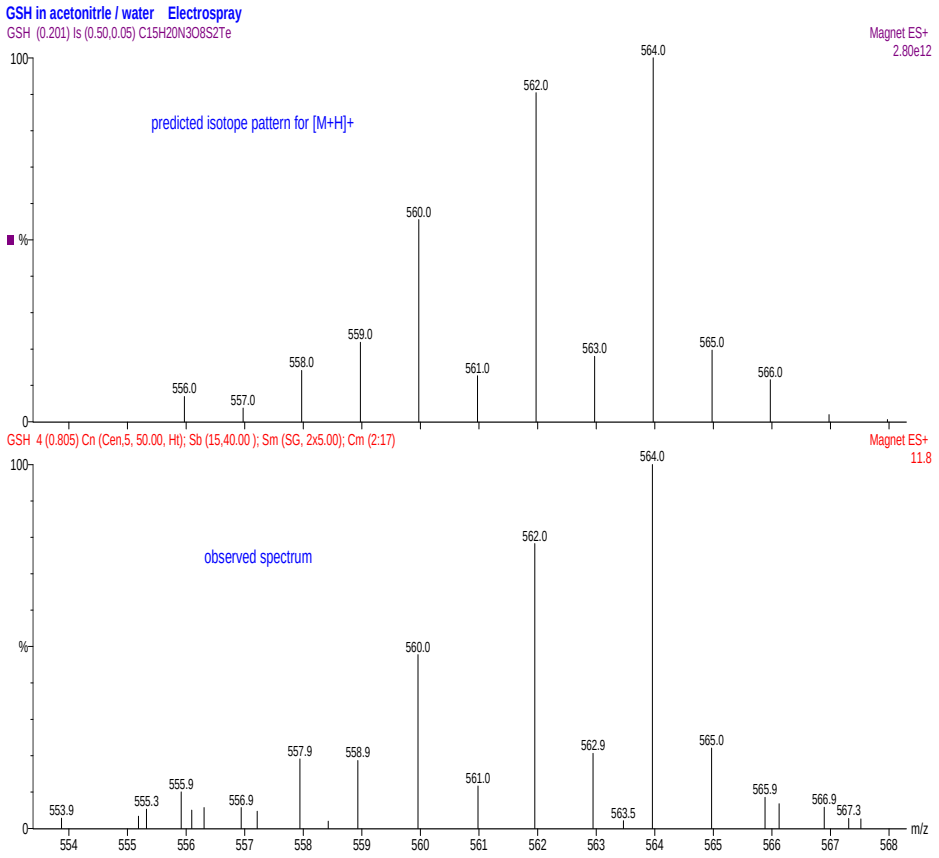

Figure 4.8 ArTeSR species was detected by mass spectrometry (electrospray) from a mixture of 5,5'-ditelluro-2,2'-dithiophenecarboxylic acid (organoditelluride **1**)/GSH (1/14, mole/mole) in CH_3CN/water (1/1, v/v).

Therefore, this UV and mass spectrometry data support the fact that ArTeTeAr does not directly react with RSNO, but a very small portion of $ArTe^-$ which is known to be immediately formed in the presence of RS^- (by **rxn 4.3**)[8] likely reacts with RSNO to generate NO. Furthermore, the kinetics of the initial burst of NO generation as well as the level of NO at steady-state in the NOA experiment is pH dependent (pH 6< 7 < 8; see

Figure 4.9). The addition of ascorbate (100 μM) as a reducing agent in place of free thiols does not generate additional NO in the NOA experiment when a fresh solution of organoditelluride **1** (2.5 μM) and GSNO (50 μM) is tested (see **Figure 4.10**).

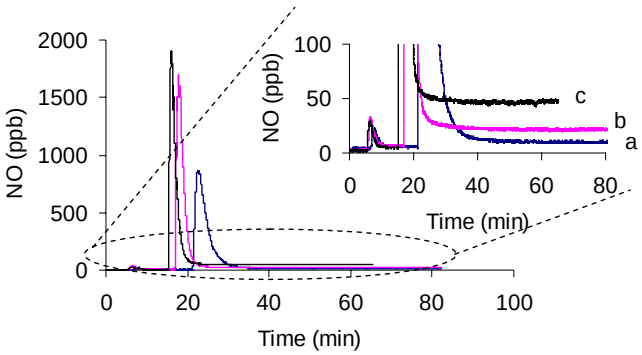

Figure 4.9 pH dependent NO generation of 1.25 μM 5,5'-ditelluro-2,2'-dithiophenecarboxylic acid (DTDTCA, organoditelluride **1**) depending on the various pH values of test solution (a= pH 6, b= pH 7, or c= pH 8) in 2 mL buffer containing 0.5 mM EDTA with 25 μM GSH and GSNO.

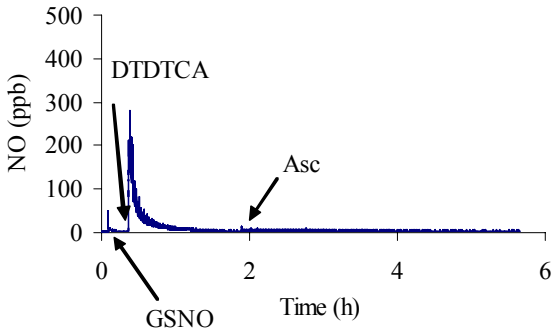

Figure 4.10 The measurements of NO generation by 2.5 μM 5,5'-ditelluro-2,2'-dithiophenecarboxylic acid (DTDTCA, organoditelluride **1**) in a solution of 50 μM GSNO and 100 μM ascorbate (Asc) in 2 mL of 10 mM PBS buffer, pH 7.4, containing 0.5 mM EDTA.

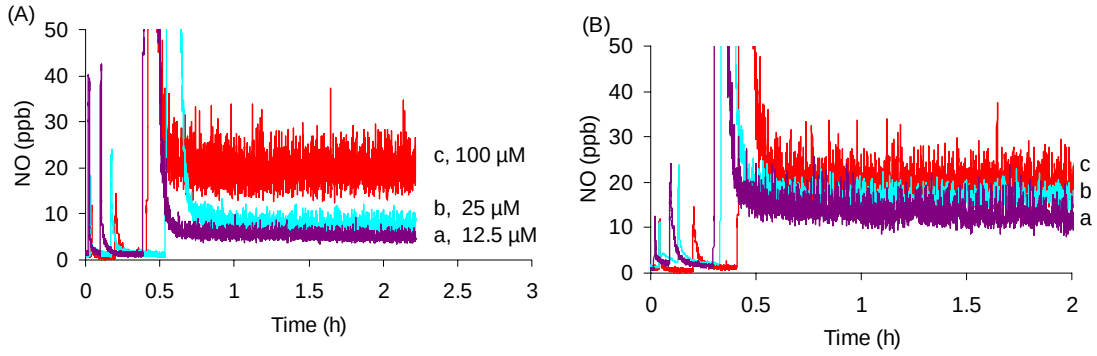

Figure 4.11 The GSH/GSNO concentration-dependent NO generation of 2.5 µM 5,5'-ditelluro-2,2'-dithiophenecarboxylic acid (DTDTCA, organoditelluride **1**) as a function of varied concentrations (a= 12.5, b= 25, and c= 100 µM) of GSH in the 100 µM GSNO (A), or (a= 12.5, b= 25, and c= 100 µM) of GSNO with 100 µM GSH (B) in 2 mL of 10 mM PBS buffer, pH 7.4, containing 0.5 mM EDTA.

Moreover, the level of NO at steady-state in the NOA experiment increases as a function of the RSH concentration in the reaction solution (see **Figure 4.11 (A)**), but not in proportion to the initial RSNO concentration (see **Figure 4.11 (B)**).

All data clearly indicate that a free thiol is the critical reducing agent required to maintain the catalytic reaction cycle, a free thiol is involved in the rate determining step, and again $ArTe^-$ formed in the presence of free thiol is the most reduced and reactive species in this redox chemistry (see **rxns 4.3** and **4.4**), and is thus responsible for NO generation. Considering that the NO generating reaction is irreversible because of $NO_{(g)}$ evolution, all the UV and NOA experimental results suggest that the equilibrium **rxn 4.4** lies far to the left as reported in earlier work.[8] Thus, this reaction (**rxn 4.4)** is likely to be a rate-determining step for NO generation.

Alternate pathways can also exist to produce the ArTeTeAr species. It has been recognized that ArTeSR may disproportionate to ArTeTeAr and RSSR (**rxn 4.5**).[8,9] In addition, oxygen competes with RSNO to oxidize $ArTe^-$ back to ArTeTeAr (**rxn 4.6**), a

well known method to synthesize organoditelluride compounds,[12] which likely takes place under the ambient conditions during the UV spectrophotometric experiments. Therefore, the mechanism for the organotellurium-mediated RSNO decay in the presence of oxygen will, in fact, be more complicated. Nontheless, when organoditelluride **1** is immobilized on an amperometric NO sensor,[14] NO liberation from GSNO still occurs under ambient coditions (see **Figure 4.12**).

$$ArTeSR \rightleftharpoons ArTeTeAr + RSSR \qquad (4.5)$$

$$ArTe^- + O_2 \rightleftharpoons 1/2\ ArTeTeAr + O_2^- \qquad (4.6)$$

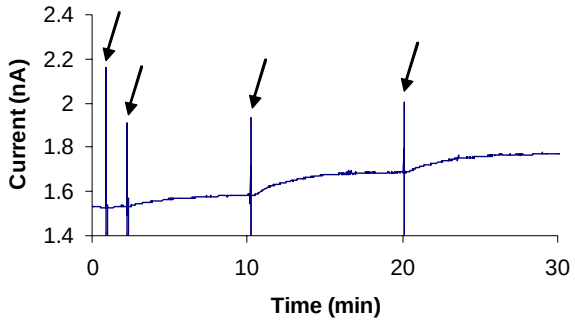

Figure 4.12 The current changes of amperometric NO sensor mounted with an organoditelluride **1**-immobilized membrane upon adding 20 μL of 5 mM GSNO solutions into 100 mL PBS buffer containing 50μM GSH and 0.1 mM EDTA under ambient oxygen; arrow indicates the addition of GSNO solution into the mixture.

However, based on reported studies, [1,3,4,7,8] the following two reactions (**rxn 4.7** and/or **4.8**) are most likely responsible for the RSNO decomposition.

$$ArTe^- + 2\ RSNO \longrightarrow ArTeSR + RS^- + 2\ NO \qquad (4.7)$$

$$ArTe^- + RSNO \longrightarrow 1/2\ ArTeTeAr + RS^- + NO \qquad (4.8)$$

First, the denitrosation of RSNO by $ArTe^-$ might directly form the ArTeSR species via **rxn 4.7**, and this intermediate (ArTeSR) could continuously participate in the catalytic cycle without further regeneration of ArTeTeAr. In contrast, **rxn 4.8** reforms the ArTeTeAr species, which is the most stable form of organotellurium species in the catalytic cycle; hence, this reaction is a thermodynamically favorable pathway. Further investigations are needed to determine whether a plausible intermediate, a nitrosotellurol species (ArTeNO), can in fact be formed during this reaction, as suggested for the similar organoselenium-mediated RSNO decomposition.[4] Nonetheless, it is difficult to differentiate between ArTeTeAr and ArTeSR species in the presence of RSH and/or RSNO probably due to the fast equilibria reactions involving all of these species (**rxns 4.3 - 4.8**). However, when considering the transnitrosation chemistry between RSH and RSNO,[15] the transnitrosation of RSe^- and RSNO (or RTe^- and RSNO) also likely occurs to form RSeNO[4] (or RTeNO), which is an unstable species compared with RSNO; hence it immediately liberates NO to turn into the original form, RSeSeR (or RTeTeR). This plausible transnitrosation supports the pathway of **rxn 4.8** as the primary NO generation reaction.

Based on the discussion and reactions outlined above, most of NOA experimental results can be interpretated. That is, any trace amounts of $ArTe^-$ initially formed via the **rxn 4.3** will quickly react with RSNO to generate NO via **rxn 4.8** (and/or **rxn 4.7)**, which keeps the equilibrium for **rxn 4.3** shifted to the right. In proportion to NO evolved, ArTeTeAr will diminish as ArTeSR accumulates regardless of the reformation of ArTeTeAr via the **rxns 4.5**, **4.6**, and **4.8**, because the NO liberation reaction(s) should be

fast and irreversible, and the equilibrium for **rxn 4.4** favors the reactants. Therefore, the burst of NO initially detected in the absence of added reducing agent depends on the amount of thiolate species initially available based on levels provided by the original nitrosothiol substrate (**rxn 4.1** and **4.2**).

4.4. Conclusions

5,5'-Ditelluro-2,2'-dithiophenecarboxylic acid (DTDTCA, organoditelluride **1**) was synthesized, and fully characterized by ^{1}H, ^{13}C, and ^{125}Te NMR, IR, and HRMS (high resolution mass spectrometry). It was found that organoditelluride **1** (ArTeTeAr) catalytically denitrosates RSNO to NO in the presence of free thiols at physiological pH (see **Figure 4.2** for the proposed mechanism). Various experiments including NOA, UV, and mass spectrometry clearly indicate that organoditelluride **1** does not directly react with RSNO, but the tellurolate ($ArTe^{-}$) species formed by thiolate (RS^{-}) that always exists in an RSNO solution at physiological pH due to the equilibrium process (**rxn 4.1** and **4.2)** does react with RSNO. The key intermediate, tellurosulfide (ArTeSR) is also produced when ArTeTeAr reacts with RS^{-}. More complicated reactions are reported to be involved in the organoditelluride redox chemistry, such as the disproportion reaction (**rxn 4.5**) and oxidation in the presence of oxygen (**rxn 4.6**).

Two different pathways to liberate NO from RSNO are plausible (**rxn 4.7** and **4.8**), but **rxn 4.8** is more likely responsible for this reaction, which is thermodynamically favorable. In this preferred pathway, a nitrosotellurol (ArTeNO) may be formed as an intermediate which is an unstable species and immediately liberates NO as proposed for organodiselenide-mediated RSNO decomposition.[4] Although further investigation is

necessary to fully understand all possible reactions involved, this discovery is considered significant, as it explores potential new applications of organoditelluride redox chemistry. This new catalyst is expected to be useful for preparing different types of NOGPs, which can be applied to prepare new RSNO selective electrochemical sensors[14] and potentially to fabricate more biocompatible coatings for blood contacting medical devices.[16]

4.5. References

1. Hou, Y. C.; Guo, Z. M.; Li, J.; Wang, P. G., Seleno compounds and glutathione peroxidase catalyzed decomposition of S-nitrosothiols. *Biochemical and Biophysical Research Communications* **1996,** 228, (1), 88-93.
2. Cha, W.; Meyerhoff, M. E., S-Nitrosothiol detection via amperometric nitric oxide sensor with surface modified hydrogel layer containing immobilized organoselenium catalyst. *Langmuir* **2006,** 22, (25), 10830-10836.
3. Cha, W.; Meyerhoff, M. E., Catalytic generation of nitric oxide from S-nitrosothiols using immobilized organoselenium species. *Biomaterials* **2007,** 28, (1), 19-27.
4. Wismach, C.; du Mont, W. W.; Jones, P. G.; Ernst, L.; Papke, U.; Mugesh, G.; Kaim, W.; Wanner, M.; Becker, K. D., Selenol nitrosation and Se-nitrososelenol homolysis: A reaction path with possible biochemical implications. *Angewandte Chemie-International Edition* **2004,** 43, (30), 3970-3974.
5. Mugesh, G.; Panda, A.; Singh, H. B.; Punekar, N. S.; Butcher, R. J., Glutathione peroxidase-like antioxidant activity of diaryl diselenides: A mechanistic study. *Journal of the American Chemical Society* **2001,** 123, (5), 839-850.
6. Wilson, S. R.; Zucker, P. A.; Huang, R. R. C.; Spector, A., Development of synthetic compounds with glutathione-peroxidase activity. *Journal of the American Chemical Society* **1989,** 111, (15), 5936-5939.
7. Engman, L.; Stern, D.; Cotgreave, I. A.; Andersson, C. M., Thiol peroxidase-activity of diaryl ditellurides as determined by a H^1-NMR method. *Journal of the American Chemical Society* **1992,** 114, (25), 9737-9743.
8. Dong, Z.; Liu, J.; Mao, S.; Huang, X.; Yang, B.; Ren, X.; Luo, G.; Shen, J., Aryl thiol substrate 3-carboxy-4-nitrobenzenethiol strongly stimulating thiol peroxidase activity of glutathione peroxidase mimic 2, 2'-ditellurobis(2-deoxy-b-cyclodextrin). *Journal of the American Chemical Society* **2004,** 126, (50), 16395-16404.
9. Mugesh, G.; Panda, A.; Kumar, S.; Apte, S. D.; Singh, H. B.; Butcher, R. J., Intramolecularly coordinated diorganyl ditellurides: Thiol peroxidase-like antioxidants. *Organometallics* **2002,** 21, (5), 884-892.
10. Stamler, J. S.; Loscalzo, J., Capillary Zone Electrophoretic Detection of biological thiols and their S-nitrosated derivatives. *Analytical Chemistry* **1992,** 64, (7), 779-785.
11. Szacilowski, K.; Stasicka, Z., S-Nitrosothiols: Materials, reactivity and mechanisms. *Progress in Reaction Kinetics and Mechanism* **2001,** 26, (1), 1-58.
12. Engman, L.; Cava, M. P., Organotellurium compounds.6. Synthesis and reactions of some heterocyclic lithium tellurolates. *Organometallics* **1982,** 1, (3), 470-473.
13. Williams, D. L. H., The chemistry of S-nitrosothiols. *Accounts of Chemical Research* **1999,** 32, (10), 869-876.
14. Cha, W.; Lee, Y.; Oh, B. K.; Meyerhoff, M. E., Direct detection of S-nitrosothiols using planar amperometric nitric oxide sensor modified with polymeric films containing catalytic copper species. *Analytical Chemistry* **2005,** 77, (11), 3516-3524.

15. Hogg, N., The kinetics of S-transnitrosation - A reversible second-order reaction. *Analytical Biochemistry* **1999,** 272, (2), 257-262.
16. Keefer, L. K., Progress toward clinical application of the nitric oxide-releasing diazeniumdiolates. *Annual Review of Pharmacology and Toxicology* **2003,** 43, 585-607.
17. Cai, T. B.; Wang, P. G., Recent developments in anticancer nitric oxide donors. *Expert Opinion on Therapeutic Patents* **2004,** 14, (6), 849-857.

CHAPTER 5

Organoditelluride-Tethered Polymeric Materials as New Nitric Oxide Generating Polymers (NOGPs)

5.1. Introduction

Nitric oxide generating polymers (NOGPs) possess catalytic sites that can catalytically liberate nitric oxide (NO) from S-nitrosothiols (RSNOs) such as S-nitrosoglutathione (GSNO) or S-nitrosocysteine (CySNO) in the presence of reducing equivalents such as free thiols (RSHs; glutathione (GSH), cysteine (CySH), etc.) or ascorbate,[1, 2] where all substrates (RSNOs, RSHs, and ascorbate) are already present in blood.[3] Hence, NOGPs are expected to locally produce enhanced NO levels for prolonged time periods at any polymer/blood interface, mimicking the endothelium cell layer that lines the inner walls of all healthy blood vessels. Because NO is known to play a key role in vasoprotection, such as the inhibition of platelet adhesion/activation,[4-6] and smooth cell proliferation,[7] NOGPs are potentially useful biomimetic materials that can be adapted into a variety of biomedical devices such as catheters, vascular grafts, extracorporeal circuits, and indwelling sensors, etc. to improve their inherent hemocompatibility.

Efforts to discover new NOGPs has focused on the use of the known chemistry of copper ions[8] and organodiselenides (RSeSeR)[9] with respect to their catalytic

decomposition of RSNOs to NO. For example, polymeric materials have been covalently modified with Cu(II)-cyclen[2] or selenocystamine,[10] and these new materials have been shown to generate NO when in contact with a fresh animal blood *in vitro*, supporting the potential usefulness of the basic concept of NOGPs. Therefore, it is now worthwhile to investigate a variety of other types of catalysts in order to provide many potentially useful NOGP polymeric materials for diverse applications within the biomedical area. Besides, known chemicals (Cu^{+}, Fe^{2+}, Hg^{2+}, Ag^{+}, and RSeSeR) for the catalytic RSNO denitrosation,[9, 11] a new chemistry based on use of organoditellurides (RTeTeR) has been introduced in Chapter 4, suggesting the use of such compounds for the preparation of additional NOGPs.

In order to utilize organoditelluride chemistry for creating NOGPs, we herein report novel polymeric materials possessing covalently attached organoditelluride species, specifically 5,5'-ditelluro-2,2'-dithiophenecarboxylic acid (DTDTCA) (see **Scheme 5.1**). Various base polymeric materials are examined in this work: hydrophilic thermoplastic polyurethane (PU; Tecophilic, SP-93A-100) as well as an interpenetrating polymer network (polymer **5**) consisting of a water soluble poly(allylamine hydrochloride) (PAH) with covalently linked DTDTCA and a cellulose membrane (see **Scheme 5.1**). The catalytic NO generation of these new materials (polymers **3, 4** and **5**) from endogenous RSNOs and RSHs at physiological pH are demonstrated. Tunable NO fluxes from polymer **5** are achieved by adjusting the amounts of catalytic sites (the polymer **4**) loaded within the cellulose membrane. The leaching of tellurium (Te) species from polymer **5** is examined as well. Finally, polymer **5**-mediated spontaneous NO generation when in contact with fresh sheep blood *in vitro* is demonstrated via use of an electrochemical

RSNO sensor in which polymer **5** is employed as an outer catalytic membrane. Results from this study suggests that new types of NOGPs based on appending an organoditelluride catalyst are potentially useful for applications in a variety of biomedical areas such as the development of RSNO sensors,[12, 13] as well as the preparation of medical devices with improved hemocompatbility.[14-18]

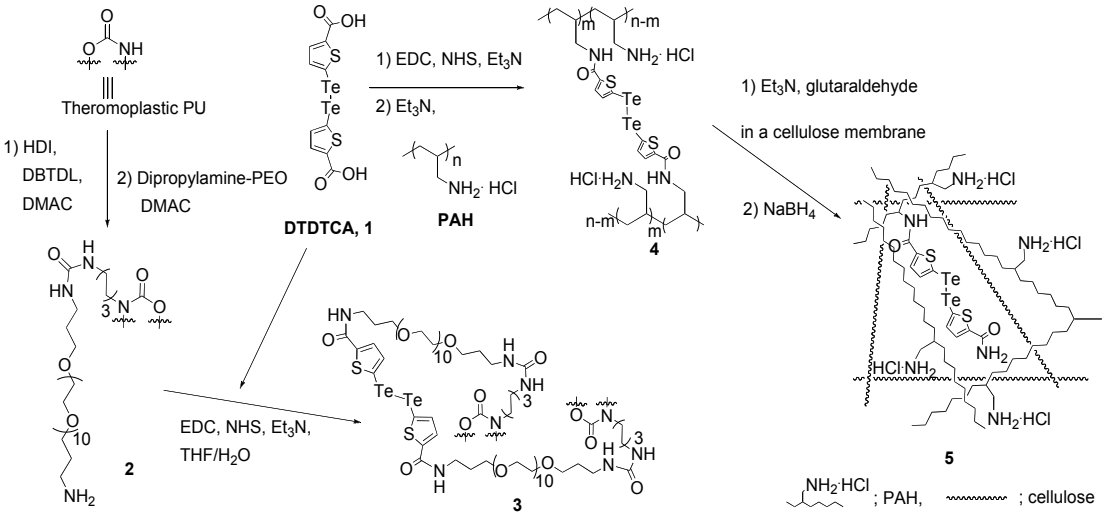

Scheme 5.1 Synthetic schemes used for preparing new types of nitric oxide generating polymers (NOGPs; polymers **3, 4**, and **5**) covalently attached with an organoditelluride species (DTDTCA, **1**), where different polymeric matrices are used; hydrophilic thermoplastic polyurethane (PU) for polymer **3**, a water soluble poly(allylamine hydrochloride) (PAH) for polymer **4**, and an interpenetrating polymer network (IPN) consisting of polymer **4** and a cellulose membrane for polymer **5** (see section 5.2.3 for details).

5.2. Experimental

5.2.1. Materials

2-Thiophene carboxylic acid, tellurium, dibutyltin dilaurate (DBTDL), hexamethylene diisocyanate (HDI), and N,N'-dimethyl acetamide (DMAC), were

purchased from Aldrich (Milwaukee, WI). N-(3-dimethylaminopropyl)-N'-ethylcarbodiimide hydrochloride (EDC·HCl), N-hydroxysuccinimide (NHS), glutathione (GSH) and cysteine (CySH) were products of Sigma (St. Louis, MO). Hydrophilic thermoplastic polyurethane (Tecophilic, SP-93A-100) was a gift from Lubrizol Advanced Materials, Inc. (formerly Noveon Inc.) (Cleveland, OH). Dipropylamine-PEO (DPA-400E, F.W.= 573.73) was a gift from Tomah products (Milton, WI). Other reagents from Aldrich, solvents from Fisher Scientific (Fair Lawn, NJ), and NMR reagents from Cambridge Isotope Laboratories, Inc. (Andover, MA) were used without further purification unless otherwise noted. Distillation was employed for the purification of HDI, Et_3N, THF, and DMAC prior to use. DI water was prepared by a Milli-Q filter system (18 MΩ cm^{-1}: Millipore Corp., Billerica, MA). Dialysis membranes were purchased from Spectrum Laboratory Inc. (Rancho Dominguez, CA).

5.2.2. Measurements

FTIR spectra were collected with a Perkin-Elmer spectrum BX FT-IR system. UV-Vis spectra were recorded by a Perkin-Elmer Lambda 35 UV/VIS spectrometer. The tellurium (Te) content of the polymers was determined by inductively coupled plasma-high resolution mass spectrometry (ICP-HRMS), using a Thermo Finnigan Element. NO measurements were made using a nitric oxide analyzer (NOA) (Sievers, model 280).

5.2.3. Synthesis

*Polymer **2**:*

The preparation of polymer **2** was performed by a modified method from the reported procedures[19, 20] as well as Chapter 3. In brief, the well-dried hydrophilic thermoplastic polyurethane (Tecophilic, SP-93A-100; 2.0 g; ca 4.8 mmole of urethane

group) purified by the soxhlet extraction was dissolved in anhydrous DMAC (40 mL). This solution was added dropwise into a stirred solution of HDI (3.89 mL, 24 mmole) and DBTDL (72 μL, 0.12 mmole) in DMAC (4 mL) at 40 - 45 °C for 3 h. After 1.5 d, the mixture was cooled to RT and then slowly added into anhydrous Et_2O (400 mL). The solid formed was filtered and washed with anhydrous Et_2O (600 mL). The filter cake was dried with N_2 blowing followed by vacuum drying to afford a white polymer. This polymer (1.86 g) was dissolved in anhydrous DMAC (30 mL), and then slowly added into a stirred solution of dipropylamine-PEO (10.4 g) in DMAC (12 mL) at 40 °C for 3 h. The mixture was stirred for 1 d at 40 °C and then slowly added into Et_2O (400 mL). The yellowish polymer formed was filtered and washed with Et_2O (600 mL). The filter cake was soxhlet extracted with MeOH for 2 d. After cooling to RT, the solid cake was again washed with MeOH and then dried by vacuum pump for 2 d to yield polymer **2** (0.82 g). A solution of aminated polymer **2** in DMAC was titrated by a colorimetric method using bromophenol blue and p-toluenesulfonic acid in isopropanol (0.2 mmole of amine sites/g of polymer **2,** see section 5.2.4 for details).

IR (neat)= 3323 cm^{-1} (N-H), 2916, 2857 cm^{-1} (CH_2), 1715 cm^{-1} (C=O), 1614 cm^{-1} (HNCONH), 1529 cm^{-1} (C-N, N-H), 1102 cm^{-1} (CH-O-CH).

*Polymer **3**:*

An organoditelluride compound (DTDTCA, **1**, see **Scheme 5.1**, 17 mg, 33 μmole), which was synthesized as described in Chapter 4, was dissolved in THF (5 mL), and mixed with EDC·HCl (15 mg, 78 μmole) in DI water (5 mL). The cloudy mixture was stirred and became clear by adding Et_3N (20 mg, 198 μmole). Then, NHS (9 mg, 78 μmole) was added into the mixture at RT. A solution of polymer **2** (0.34 g, 68 μmole of

free amine) in THF (12 mL) was then mixed with the above solution and stirred at RT overnight. The mixture was slowly added into Et_2O (900 mL) to form a slightly reddish yellow polymer. The solid was washed with Et_2O and DI water. The filter cake was stirred in MeOH at RT overnight. The residue was again filtered and washed with MeOH and then dried with a vacuum pump to give a yellowish polymer **3** (0.2 g). Based on the ICP-HRMS analysis, the total tellurium amount in the prepared polymer was 5.3 mg per g of polymer, which corresponds to 10.5 mg/cm^3 of DTDTCA, **1**, if the density of polymer is considered as 1 g/cm^3.

IR (neat)= 3320 cm^{-1} (N-H), 2915, 2849 cm^{-1} (=C-H), 1715 cm^{-1} (C=O), 1616 cm^{-1} (HNCONH), 1526 cm^{-1} (C-N, N-H), 1445 cm^{-1} (=C-H), 1099 cm^{-1} (CH_2-O-CH_2).

*Polymer **4**:*

To a solution of 5,5'-ditelluro-2,2'-dithiophenecarboxylic acid (DTDTCA, **1**; 82 mg, 0.16 mmole), Et_3N (130 mg, 1.28 mmole), EDC (76 mg, 0.40 mmole), and NHS (50 mg, 0.43 mmole) in THF/water (2 mL/0.1 mL) was added a solution of PAH (0.3 g, equivalent to 3.2 mmole of amine groups in the polymer, Mn= 15,000 g/mol) and triethylamine (130 mg, 1.28 mmole) in DI water (8 mL). After the reaction mixture was stirred overnight at RT, the mixture was filtered with membrane filters (MWCO= 5 kD) and washed with DI water several times using a centrifuge to remove any low molecular weight compounds. The filtercake was collected and freeze-dried to give a light reddish brown colored polymer **4**. The color and UV-Vis spectrum of polymer **4** exhibited the characteristics of DTDTCA, **1** (λ_{max}= 306 nm).[13] ICP-HRMS analysis yielded 7. 5 wt % Te content in polymer **4**, which corresponds to ca. 0.3 mmole DTDTCA, **1,** in 1 g of the polymer **4** (y= 56%). On the other hand, due to the dicarboxylic acid groups of

DTDTCA, **1**, it also acts as a crosslinking agent during the coupling reaction; hence, this affects the water solubility of resulting polymer **4**. Nonetheless, under the given reaction conditions described above, most of polymer **4** was found to be soluble when used as a diluted solution (0.1 mg/mL).

IR (KBr)= 3424 cm^{-1} (COO-H, N-H), 2924, 2864 cm^{-1} (=C-H), 1635 cm^{-1} (C=O), 1559 cm^{-1} (HNCONH), 1457 cm^{-1} (C-N, N-H), 1406 cm^{-1} (=C-H).

*Polymer **5***:

A cellulose membrane (Spectra/Por, MWCO = 50 kD) was cut into smaller square sized films (1 cm x 1 cm). After they were extensively washed with 0.1 M EDTA in DI water to remove any metal ion impurities, they were separately put into three different concentrations of polymer **4** solutions (0.9, 2.7, and 9 wt % in 1 mL of DI water), and then shaken overnight at RT. Each film was placed on a glass slide. Three different solutions of polymer **4** (0.2 mL of 0.9, 2.7, and 9 wt % solution respectively) containing triethylamine (ca. 10 wt %) were individually placed onto each film, followed by addition of a glutaraldehyde solution (0.1 mL of 5 wt % in DI water). The resultant films were allowed to stand for 2 d at RT. Each film was then washed extensively with DI water and then shaken in a $NaBH_4$ solution (0.1 M in 5 mL DI water) for 1 h at RT. Each film was then stirred in a buffered solution, pH 4.3, overnight at RT to remove any residual $NaBH_4$, and then stored in PBS buffer, pH 7.4, prior to NOA experiments.

5.2.4. Determination of free amine equivalents in polymer 2

Free amine equivalents in polymer **2** were determined by a titration method as described in Chapter 3.

5.2.5. Preparation of RSNO solutions

S-nitrosocysteine (CySNO) and s-nitosoglutathione (GSNO) solutions were prepared according to the method described in Chapter 2 and in the literature.[12, 21]

5.2.6. Procedure for the treatment of polymer 3 with excess of GSH/GSNO

A small film of polymer **3** (3.92 mg; size, 0.9 cm X 1.8 cm; thickness, < 5 μm) was soaked in a solution of GSH/GSNO (100 μM/100 μM) in 10 mL of PBS buffer (10 mM), pH 7.4, containing 0.5 mM EDTA (the same PBS buffer used for all experiments unless otherwise noted). After the mixture was shaken overnight at RT, the film was removed from the mixture. This film was again shaken in a fresh solution of GSH/GSNO (200 μM/200 μM) in 10 mL of PBS buffer for 6 h. The film was removed from the solution and placed into a fresh solution of 10 mL PBS buffer. The same procedure to wash the film was carried out a couple of times to ensure that the film is in a fully hydrated state immediately before testing in the NOA experiments.

5.2.7. Sample preparation for analyzing Te content in the polymers

A procedure similar to that employed for the analysis of copper content in the polymer films described in Chapter 2 was followed for analysis of the Te content of the new polymers reported here. In brief, a given amount of polymer was dried using the vacuum pump, and completely dissolved in 0.5 mL of concentrated HNO_3, and then diluted with DI water to give a 5 mL solution. Each solution was then quickly filtered with a syringe filter (a product of National Scientific Company; Rockwood, TN), and the filtrate was analyzed by ICP-HRMS.

5.2.8. General procedures for the NO measurements using a chemiluminescence NO analyzer (NOA)

The typical procedure for all NO measurements (to assess NO generated from RSNO species) using the NOA was described in Chapter 2.

5.2.9. Tellurium (Te) leaching study

A polymer film (polymer **5**) was fully immersed in a solution of 10 μM GSH/GSNO solution in 5 mL of PBS buffer, pH 7.4, for 1 d at RT. After a small amount of sample (30 μL) was withdrawn from the mixture, and a fresh solution of concentrated GSH/GSNO was added into the mixture (the total volume was maintained). This process of sampling and injecting fresh GSH/GSNO solutions was carried out daily for 15 d. The Te content in some of sample solutions were then determined by ICP-HRMS.

5.2.10. Amperometric NO detection in blood

Amperometric NO sensors were fabricated and used for RSNO detection in whole sheep blood, according to the procedure described in Chapter 3. A small piece of polymer **5** was mounted at the surface of the NO sensor as the outermost layer, while a blank cellulose membrane was similarly employed at the surface of a second "control" NO sensor placed in the same blood sample.

5.3. Results and discussion

5.3.1. Synthesis and characterization

5.3.1.1. Preparation of polymer 3

A modification of biomedical grade thermoplastic polyurethane (PU) (Tecophilic, SP-93A-100) was initially tried for the development of an organoditelluride-immobilized

NOGP because of the multiple advantages of PU materials, including good mechanical properties, processability, and relatively good inherent biocompatibility.

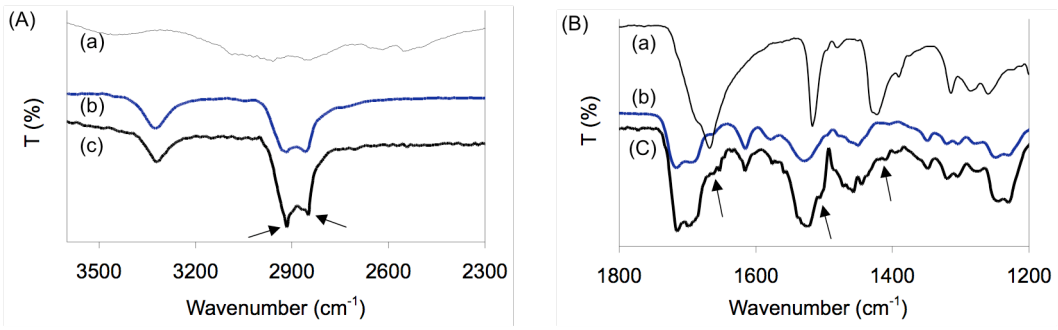

Figure 5.1 Comparison of IR spectra between 5,5'-ditelluro-2,2'-dithiophenecarboxylic acid; DTDTCA, **1** (a), the aminated thermoplastic PU; polymer **2** (b), and the conjugated product with (a) and (b); polymer **3** (c). Arrows indicate that all of characteristic peaks of DTDTCA, **1,** appears in the spectrum of polymer **3** as shown the regions (A) and (B), corresponding to the stretching and bending of (=C-H) and (C=O) groups.

First, DTDTCA (**1)** was synthesized as described in Chapter 4, and the aminated polymer **2** was prepared as described in Chapter 3, in which the free amine sites were created at a level of 0.2 mmole per 1 g of the polymer, as determined by the colorimetric titration (see section 5.2.4). The EDC coupling chemistry of DTDTCA, **1,** with polymer **2,** yielded polymer **3**, possessing the characteristic IR bands of DTDTCA in the IR spectrum (see **Figure 5.1**). This suggests the successful incorporation of organoditelluride species within the PU matrix. Polymer **3** was analyzed via ICP-HRMS to contain 5.3 mg of tellurium per gram of polymer, which corresponds to 10.5 mg/cm^3, assuming a polymer density of 1 g/cm^3.

5.3.1.2. Preparation of polymer 4

DTDTCA, **1**, was covalently linked into a water soluble polymer, poly(allylamine hydrochloride) (PAH, M_n= 15,000) through the EDC coupling chemistry, resulting in the

formation of polymer **4** (see section 5.2.3 for details) possessing 7.5 wt % of tellurium (Te) as analyzed by ICP-HRMS. Several new IR bands including those at 2924 cm^{-1} (=C-H), 2864 cm^{-1} (=C-H), 1635 cm^{-1} (C=O), 1559 cm^{-1} (-NHCO-), 1406 cm^{-1} (=C-H) appeared in the product, revealing the presence of the newly incorporated DTDTCA, **1,** in polymer **4** (see **Figure 5.2(A)**). This polymer displayed the characteristic color (light reddish brown) and absorption band (λ= 306 nm) of DTDTCA, **1** (see **Figure 5.2(B)**).[22]

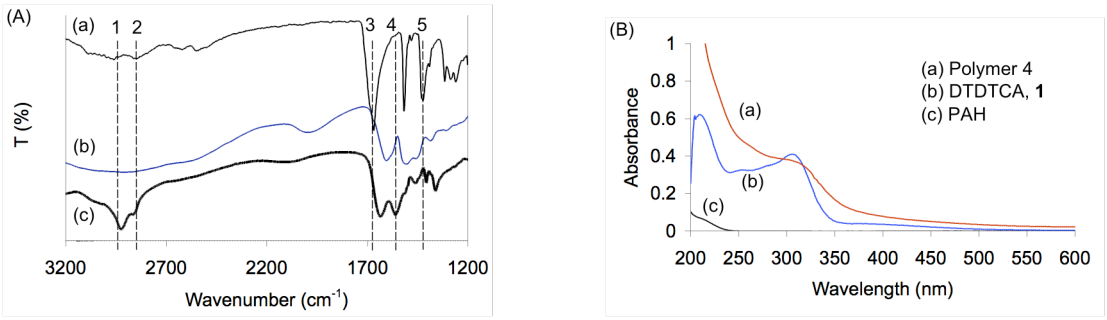

Figure 5.2 IR and UV spectra of polymer **4**, PAH, and DTDTCA (**1**); (A) The IR spectrum of polymer **4** (c) matches with most of the bands in DTDTCA (**1)** (a) (the dashed line 1, 2, and 5 for the aromatic C-H stretching and bending; 3 for the C=O stretching), poly(allylamine hydrochloride) (PAH) (b), as well as a new band indicating the amide bond formation between PAH and DTDTCA (the dashed line 4); (B) UV spectra of polymer **4:** (a) shows the distinctive absorption band (shoulder, λ= 306 nm) of DTDTCA (**1)** (b) in the UV-Vis spectrum after immobilizing DTDTCA on PAH (c).

5.3.1.3. Preparation of polymer 5

In order to maximize the catalytic NO generation of polymer **5**, polymer **4** possessing the catalyst (DTDTCA, **1**) was crosslinked within a small piece of cellulose membrane (the bulk phase as well as the surface). Since the small molecules RSNOs and RSHs could diffuse into a porous cellulose membrane, the NO generation is likely to occur throughout the film. Further, by varying the concentration of polymer **4** (0.9 wt % (L): 2.7 wt % (M): 9.0 wt % (H)= 1: 3: 10) when loaded in the same sized cellulose

membrane, the resulting polymer **5** can possess different densities of polymer **4** as determined by the amount of tellurium (Te) found within the resultant films (see **Table 5.1),** as well as the slight color differences observed, in proportional to the amount of applied polymer **4** (see section 5.2.3 for details).

Table 5.1 Comparison of three different polymers (**5**) prepared by altering the amounts of polymer **4** (0.9 wt % (L): 2.7 wt % (M): 9.0 wt % (H)= 1: 3: 10) when loaded in the cellulose membrane (size= 1 cm x 1 cm x 50 μm). The analyzed data were obtained by ICP-HRMS.[a]

Polymer **5**	L	M	H
The ratio of the amounts of polymer **4** when loaded in the cellulose membrane = the theoretical Te ratio	1	3	10
The analyzed Te ratio in the polymer **5** (μg)	1 (2.74)	3 (7.95)	8 (21.75)
The density of DTDTCA, **1** (μg/cm^3) in the polymer **5**[b]	1.1	3.2	8.7
The density of polymer **4** (μg/cm^3) in the polymer **5**[c]	7.3	21.2	58.0

[a] See section 5.2.7 for the sample preparation; [b] based on the molecular weight of DTDTCA, **1,** (509 g/mol) consisting 2 equivalents of Te, and the volume of polymer **5** (0.005 cm^3); [c] based on the 7.5 wt % of Te in the polymer **4**.

Because polymer **4** has inherent color, the more that was added during the crosslinking, the darker the color of the final polymer **5**. ICP-HRMS analysis of the various polymer **5** samples yielded a ratio of Te in three different samples (polymer **5**) that was close to the ratio of the loaded amounts of polymer **4** (see **Table 1**). The analyzed ratio of Te within polymer **5** samples suggests that the yield of the loading process is slightly decreased at higher loading concentrations, which is reasonable to

expect in preparing this type of IPN given the limited pore size and total internal volume of the cellulose membrane matrix.

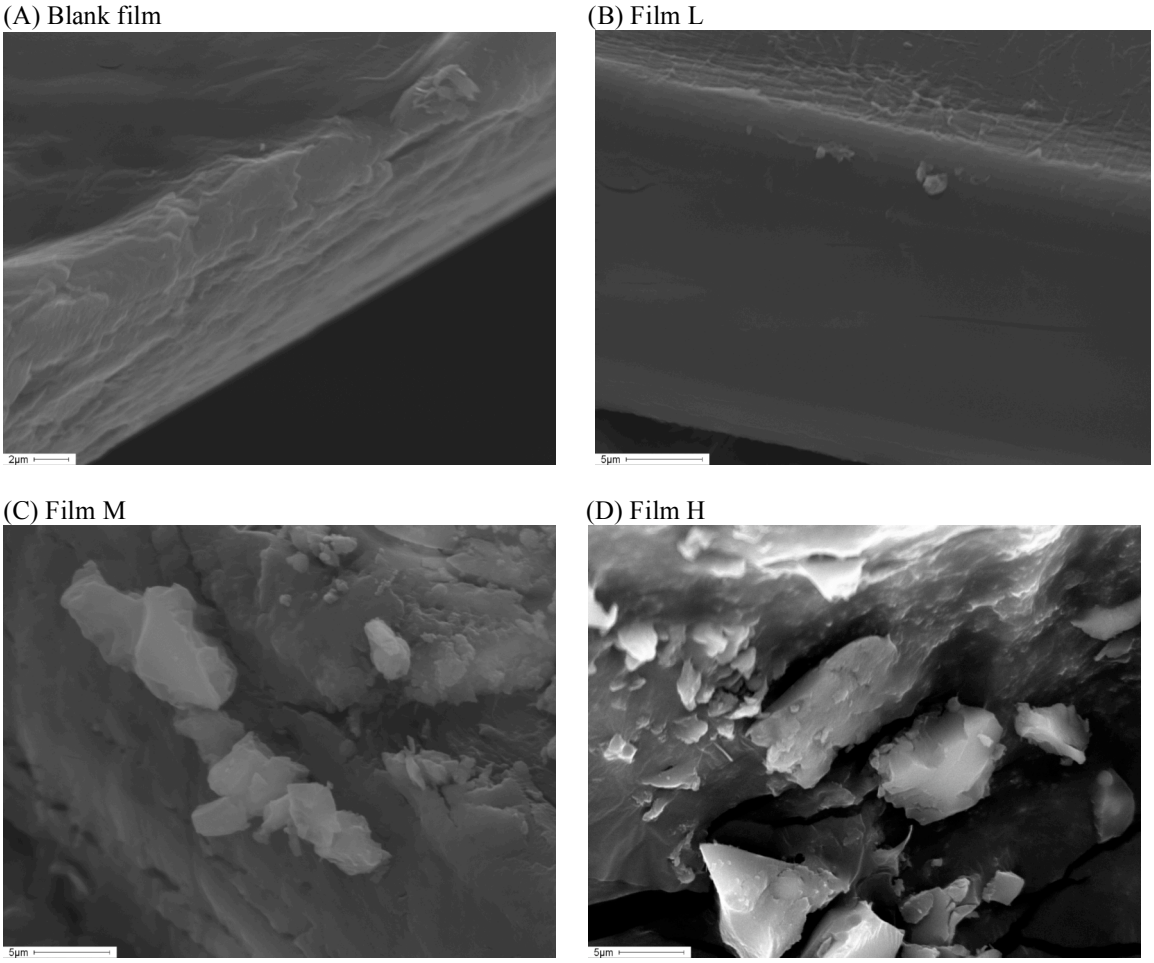

Figure 5.3 Scanning electron microscopy (SEM) image of a part of the intersected polymer **5** film in a dried state after gold coating; the blank (A), L (B), M (C), H (D) film. Polymer **4** is scattered everywhere (bulk phase and surface) in the L, M, and H films (the polymer **5**) in proportional to the amount of polymer **4** loaded in the polymerization process.

As shown **Figure 5.3,** images of the intersected parts of the films (blank, L, M, and H) as captured by scanning electron microscopy (SEM) showed that the various amounts of polymer **4** were scattered (as observed brighter islands in the film) within L, M, and H, while the blank cellulose membrane had a clean surface. The brighter polymers in the IPN were proven to possess Te (ca. 8 %) as measured by energy

dispersed X-ray analysis (EDX), where the Te content is very close to the value (7.5 %) determined by the ICP-HRMS, further confirming that polymer **4** contains the catalyst (DTDTCA, **1**). The sizes of polymer **4** regions varied up to several μm, and they were dispersed in the interior as well as exterior of polymer **5** along with an increased relative density of polymer **4** from the film L to H, as desired. Taken together, all data including IR, UV, ICP-HRMS, and SEM support that polymer **4** with the appended organoditelluride species was successfully immobilized within the cellulose membrane to form a new IPN.

5.3.2. Catalytic NO generation from RSNO species

5.3.2.1. Polymer 3-mediated NO production

To remove any unbound species, or any half of the original DTDTCA species not covalently linked to the PU backbone in polymer **3**, a small piece of film (polymer **3**) was treated with a solution of excess GSH/GSNO (see section 5.2.6 for details) prior to testing for catalytic NO generation from RSNO species. The catalytic NO generation mediated by the resulting polymer in a solution of GSH/GSNO in phosphate-buffered saline (PBS) solution, pH 7.4, containing excess EDTA (0.5 mM, which can entirely block any metal ion-induced RSNO decomposition by impurities) was demonstrated via NOA measurements (see **Figure 5.4**).

In brief, the first immersion of the polymer film into a fresh solution of GSNO/GSH yields an increase in the NO flux, which reaches a relatively low steady-state level. The NO flux returns to baseline by removing the polymer film from the solution. Subsequent re-immersion/removal cycles of the same film demonstrate that this polymer reversibly achieves nearly the same steady-state NO generation. The

demonstration of such catalytic behavior by means of the polymeric material with the appended organoditelluride species again reinforces the proposed mechanism of organoditelluride-mediated catalytic RSNO denitrosation as suggested in Chapter 4, and also supports the potential usefulness of this polymeric material as a novel NOGP. By utilizing the inherent advantages of polymer **3**, the catalytic production of biologically active NO from the surface of a biomedical grade polymeric matrix has been achieved. Hence, polymer **3** is a potential candidate NOGP for coating a variety of existing biomedical devices to improve their inherent hemocompatibility since only a very low concentration of surface NO (< 1 nM) is known to be effective to provide a thromboresistive surface.[23-26]

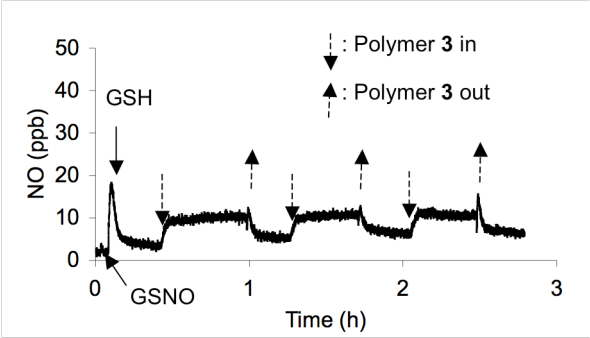

Figure 5.4 The catalytic NO generation mediated by a piece (ca. 3.9 mg and 3.2 cm^2) of polymer **3** in a solution of 100 μM GSH and 25 μM GSNO in PBS buffer, pH 7.4, (with 0.5 mM EDTA) as monitored using a chemiluminescence NO analyzer.

5.3.2.2. Polymer 4-mediated NO production

The catalytic activity of a water-soluble polymer **4** for generation of NO from RSNO was tested as well. When a catalytic amount of polymer **4** in DI water solution (50 μL of the 0.1 mg/ml solution, corresponding to ca. 0.75 μM of DTDTCA, **1**) was added into a mixture of GSH (50 μM) and GSNO (10 μM) in the PBS buffer, pH 7.4, all

NO equivalents corresponding to GSNO concentration in the reaction mixture were detected via the NOA (see **Figure 5.5**).

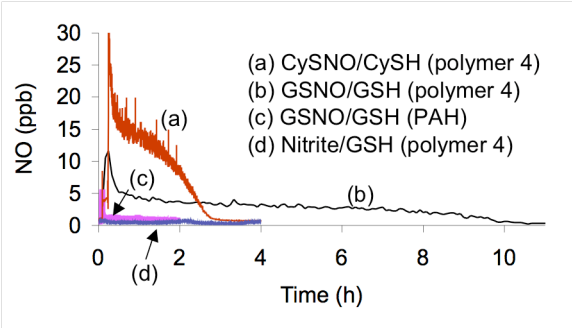

Figure 5.5 The complete denitrosations of S-nitrosothiols (10 μM) catalyzed by the water soluble polymer **4** (~0.75 μM DTDTCA, **1**) were observed via the NOA ((a) and (b)); the same amount of poly(allylamine hydrochloride) (PAH) did not catalyze the reaction (c); nitrite (1 mM $NaNO_2$) was not reduced by polymer **4** (d) (in 2 mL of PBS buffer, pH 7.4, containing 0.5 mM EDTA and 50 μM RSH).

The results obtained with a CySNO/CySH substrate solution under similar conditions also demonstrated the activity of polymer **4,** but with somewhat faster kinetics. It is worthwhile to note that nitrite ($NaNO_2$, 1 mM) was not reduced to NO under the same experimental conditions, implying that this polymer is a selective catalyst toward RSNO decomposition whereas copper ion catalysts can reduce both RSNOs and nitrite.[27] As a control experiment, when the equivalent amount of PAH (50 μL of the 0.1 mg/mL in DI water solution) was added into a new GSNO/GSH solution, a change of NO baseline was not observed, verifying that the organoditelluride species in polymer **4** is the real catalytic species (see **Figure 5.5**).

5.3.2.3. Polymer 5-mediated NO production

Polymer **5** was also studied for its catalytic denitrosation of RSNOs under comparable conditions. Indeed, several experiments with the films L, M, and H revealed

their high catalytic function in conjunction with their ability to generate diverse NO fluxes (see **Figure 5.6**) based on Te content. First, in the presence and absence of a blank film (cellulose membrane) in a GSNO/GSH solution, the baseline level of NO produced from the GSNO was not significantly changed, as shown **Figure 5.6(A)**. Trivial changes of these baselines are likely due to the intrinsic stability of RSNOs (light and thermal sensitivity).[28]

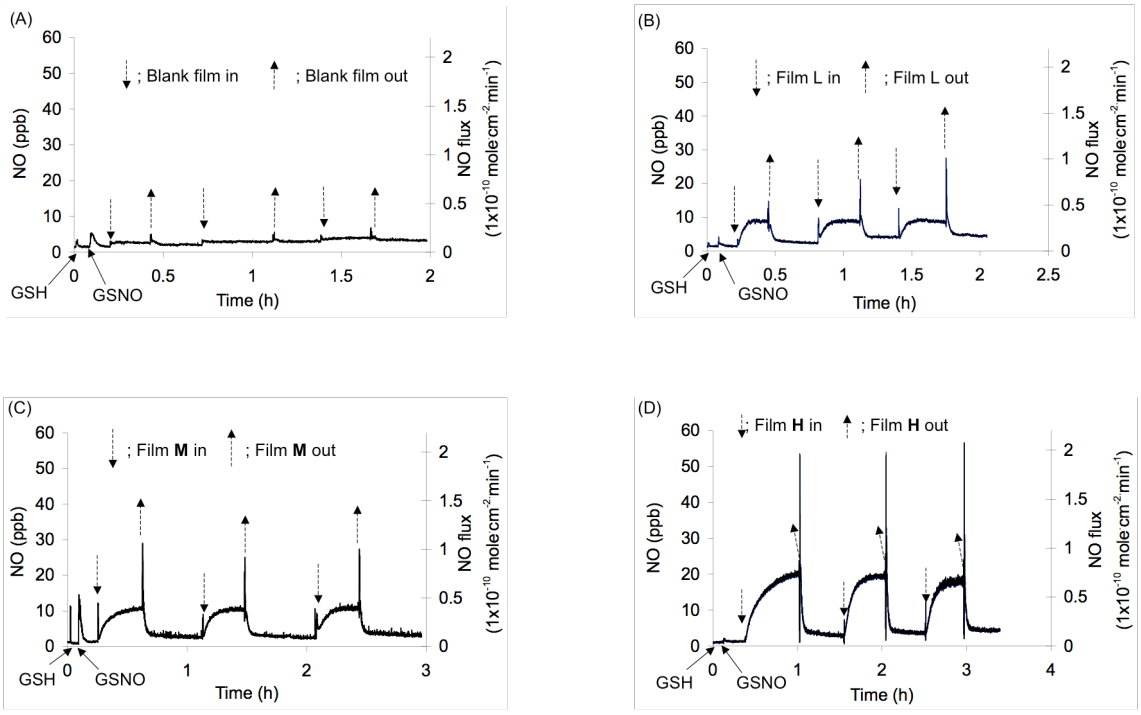

Figure 5.6 The NO generation profiles using the blank (A), film L (B), M (C), and H (D) (1 cm x 1 cm x 50 µm, polymer **5**) from GSNO (50 µM) and GSH (50 µM) in the 2 mL of PBS buffer (10 mM), pH 7.4, containing EDTA (0.5 mM) monitored via a chemiluminescence NO analyzer (NOA). Arrow indicates additions/removals of given species/film into the mixture.

Alternatively, placing the polymer **5** film L into the reaction mixture under the same conditions caused the NO signal to reach a higher steady-state value, and withdrawing the film L from the solution induced a decrease in the observed NO signal to a near baseline

value. Such a slight increase of baseline might originate from the natural decomposition of GSNO or be caused by any catalytic species leached from the membrane; e.g., a tiny amount of half of DTDTCA, **1,** in which only one carboxylic group had been linked to the PAH backbone. This species is expected to separate from the polymer backbone during the catalytic process and dissolve into the aqueous phase of the reaction mixture according to the proposed catalytic mechanism (see **Figure 4.2** in Chapter 4).[22] However, continuing the insertion/removal cycles of film L yields a similar level of NO signal at a steady-state, indicating that this film catalytically liberates NO from GSNO at physiological pH (see **Figure 5.6(B)**). Both films M and H display similar catalytic GSNO decomposition to NO under the same conditions, as shown **Figures 5.6(C)** and **(D)**. Additionally, the maximum NO flux at a steady-state was gradually enhanced from the film L to H (L < M < H), where the density of polymer **4**, i.e., DTDTCA, **1,** in the polymer **5** also increases in the same order, although the apparent NO flux does not seem to increase in direct proportion to the amount of catalyst in the various polymer **5** compositions. This is likely related to the heterogeneous nature of the catalytic process, and hence mass transfer or RSNO and RSH to the surface may become the rate-limiting step, not amount of bound catalyst. Nonetheless, this study proposes a useful approach to preparing a new type of NOGP based on IPN type films with an ability to adjust the level of NO flux emitted in the presence of a given amount of RSNO species.

5.3.4. Tellurium leaching experiment

To evaluate any potential leaching of catalytic species from polymer **5**, a soaking experiment using the H film was conducted (see section 5.2.9 for details). Approximately 10 % of Te in the film was found in the GSH/GSNO solution after 1 d, as

determined by the ICP-HRMS analysis. Thereafter, the total amount of Te leached from the film slowly increased to up to 20 % of the original amount, and apparently levelled off after 15 d (see **Figure 5.7**).

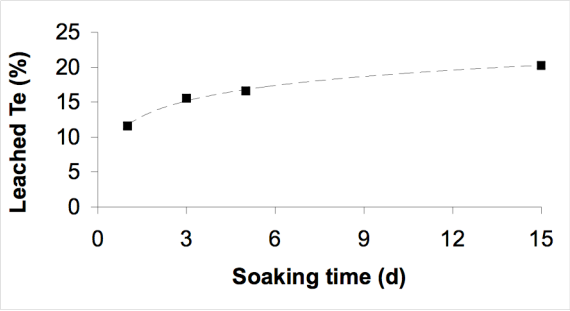

Figure 5.7. A plot of soaking time vs. the accumulated Te amount in sample solution which was withdrawn daily from the solution of 10 μM GSH/GSH with the fully immersed polymer **5**, while a fresh solution of 10 μM GSH/GSNO was correspondingly added into the original solution resulting in an increasing concentration of GSH.

This result can be explained by considering the proposed mechanism of the organoditelluride-mediated RSNO decomposition in which RSH added reduces an organoditelluride species to break the ditelluride bond. Therefore, any half side of DTDTCA, **1,** species in which only one carboxylic acid group is attached to the polymer backbone can be freed from the polymer in the presence of GSH/GSNO solution to dissolve in the aqueous phase. Further, in the same manner, even when both carboxylic groups in the DTDTCA, **1,** are linked covalently to the PAH, the GSH-mediated disconnection of ditelluride bond causes the molecular weight of polymer **4** to partially decrease; hence, some physically crosslinked polymers and/or relatively small molecular weight polymers (> 50 kD, MWCO of cellulose membrane) that have good water solubility may slowly dissolve into the GSH/GSNO solution phase until all of such polymeric species are removed from the IPN (polymer **5**). Indeed, the rate of Te leaching

was opposite to the concentration changes of GSH/GSNO solution (because of continuous addition of RSH/RSNO solution into the original solution), excluding the probability of a direct and continuous decomposition of the organoditelluride catalyst in this environment. This reinforces the proposed mechanism of organoditelluride-mediated RSNO denitrosation described in detail within Chapter 4. The result of this study suggests that effective catalytic NO production activity of polymer **5** can be achieved for extended periods of time, indicating the potential usefulness of such polymers for biomedical applications. It is clear that a large number of *in vivo* studies over varying time periods are required to fully assess the effectiveness as well as the life-time of this type of NOGP in such potential applications.

5.3.5. Spontaneous NO generation in blood

Finally, to further assess whether these new polymeric materials (polymer **5**) can mediate spontaneous NO generation in fresh whole blood, an amperometric RSNO sensor was assembled using polymer **5** (H film) as an external film on the surface of a NO selective electrochemical sensor. A control NO sensor was also fabricated with a cellulose blank film instead of the polymer **5** in analogous fashion as the experiments described in Chapters 2 and 3, to test NO generation in blood using the Cu(II)-cylcen appended polymers. Each sensor was calibrated for the intrinsic direct amperometric response to NO prior to use (see **Figure 5.8(A)**), and then simultaneously and respectively measured NO and RSNO levels in fresh sheep blood diluted with PBS buffer at 35 °C. As shown in **Figure 5.9**, each sensor exhibits independent amperometric signals, which were converted to NO equivalents by the prior NO calibration curve. The difference of NO equivalents between the two sensors indicates that the spontaneous

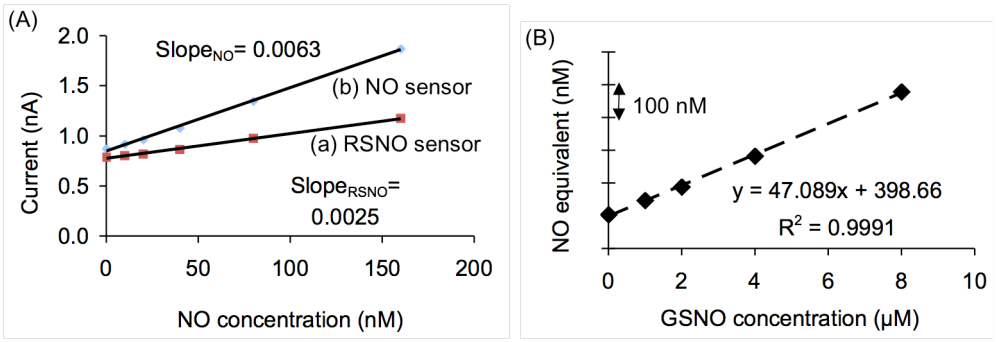

Figure 5.8 (A) Calibration curves for the inherent NO responses of both RSNO (a) and NO sensors (b) in the PBS buffer (pH 7.4, 100 mL) at 35 °C; (B) calibration curve for the inherent RSNO response of RSNO sensor (a) in a blood sample (30 mL) diluted in PBS buffer (pH 7.4, 70 mL) at 35 °C.

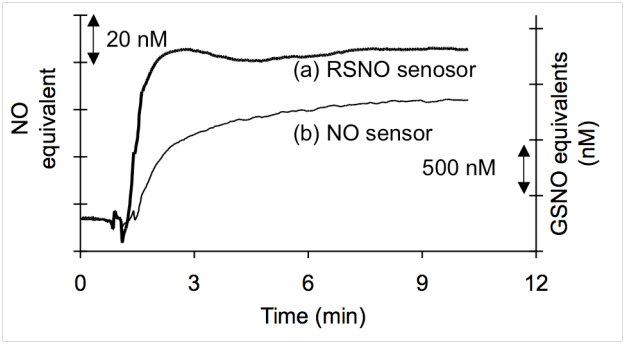

Figure 5.9. The amperometric NO measurements in a fresh sheep whole blood (30 mL) diluted with PBS buffer (70 mL, pH 7.4) at 35 °C using two sensors; RSNO (a) and NO sensor (b), where the amperometric signals were converted to the NO or GSNO equivalents (nM) from their calibration curves (see **Figure 5.8**).

denitrosation of endogenous RSNO species in the blood locally occurs at the outer membrane of RSNO sensor (but not the control sensor) in which the catalyst in the polymer **5** is exposed to the blood components (see **Figure 5.9**). Thus, this value should be proportional to the total concentration of all RSNO species in the blood, which corresponds to ~500 nM (based on GSNO calibration of the RSNO sensor from a post-calibration curve continuously obtained in the same blood sample) (see **Figure 5.8(B)**).

The ability of polymer **5** in generating NO in contact with blood *in vitro* was, herein, clearly demonstrated via the RSNO sensor measurements.

5.4. Conclusions

In summary, various polymeric materials possessing covalently linked organoditelluride species (DTDTCA, **1**) were prepared and studied for their catalytic NO generation abilities. In this work, the thermoplastic PU used to prepare polymer **3**, the water-soluble PAH for creating polymer **4**, and the IPN using the cellulose membrane for developing polymer **5,** were all shown to be useful polymeric matrices for creating NOGPs. Their catalytic activities were successfully demonstrated using the RSNOs/RSHs solutions at physiological pH via the NOA measurements. Especially exciting is the ability to the tune NO fluxes of polymer **5** materials by varying the amount of polymer **4** employed during the crosslinking reaction in the cellulose membrane. The Te leaching experiments conducted with polymer **5** indicate that most of the catalyst remains in the polymer phase even after soaking in high concentrations of fresh GSH/GSNO solution for two weeks, reinforcing the proposed mechanism for organoditelluride-mediated RSNO denitrosation as well as reflecting the potential long-term utility of the new polymers. Finally, the spontaneous NO generation in a fresh sheep blood *in vitro* mediated by polymer **5** was clearly demonstrated via amperometric NO gas sensor measurements, suggesting the usefulness of the NOGP because endogenous RSNOs and free thiol reducing agents in blood would provide the substrates necessary for such polymers to generate a surface enhanced level of NO, which could prevent platelet activation and adhesion and hence reduce the risk of thrombosis on

medical devices possessing such polymers. For example, polymer **3** can be used as a coating for the already existing biomedical devices, while the water-soluble polymer **4** may be effective as an anti-cancer agent[29, 30] as well as an alternative of anticoagulant used in a hemodialysis membrane,[31] and the polymer **5** can be applied to a membrane layer such as in the hemodialysis or in construction of RSNO sensors,[12, 13] Obviously, extensive *in vivo* studies must be carried out to fully test the effectiveness, life-time, as well as any toxicity of those new NOGPs. An RSNO sensor prepared with organoditelluride-tethered polymers will be reported soon.

5.5. References

1. Oh, B. K.; Meyerhoff, M. E., Spontaneous catalytic generation of nitric oxide from S-nitrosothiols at the surface of polymer films doped with lipophilic copper(II) complex. *Journal of the American Chemical Society* **2003,** 125, (32), 9552-9553.
2. Hwang, S.; Cha, W.; Meyerhoff, M. E., Polymethacrylates with a covalently linked Cu-II-cyclen complex for the in situ generation of nitric oxide from nitrosothiols in blood. *Angewandte Chemie-International Edition* **2006,** 45, (17), 2745-2748.
3. Kelm, M., Nitric oxide metabolism and breakdown. *Biochimica et Biophysica Acta* **1999,** 1411, (2-3), 273-289.
4. Krejcy, K.; Schmetterer, L.; Kastner, J.; Nieszpaurlos, M.; Monitzer, B.; Schutz, W.; Eichler, H. G.; Kyrle, P. A., Role of nitric-oxide in hemostatic system activation in-vivo in humans. *Arteriosclerosis Thrombosis and Vascular Biology* **1995,** 15, (11), 2063-2067.
5. Salvemini, D.; Masini, E.; Anggard, E.; Mannaioni, P. F.; Vane, J., Synthesis of a nitric oxide-like factor from L-arginine by rat serosal mast-cells - Stimulation of guanylate-cyclase and inhibition of platelet-aggregation. *Biochemical and Biophysical Research Communications* **1990,** 169, (2), 596-601.
6. Samama, C. M.; Diaby, M.; Fellahi, J. L.; Mdhafar, A.; Eyraud, D.; Arock, M.; Guillosson, J. J.; Coriat, P.; Rouby, J. J., Inhibition of platelet-aggregation by inhaled nitric-oxide in patients with acute respiratory-distress syndrome. *Anesthesiology* **1995,** 83, (1), 56-65.
7. Sarkar, R.; Webb, R. C., Does nitric oxide regulate smooth muscle proliferation? A critical appraisal. *Journal of Vascular Research* **1998,** 35, (3), 135-142.
8. Mcaninly, J.; Williams, D. L. H.; Askew, S. C.; Butler, A. R.; Russell, C., Metal-ion catalysis in nitrosothiol (RSNO) decomposition. *Journal of the Chemical Society-Chemical Communications* **1993**, (23), 1758-1759.
9. Hou, Y. C.; Guo, Z. M.; Li, J.; Wang, P. G., Seleno compounds and glutathione peroxidase catalyzed decomposition of S-nitrosothiols. *Biochemical and Biophysical Research Communications* **1996,** 228, (1), 88-93.
10. Cha, W.; Meyerhoff, M. E., Catalytic generation of nitric oxide from S-nitrosothiols using immobilized organoselenium species. *Biomaterials* **2007,** 28, (1), 19-27.
11. Wang, P. G.; Xian, M.; Tang, X. P.; Wu, X. J.; Wen, Z.; Cai, T. W.; Janczuk, A. J., Nitric oxide donors: Chemical activities and biological applications. *Chemical Reviews* **2002,** 102, (4), 1091-1134.
12. Cha, W.; Lee, Y.; Oh, B. K.; Meyerhoff, M. E., Direct detection of S-nitrosothiols using planar amperometric nitric oxide sensor modified with polymeric films containing catalytic copper species. *Analytical Chemistry* **2005,** 77, (11), 3516-3524.
13. Cha, W.; Meyerhoff, M. E., S-Nitrosothiol detection via amperometric nitric oxide sensor with surface modified hydrogel layer containing immobilized organoselenium catalyst. *Langmuir* **2006,** 22, (25), 10830-10836.

14. Zhang, H. P.; Annich, G. M.; Miskulin, J.; Osterholzer, K.; Merz, S. I.; Bartlett, R. H.; Meyerhoff, M. E., Nitric oxide releasing silicone rubbers with improved blood compatibility: preparation, characterization, and in vivo evaluation. *Biomaterials* **2002,** 23, (6), 1485-1494.
15. Smith, D. J.; Chakravarthy, D.; Pulfer, S.; Simmons, M. L.; Hrabie, J. A.; Citro, M. L.; Saavedra, J. E.; Davies, K. M.; Hutsell, T. C.; Mooradian, D. L.; Hanson, S. R.; Keefer, L. K., Nitric oxide-releasing polymers containing the [N(O)NO](-) group. *Journal of Medicinal Chemistry* **1996,** 39, (5), 1148-1156.
16. Bohl, K. S.; West, J. L., Nitric oxide-releasing hydrogels for the prevention of thrombosis and restenosis. *Circulation* **2000,** 102, (18), 734-734.
17. Kaul, S.; Cercek, B.; Rengstrom, J.; Xu, X. P.; Molloy, M. D.; Dimayuga, P.; Parikh, A. K.; Fishbein, M. C.; Nilsson, J.; Rajavashisth, T. B.; Shah, P. K., Polymeric-based perivascular delivery of a nitric oxide donor inhibits intimal thickening after balloon denudation arterial injury: Role of nuclear factor-kappaB. *Journal of the American College of Cardiology* **2000,** 35, (2), 493-501.
18. Baek, S. H.; Hrabie, J. A.; Keefer, L. K.; Hou, D. M.; Fineberg, N.; Rhoades, R.; March, K. L., Augmentation of intrapericardial nitric oxide level by a prolonged-release nitric oxide donor reduces luminal narrowing after porcine coronary angioplasty. *Circulation* **2002,** 105, (23), 2779-2784.
19. Archambault, J. G.; Brash, J. L., Protein resistant polyurethane surfaces by chemical grafting of PEO: amino-terminated PEO as grafting reagent. *Colloids and Surfaces B-Biointerfaces* **2004,** 39, (1-2), 9-16.
20. Park, K. D.; Okano, T.; Nojiri, C.; Kim, S. W., Heparin immobilization onto segmented polyurethaneurea surfaces - effect of hydrophilic spacers. *Journal of Biomedical Materials Research* **1988,** 22, (11), 977-992.
21. Stamler, J. S.; Loscalzo, J., Capillary Zone Electrophoretic detection of biological thiols and their S-nitrosated derivatives. *Analytical Chemistry* **1992,** 64, (7), 779-785.
22. Hwang, S.; Meyerhoff, M. E., Organoditelluride-mediated catalytic S-nitrosothiol decomposition. *Journal of Materials Chemistry* **2007,** 17, (15), 1462-1465.
23. Siney, L.; Lewis, M. J., Endothelium-derived relaxing factor inhibits platelet-adhesion to cultured porcine endocardial endothelium. *European Journal of Pharmacology* **1992,** 229, (2-3), 223-226.
24. Radomski, M. W.; Palmer, R. M. J.; Moncada, S., The anti-aggregating properties of vascular endothelium - Interactions between prostacyclin and nitric-oxide. *British Journal of Pharmacology* **1987,** 92, (3), 639-646.
25. Radomski, M. W.; Palmer, R. M. J.; Moncada, S., The role of nitric-oxide and cGMP in platelet-adhesion to vascular endothelium. *Biochemical and Biophysical Research Communications* **1987,** 148, (3), 1482-1489.
26. Sneddon, J. M.; Vane, J. R., Endothelium-derived relaxing factor reduces platelet-adhesion to bovine endothelial-cells. *Proceedings of the National Academy of Sciences of the United States of America* **1988,** 85, (8), 2800-2804.
27. Oh, B. K.; Meyerhoff, M. E., Catalytic generation of nitric oxide from nitrite at the interface of polymeric films doped with lipophilic Cu(Il)-complex: a potential route to the preparation of thromboresistant coatings. *Biomaterials* **2004,** 25, (2), 283-293.

28. Szacilowski, K.; Stasicka, Z., S-Nitrosothiols: Materials, reactivity and mechanisms. *Progress in Reaction Kinetics and Mechanism* **2001,** 26, (1), 1-58.
29. Hibbs, J. B.; Taintor, R. R.; Vavrin, Z., Macrophage cytotoxicity - Role for L-arginine deiminase and imino-nitrogen oxidation to nitrite. *Science* **1987,** 235, (4787), 473-476.
30. Stuehr, D. J.; Gross, S. S.; Sakuma, I.; Levi, R.; Nathan, C. F., Activated murine macrophages secrete a metabolite of arginine with the bioactivity of endothelium-derived relaxing factor and the chemical-reactivity of nitric-oxide. *Journal of Experimental Medicine* **1989,** 169, (3), 1011-1020.
31. Zhou, Z. R.; Annich, G. M.; Wu, Y. D.; Meyerhoff, M. E., Water-soluble poly(ethylenimine)-based nitric oxide donors: Preparation, characterization, and potential application in hemodialysis. *Biomacromolecules* **2006,** 7, (9), 2565-2574.

Chapter 6

Amperometric Nitrosothiol Sensor Using Immobilized Organoditelluride Species as Selective Catalyst

6.1. Introduction

S-Nitrosothiols (RSNOs) are an important group of molecules found in blood and consist of both low molecular weight (LMW) species such as S-nitrosoglutathione (GSNO) and S-nitrosocysteine (CySNO), as well as high molecular weight (HMW) RSNO macromolecules such as S-nitrosoalbumin (AlbSNO) and S-nitrosohemoglobin (HbSNO).[1] The typical biological pathway to form RSNOs is nitric oxide (NO)-mediated S-nitrosation of sulfhydryl groups in amino acids, peptides, and proteins. For example, one of the identified processes for RSNO formation involves reactions with intermediates of the NO oxidation pathway such as nitrogen dioxide (NO_2) and dinitrogen trioxide (N_2O_3) as nitrosating agents of free thiols (RSHs).[2, 3] Nitrosylated metal centers (copper or iron)[4, 5] as well as a radical adducts of RSH and NO (RS-N$^{\bullet}$-OH)[6] are also recognized intermediates in the production of RSNOs in the presence of an electron accepter. Additionally, another important conduit for RSNO formation is the reallocation of NO from species to species through exchange with sulfhydryl groups, which is termed transnitrosation.[7]

Endogenous RSNOs have been recognized as a molecular vehicle to transfer and store transient NO molecules produced enzymatically by nitric oxide synthase (NOS) within endothelial and other cells. Nitric oxide participates in many physiological processes ranging from cytoprotection to cytotoxicity. In fact, endogenous RSNOs exhibit many of the same physiological functions as NO, such as inhibition of platelet aggregation[8] and relaxation of vascular smooth muscles.[9] RSNOs are also known to participate in host defense processes such as killing tumors[10] and intracellular pathogens,[11] in addition to intracellular signaling,[12] ion channel regulation,[13, 14] apoptosis,[15, 16] etc. Hence, the decrease or increase in the physiological production of NO, which appears to occur in certain diseases such as atherosclerosis, hypertension, and diabetes, has been associated with not only a dysfunctional endothelium cell layer,[17-20] but also the improper storage and/or delivery of NO by means of RSNOs.[21, 22] Indeed, an inverse correlation between NO and RSNO concentrations have been recently reported in specific NO-related disorders. For instance, the suppressed NO levels due to the endothelial dysfunction caused by oxidative stress (typically by lack of adequate ascorbate) are characteristic of preeclampsia,[23, 24] a pregnancy-specific syndrome known for the major cause of both maternal and fetal morbidity and mortality, where the RSNO levels in preeclampsia plasma were found to be higher compared with normal pregnancy and nonpregnancy plasma.[22] Further, it has been reported that while NO concentrations are generally higher in the expired air of asthma patients (vs. controls), a recent study showed that the average RSNO levels of the expired air in asthmatic children were lower than in normal children.[21] In addition, a recent report demonstrated that patients who had more risk factors for heart attacks and strokes had a lower level of RSNOs in their

blood, presumably since these risk factors (high cholesterol, high blood pressure, smoking, etc.) contributed to endothelial dysfunction in these individuals.[25] Therefore, the detection and monitoring of endogenous RSNO levels have become of great interest for the purpose of disease diagnosis and treatment as well as risk assessment.

There are several known approaches to measure RSNO species. Fundamentally, NO oxidative products (NO, NO_2^-, and/or NO_3^-) resulting from the reductive reaction of RSNOs using redox-active species (iodine/iodide, cysteine/$CuCl_2$, VCl_3/HCl, or ferricyanide, etc.) can be detected by chemiluminescence or electrochemical methods.[26-29] Sometimes, these NO products react with reagents to form a detectable product (Griess nitrite reagent or fluorescent chemicals) that can be quantitated by spectrophotometric or flourometric assays.[30, 31] Despite the good sensitivity of present approaches (especially chemiluminescence based assays), their ability to quantify RSNOs accurately are often doubted because all existing methods require a number of tedious pretreatment or separation steps to eliminate interfering substances (e.g., nitrite, antioxidants, and/or proteins, etc.).[30, 32-34] Since RSNOs are known to be highly labile molecules that can decompose in the presence of light or trace metal ions,[35, 36] such pretreatment steps can lead to loss of the analyte.

To deal with the accuracy problems as well as existing complicated procedures, recent research in this laboratory has proposed the direct measurement of RSNO levels in fresh whole blood samples via planar amperometric RSNO sensors.[37, 38] These sensors are prepared by immobilizing a nitric oxide generating polymer (NOGP) at the surface of a highly selective amperometric NO sensor.[39, 40] As described in this thesis, the NOGP, a polymeric material appended with an NO generating catalyst, can spontaneously

denitrosate RSNOs to NO when in contact with blood to locally increase the NO concentration at the surface of the polymer layer. Hence, the amperometric NO sensor with the immobilized NOGP can detect the locally elevated NO levels in proportional to RSNO concentrations in blood. Thus far, a variety of polymeric materials immobilized with copper(II) species and organodiselenides (RSeSeR), compounds known for their NO generating capability,[41, 42] have been utilized to fabricate RSNO sensors.[37, 38] Results have indicated that the sensor performance is largely dependent on the characteristics of the NO generating catalyst. For example, the copper based RSNO sensors exhibit significantly different amperometric sensitivities to various LMW RSNO species,[37] while the organodiselenide-based RSNO sensor displays comparable sensitivities to all LMW RSNOs.[38] Hence, research regarding the fundamental reaction chemistry between RSNO species and potential NO generating catalysts is very important with respect to understanding the potential reactivity of endogenous RSNOs as well as to develop NOGPs for a variety of biomedical applications, including the preparation of new RSNO sensors.

Polymeric materials linked with an organoditelluride (RTeTeR) species have recently been developed as a new type of NOGP (see Chapter 5). In this chapter, a detailed study on the use of such an organoditelluride-tethered polymer as an immobilized selective catalytic layer for the development of a useful RSNO sensor is presented. Amperometric NO sensors fabricated as described previously[38] (and in Chapter 3) are modified with a dialysis membrane consisting of an impregnated organdoditelluride-linked hydrogel (see **Figure 6.1**), in which poly(allylamine hydrochloride) (PAH) with covalently attached 5'-ditelluro-2,2'-dithiophenecarboxylic

acid (DTDTCA) is further crosslinked on a dialysis membrane support. The NO gas produced from the RSNO decomposition via this polymeric layer diffuses through a gas permeable membrane (teflon) of the NO sensor to a platinized platinum anode, where it is oxidized and the resulting current in proportional to the RSNO levels present.

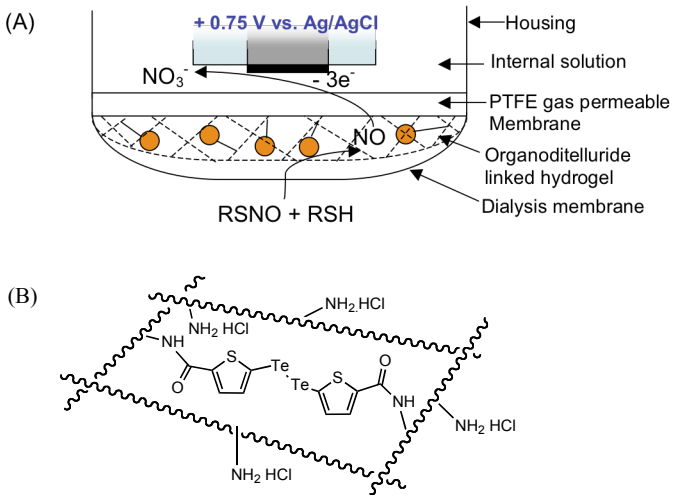

Figure 6.1 (A) Schematic of RSNO detection using the proposed amperometric sensor modified with a NO generating catalytic layer; (B) the schematic structure of organoditelluride-linked hydrogel used in this work.

It will be shown that this new RSNO sensor configuration is able to directly detect various LMW RSNO species at 0.1 μM levels, with an excellent operational life-time (up to a month). In addition, speculation regarding transnitrosation between RSNO/RSHs is discussed with respect to the potential to detect higher molecular weight RSNOs. Finally, the measurement of RSNO species in the fresh animal blood sample is demonstrated via this device.

6.2. Experimental

6.2.1. Materials

Dialysis membranes were purchased from Spectrum Laboratory Inc. (Rancho Dominguez, CA). Bovine serum albumin (BSA, gamma-globulin and protease free, fatty acid content = 0.005 %), glutaraldehyde (25 wt %), N-(3-dimethylaminopropyl)-N'-ethylcarbodiimide hydrochloride (EDC·HCl), N-hydroxysuccinimide (NHS), N-acetyl-penicillamine (NAP), glutathione (GSH) and cysteine (CySH) were products of Sigma (St. Louis, MO). All other chemicals including poly(allylamine hydrochloride) (PAH, Avg. M.W.= 15 kD) from Aldrich (Milwaukee, WI) and solvents from Fisher Scientific (Fair Lawn, NJ) were used without further purification unless otherwise noted. Distillation was employed for the purification of Et_3N, and THF prior to use. DI water was prepared by a Milli-Q filter system (18 MΩ cm^{-1}: Millipore Corp., Billerica, MA, USA).

6.2.2. Preparation of S-nitrosothiols

S-Nitrosocysteine (CySNO), S-nitroso-N-acetyl penicillamine (SNAP), and S-nitosoglutathione (GSNO) solutions were prepared according to the method described in the literature (see also Chapter 2).[43] All solutions were freshly prepared in a timely-manner as needed from stock solutions prepared daily. S-Nitroso-albumin (AlbSNO) was also prepared using BSA as previously reported.[44] The concentration of AlbSNO was determined by using a chemiluminescence NO analyzer (NOA) (Seivers 280, Boulder, CO) and excess copper ions to quantitatively liberate the NO.[37]

6.2.3. Preparation of the organoditelluride-linked hydrogel

The conjugation of 5'-ditelluro-2,2'-dithiophenecarboxylic acid (DTDTCA, refer to **Figure 6.1** for the structure; prepared as described in Chapter 4) with poly(allylamine hydrochloride) (PAH) was carried out via an EDC coupling chemistry according to the method described in Chapter 5. The resulting polymer was analyzed to possess 7.5 wt % of Te, as determined by inductively coupled plasma-high resolution mass spectrometry (ICP-HRMS). The general method used to prepare the catalytic hydrogel layer within a dialysis membrane that could be mounted over the outer gas permeable membrane of the amperometric sensor was a slightly modified procedure of that described in Chapter 5. In brief, a small volume (40 μL) of a mixture (DTDTCA-tethered PAH (0.2 mL, 4 wt %), Et_3N (0.1 mL, 1 wt %), and glutaraldehyde (0.1 mL, 1 wt %) in DI water) was placed onto a dried dialysis membrane (MWCO, 50 kD; 1 cm^2) previously purified by extensively washing with 0.1 mM EDTA solution to eliminate metal ion impurities within the membrane, and then further washing with DI water. The resulting membrane was allowed to stand a few days at RT and washed with DI water prior to use.

6.2.4. Fabrication of amperometric RSNO/NO sensors

Amperometric NO sensors were fabricated according to the procedures described in Chapters 3 and 5. A control NO sensor was fabricated by mounting a plain dialysis membrane over the gas permeable membrane of the NO sensor, while the organoditelluride-linked hydrogel impregnated dialysis membrane was employed as the outer layer to fabricate the RSNO sensor.

6.2.5. Detection of S-nitrosothiols

All measurements of RSNO solutions were carried out in PBS buffer (10 mM, pH 7.4) containing 0.1 mM EDTA (necessary to sequester metal ion impurities, especially copper ions known to be an excellent catalyst for RSNO decomposition) in a brown amber vial (100 mL) at RT. Prior to use, calibration curves for both the RSNO and NO sensors were obtained by measuring their intrinsic amperometric responses toward a NO standard solution. The background NO levels in bulk RSNO solutions were also monitored via the NO sensor, as needed, by simultaneously placing both the RSNO and NO sensors into the same solution and then converting to NO concentrations based on the prior calibration curve for each sensor using the standard NO solutions. The long-term stability of the RSNO sensor was determined by assessing the sensitivity of amperometric response toward GSNO (using GSH as reducing agent) every few days.

6.2.6. Detection of RSNOs in blood

The experimental methods for the detection of endogenous RSNOs in animal blood were analogous to those reported previously in the literature[37, 38] (and as described in Chapters 2 – 5). In brief, heparinzied fresh sheep blood (obtained from Extracorporeal Membrane Oxygenation (ECMO) laboratory at the University of Michigan Medical School) was kept at 35 °C before and during the experiments. Both NO and RSNO sensors were pre-calibrated to determine their inherent amperometric NO response in stirred PBS buffer (pH 7.4) at 35 °C. Then, the amperometric signal of each sensor was monitored by adding the fresh sheep blood (30 mL) into the PBS buffer, pH 7.4 (70 mL, saturated with N_2) containing GSH and EDTA (final concentrations of 50 μM and 0.1 mM, respectively, after the blood was added). For the estimation of RSNO concentrations in blood, the RSNO sensor's inherent response to the exogenous GSNO

was post-calibrated by injecting the GSNO standard solution in the same blood sample (i.e., standard addition method).

6.3. Results and discussion

6.3.1. RSNO sensor performance

Due to the catalytic activity of organoditelluride species and corresponding polymeric materials that possess covalently linked RTe sites in denitrosating RSNOs (see Chapters 4 and 5), an amperometric NO sensor with an external dialysis membrane containing an organoditelluride-linked polymer is expected to detect NO and RSNO levels in test samples. An electrochemical NO sensor covered with a "blank" dialysis membrane should only detect NO concentrations in the same samples. Thus, to evaluate the basic analytical performance of the proposed RSNO sensor, both an RSNO and NO sensor were prepared and tested for their direct response toward NO and various RSNO species.

For preliminary studies, both sensors were concurrently placed in a working buffer solution containing a suitable reducing agent (50 μM GSH) (along with 0.1 mM EDTA in phosphate buffered saline (PBS), pH 7.4) and were monitored for their amperometric responses toward added NO or GSNO solutions as shown in **Figure 6.2**. The expected current responses of both sensors toward added NO standard solution confirmed their suitable function for amperometric NO detection (see **Figure 6.2(A)**). The intrinsic NO sensitivities obtained from this experiment can be used to prepare

calibration curves for each sensor to convert the current values recorded for each device into NO equivalent levels.

Upon adding increasing concentrations of GSNO into a fresh working buffer solution (with added GSH), the RSNO sensor displays a significant current change in proportional to the GSNO levels present (see **Figure 6.2(B)**), while the current of the "control" NO sensor in the same solution does change appreciably. This confirms that the presence of the organoditelluride polymer immobilized within the dialysis membrane mounted over the gas permeable membrane is responsible for the catalytic conversion of GSNO to NO at the surface of the RSNO sensor.

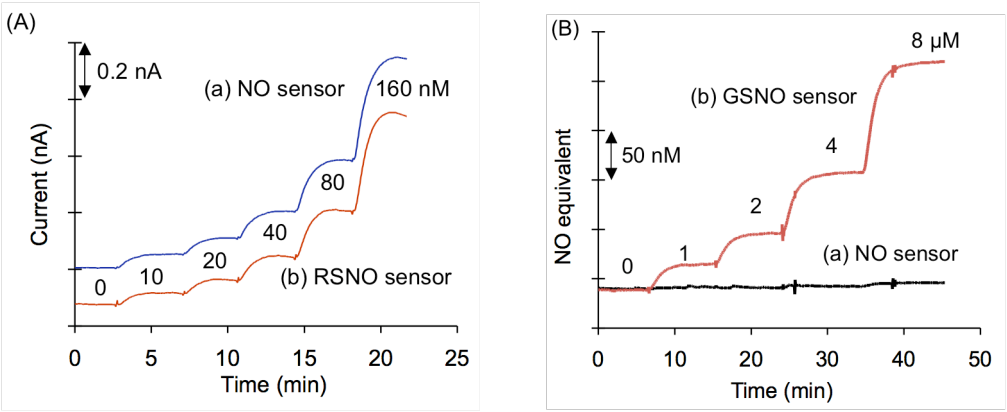

Figure 6.2 The inherent amperometric responses of (a) NO and (b) RSNO sensor monitored by intermittently adding a small aliquots of a standard (A) NO or (B) GSNO solution into the stirred solution of PBS buffer, pH 7.4, containing 0.1 mM EDTA and 50 μM GSH at RT (the working buffer solution); the numbers in the graph indicate the accumulated concentrations of the given species in the working buffer solution.

Such catalytic function of the organoditelluride-linked hydrogel on the surface of the RSNO sensor was also demonstrated by performing a real-time reversibility test. As shown in **Figure 6.3**, the RSNO sensor dynamically responded to the change of GSNO

concentrations in real-time as concentration is increased and then decreased within the same test vessel.

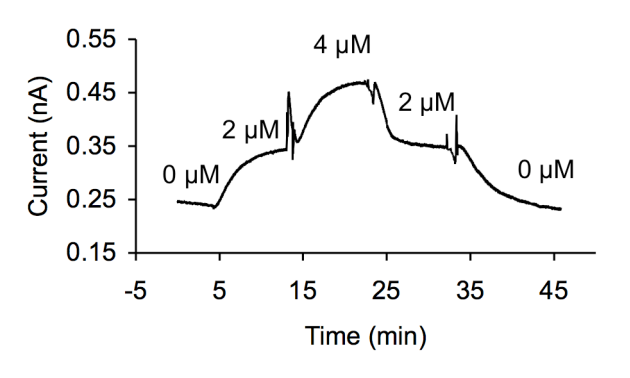

Figure 6.3 The dynamic amperometric response and reversibility of RSNO sensor by exchanging three different concentrations (0, 2, and 4 µM) of GSNO in working buffer solution at RT.

When comparing the relatively short response times (2 - 4 min) for both sensors to reach the steady-state current levels with respect to NO concentrations (see **Figure 6.2(A)**), a somewhat slower response (4 – 8 min) toward changes in GSNO concentrations was observed with the RSNO sensor, suggesting that the dialysis membrane filled with the crosslinked catalytic polymer (thickness, 20 - 40 µm) acts as a diffusion barrier for mass transfer of GSNO/GSH species into the catalytic layer, and this leads to the slower dynamic response. A design in which the catalyst is immobilized directly on the outer surface of dialysis membrane of the NO sensor would likely yield better dynamic response times. It is important to note, however, that the response time of the proposed RSNO sensor reported herein is comparable to a previously reported organdodiselenide-based RSNO sensor[38] also prepared using an outer dialysis membrane

to immobilize the polymeric catalyst (i.e., the catalytic layer was between the gas permeable membrane and dialysis membrane, see **Figure 6.1**).

The main advantage of the RSNO sensor prepared with the immobilized organoditelluride species is a very long operational lifetime (up to a month), which was determined by frequently monitoring the sensitivity (nA/μM) changes in response to both NO and GSNO. Remarkably, the sensitivity for the GSNO response is nearly maintained with time while only a slight decrease in the NO response originating from the platinized platinum working electrode. Hence, this behavior yields a small increase in the relative sensitivity for GSNO vs. NO response as a function of time ($Sensitivity_{GSNO}/Sensitivity_{NO}$) (see **Figure 6.4)**.

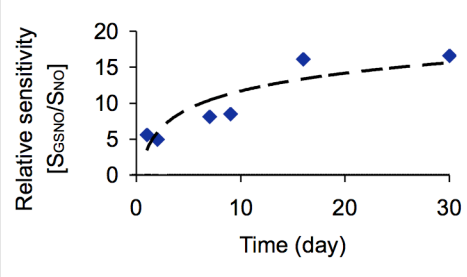

Figure 6.4 Stability of RSNO sensor, plotted as relative sensitivity (S_{GSNO}/S_{NO}) of the RSNO sensor as a function of time, where S_{GSNO} is the sensitivity (nA/μM) of RSNO sensor toward GSNO and S_{NO} is the sensitivity (nA/μM) of RSNO sensor toward NO.

The excellent stability of the proposed RSNO sensor compared to any of the previously reported amperometric RSNO sensors modified with NO generating catalysts (e.g., copper[37] and/or organodiselenide[38]-based RSNO sensor; up to 2 weeks) likely stems from the greater stability of the active organoditelluride species (DTDTCA) employed within the catalytic layer of this sensor. Considering the redox mechanism involved for NO generating catalysts (i.e., copper ions, RSeSeR, or RTeTeR), the least

stable forms of the catalysts (i.e., Cu(I), RSe^- (selenolate), or RTe^- (tellurolate)) in their redox cycles very likely determine their catalytic lifetimes, which is reflected in the RSNO sensors' stabilities. In fact, the organoditelluride species (DTDTCA) used in this study possesses a unique structure that can be further stabilized in the reduced form (RTe^-, where R = thiophenecarboxylic acid) by the aromatic resonance that can occur (see **Figure 6.1(B)**). This decreases the possibility of side reactions to form Te (Se) element and/or the adduct of small molecular thiolate (RS^-, a reducing agent), $RSTe^-$ ($RSSe^-$)[45, 46] that can be washed out from the membrane phase. Indeed, the amperometric RSNO sensors reported in previous studies did not possess such a structural benefit for the NO generating catalyst, resulting in reduce long-term stability.[38] Further, the fact that RSNO sensitivity can actually remain the same while the inherent amperometric NO response of the RSNO sensor decreases with time suggests that the mass transfer into the catalytic layer of the RSNO and reducing agent may actually increase as a function of time, as the layer becomes more fully hydrated and the crosslinked catalytic polymeric material reorganizes and/or the cellulose membrane hydrolyzes.

6.3.2. Direct amperometric detection of S-nitrosothiols

As depicted in **Figures 6.5** and **6.6**, the new organoditelluride-based RSNO sensor is capable of directly detecting various RSNO species from sub-μM to μM levels, which are the suggested ranges for RSNO species in blood,[47] although their exact concentrations in blood plasma are still in debate.[48, 49] The measurements of RSNO species by the sensor exhibit reasonable detection limits (~0.1 μM) with respect to the LMW RSNOs including GSNO, CySNO, and SNAP. An attractive feature of the proposed RSNO sensor is that the responses toward GSNO and CySNO were nearly

equal in the range of 0.1 – 4 µM as illustrated by their respective calibration curves (see **Figures 6.6(A)** and **(B)**).

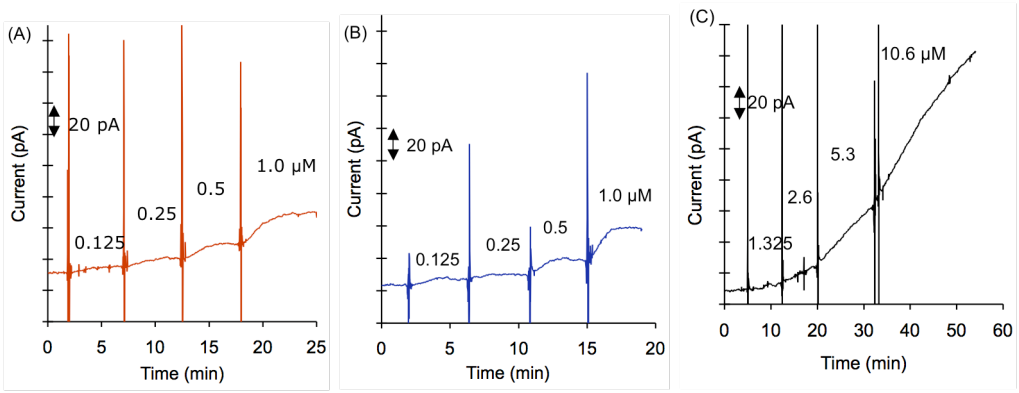

Figure 6.5 The typical dynamic amperometric responses detected by the RSNO sensor at low concentrations of various RSNOs, known as endogenous RSNO species in blood ((A) GSNO, (B) CySNO, and (C) AlbSNO) in the working buffer solution at RT.

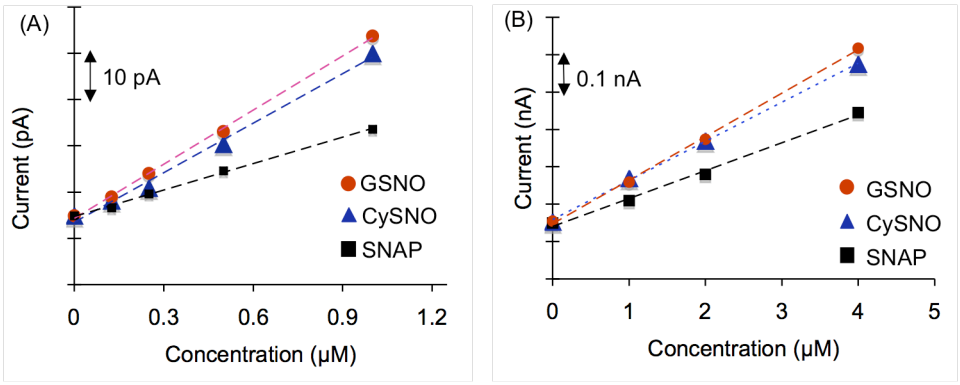

Figure 6.6 Calibration curves for the representative low molecular weight (LMW) RSNOs with various concentrations ((A) sub-µM, (B) µM levels) in the working buffer solution at RT.

Such homogeneous responses toward the various LMW endogenous RSNOs were reported previously for low concentrations (≤ 1 µM) of RSNOs using orgnodiselenide-based RSNO sensor.[38] In contrast, the Cu-based RSNO sensor reported earlier exhibits a

much greater amperometric response toward CySNO than GSNO as well as other RSNO species.[37]

6.3.3. Role of transnitrosation reaction in amperometric response

An interesting phenomenon observed in the detection of AlbSNO is that the current signals continuously increase, without yielding a final steady-state response (see **Figure 6.5(C)**). Due to the large molecular weight of AlbSNO (69 kD) compared to the molecular cutoff (MWCO, 50 kD) of the dialysis membrane mounted on the RSNO sensor, it is unlikely that AlbSNO passes through this membrane and reacts directly with the organoditelluride catalyst. However, a transnitrosation reaction between AlbSNO and excess GSH reducing agent (50 μM GSH is already present in the working buffer solution) can provide a low molecular RSNO species from the higher molecular weight AlbSNO species.[50] This speculation is further confirmed by employing CySH in place of GSH as a reducing agent in the working buffer (see **Figure 6.7**). In this case, the calibration curves for LMW RSNOs measured by the RSNO sensor (see **Figrue 6.7(A)**) exhibit enhanced sensitivities in the presence of CySH compared to GSH, in addition to a reversed order of sensitivity in the case of SNAP.

Such increases in the sensitivity toward the LMW RSNOs are also likely associated with a transnitrosation reaction, because the current signals for LMW RSNOs at various concentrations in the presence of CySH respond much slower in reaching steady-state amperometric signals (compared to when using GSH as reducing agent), especially, the very long response time with respect to SNAP additions. **Figure 6.7(B)** clearly shows the effects of various CySH concentrations on the real-time detection of a fixed concentration of GSNO when compared directly using GSH as the reducing agent

via the exact same RSNO sensor. The elongated response time that appears when CySH is employed as a reducing agent implies that the transnitrosation reaction plays a significant role in creating the increase of surface NO levels and the apparent increase in sensitivity of the proposed RSNO sensor. In fact, it has been reported that CySH and its residues in many proteins are widely involved in biological transnitrosation reactions.[51, 52] Thus the equilibrium constant for transnitrosating reaction with cysteine is likely more favorable than for GSH.[50, 53, 54]

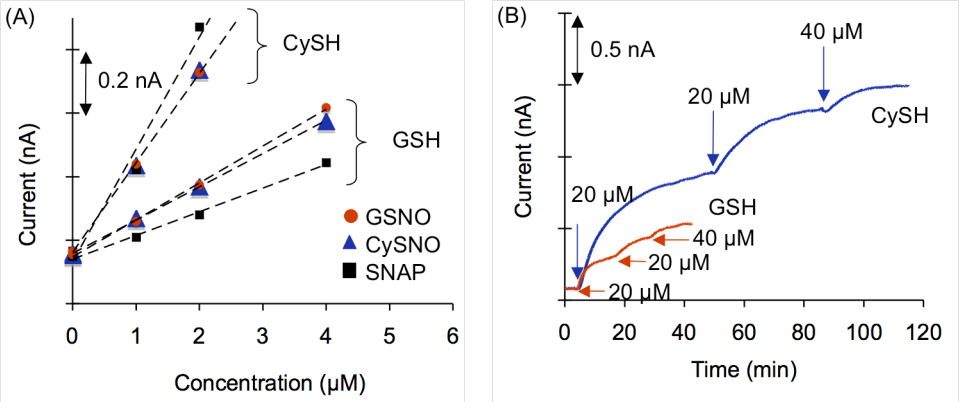

Figure 6.7 (A) Calibration curves for GSNO, CySNO, and SNAP as measured with new RSNO sensor in the presence of a different reducing agents (GSH or CySH) in the working buffer solution at RT; (B) The real-time measurements of GSNO (4 μM) via the RSNO sensor by injecting GSH or CySH in the working buffer solution at RT; arrows indicate the time the corresponding RSH concentration is added.

In contrast, any considerable S-nitrosylation of GSH from the GSNO, CySNO, or SNAP is not obvious from the response patterns observed, which is also supported by the fact that a significant background NO level in the bulk solution is not detected by the NO sensor when simultaneously monitored with the RSNO sensor in the same solution (see **Figure 6.2(B)**). However, as shown **Figure 6.5(C)**, the S-nitrosylation of GSH from AlbSNO as an analyte does appear to take place.[50] Therefore, there are somewhat

complicated relationships of S-nitrosylation between endogenous RSNOs, which are important in understanding the characteristics of RSHs/RSNOs in biological systems. Although further studies are necessary to fully understand the transnitrosation equilibria involved between all endogenous RSH/RSNO species, based on the observed experimental results presented here, the proposed RSNO sensor can directly detect various LMW RSNOs at low concentrations (0.1 – 4 μM) in the presence of GSH (50 μM), and there is also some sluggish yet considerable amperometric response observed toward protein RSNOs due to transnitrosation chemistry with the added reducing agent (GSH).

Another interesting observation made in this work is the effect of GSH concentration on the observed sensitivity of the proposed RSNO sensor. As discussed in Chapter 4, the reducing agent, RSH, participates in the rate-determining step of organoditelluride-mediated RSNO denitrosation reaction (see **Figure 4.2** in Chapter 4). Hence, the RSNO sensor's sensitivity is expected to be influenced by the concentration of RSH in the working buffer. Indeed, as shown **Figure 6.7(B)**, the addition of GSH (up to 40 μM) into the working buffer solution greatly improves the sensitivity of the RSNO sensor without changing the response time. At higher concentrations of GSH, the effect levels off, and saturates, with no change in observed response to further increase in the concentration of GSH. Therefore, the amount of GSH recommended for use in the working buffer (50 μM) seems appropriate to detect various RSNO species with optimal sensitivity.

6.3.4. Direct detection of endogenous S-nitrosothiols in blood

Initially, both the RSNO and NO sensors, which were pre-calibrated for their inherent responses with respect to a NO standard solution (see **Figure 6.8**), were concurrently placed in a new working buffer solution (70 mL) at 35 °C and their baseline amperometric signals were recorded. Upon adding the fresh sheep whole blood (30 mL) into the working buffer solution, the RSNO sensor detects the RSNO/NO levels in the blood sample, while the control NO sensor only detects the NO levels in the same blood sample (see **Figure 6.8**). The change in current signal observed between the two sensors can be converted to the NO equivalent levels by means of the prior NO calibration curves, yielding a noticeable gap between two sensors in terms of surface NO concentrations detected, as represented by Δ value (~60 nM NO concentration) in **Figure 6.9(A)**.

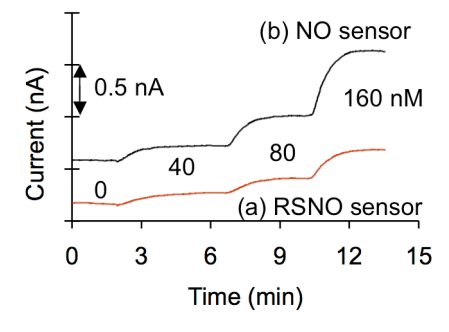

Figure 6.8 Calibration curves of both the (a) RSNO and (b) NO sensors for the individual current responses toward the NO standard solutions added in the working buffer solution at 35 ºC, where the sensitivities were calculated to be 6.8 nA/μM for the NO sensor and 3.3 nA/μM for the RSNO sensor.

Finally, the injection of a GSNO standard solution into the same blood sample illustrates clearly that the two sensors exhibit their expected functions, with the RSNO

sensor having significant response, while little or no response is seen from the control NO sensor in the same blood sample after the RSNO additions (see **Figure 6.9(B)**). From the initial response of he RSNO to the added blood, and the change in current detected when the sample is further spiked with several additions of GSNO, it is possible to utilize the method of multiple standard addition[55, 56] to determine the total GSNO equivalent concentration in the original blood sample.

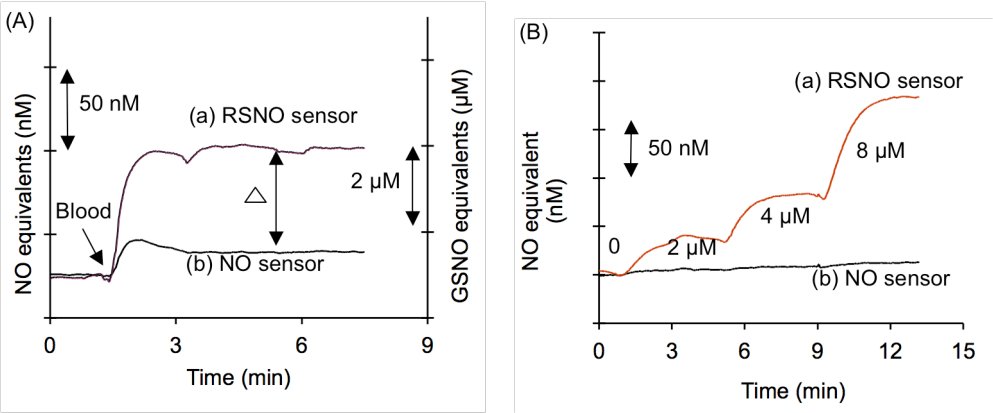

Figure 6.9 (A) The real-time amperometric detections using both the (a) RSNO and (b) NO sensors for endogenous RSNOs in the sheep whole blood sample in the working buffer solution at 35 ºC (30 mL blood, 70 mL PBS buffer, 50 μM GSH, and 0.1 mM EDTA); arrow indicates the moment the fresh sheep whole blood was injected; (B) calibration curves of two ((a) RSNO and (b) NO) sensors for their intrinsic amperometric responses toward GSNO standard solutions added in the same blood sample at 35 ºC.

Based on the NO and GSNO calibration curves, the current difference between the two sensors translates to ~2.6 μM GSNO equivalents in the sheep blood. Given the studies shown above (see **Figure 6.5(C)**) some fraction of this value would come from the AlbSNO present in the blood, which yields amperometric response via the transnitrosylation chemistry with the GSH reducing agent. If conditions can be found

where this reaction proceeds with near 100% efficiency, then the sensor value reported would be a measure of the total RSNO species in the plasma phase of the blood. Efforts to find conditions where such high efficiency takes place are currently in progress.

6.4. Conclusions

In this work, a new type of RSNO sensor has been prepared by employing a crosslinked organoditelluride-tethered PAH polymer within a dialysis membrane support mounted as an outer layer of a planar amperometric NO sensor. Due to the catalytic activity of organoditelluride-linked hydrogel for the decomposition of RSNO species to NO in the presence of appropriate RSH reducing agent, various LMW RSNO/RSH species that can pass through the diffusion barrier and liberate NO to increase the local NO levels within this catalytic layer, results in an increase in current proportional to the RSNO concentration present in solution. Compared to previously reported RSNO sensors based on immobilized Cu(II), organodiselenide and enzyme layers,[57] this new organoditelluride modified sensor has a much longer operational lifetime, presumably due the the enhanced stability of the catalyst employed. It has been further shown that a transnitrosation reaction between high molecular weight RSNO species and the necessary low molecular weight thiol reducing agent, actually yields an increase in LMW RSNO in the test solution that allows some amperometric response to the HMW AlbSNO species. The sensor provides an output signal in diluted whole blood samples that is likely proportional to the level of total RSNO species in the plasma phase of the blood sample. With further optimization of response times and more studies to determine conditions

where the catalytic layer can directly liberate NO from HMW endogenous RSNOs by changing the sensor configurations and/or via more efficient transnitrosation reactions, the proposed sensor could ultimately provide a useful new tool for rapidly determining total RSNO species concentrations whole blood samples, without pretreatment steps that can dramatically alter the levels of RSNO detected by other methodologies.

6.5. References

1. Kelm, M., Nitric oxide metabolism and breakdown. *Biochimica et Biophysica Acta* **1999,** 1411, (2-3), 273-289.
2. Kharitonov, V. G.; Sundquist, A. R.; Sharma, V. S., Kinetics of nitrosation of thiols by nitric-oxide in the presence of oxygen. *Journal of Biological Chemistry* **1995,** 270, (47), 28158-28164.
3. Wink, D. A.; Nims, R. W.; Darbyshire, J. F.; Christodoulou, D.; Hanbauer, I.; Cox, G. W.; Laval, F.; Laval, J.; Cook, J. A.; Krishna, M. C.; Degraff, W. G.; Mitchell, J. B., Reaction-kinetics for nitrosation of cysteine and glutathione in aerobic nitric-oxide solutions at neutral pH - Insights into the fate and physiological-effects of intermediates generated in the NO/O^{-2} reaction. *Chemical Research in Toxicology* **1994,** 7, (4), 519-525.
4. Gow, A. J.; Stamler, J. S., Reactions between nitric oxide and haemoglobin under physiological conditions. *Nature* **1998,** 391, (6663), 169-173.
5. Inoue, K.; Akaike, T.; Miyamoto, Y.; Okamoto, T.; Sawa, T.; Otagiri, M.; Suzuki, S.; Yoshimura, T.; Maeda, H., Nitrosothiol formation catalyzed by ceruloplasmin - Implication for cytoprotective mechanism in vivo. *Journal of Biological Chemistry* **1999,** 274, (38), 27069-27075.
6. Gow, A. J.; Buerk, D. G.; Ischiropoulos, H., A novel reaction mechanism for the formation of S-nitrosothiol in vivo. *Journal of Biological Chemistry* **1997,** 272, (5), 2841-2845.
7. Hogg, N., The kinetics of S-transnitrosation - A reversible second-order reaction. *Analytical Biochemistry* **1999,** 272, (2), 257-262.
8. Pawloski, J. R.; Swaminathan, R. V.; Stamler, J. S., Cell-free and erythrocytic S-nitrosohemoglobin inhibits human platelet aggregation. *Circulation* **1998,** 97, (3), 263-267.
9. Ignarro, L. J.; Lippton, H.; Edwards, J. C.; Baricos, W. H.; Hyman, A. L.; Kadowitz, P. J.; Gruetter, C. A., Mechanism of vascular smooth-muscle relaxation by organic nitrates, nitrites, nitroprusside and nitric-oxide - Evidence for the involvement of S-sitrosothiols as active intermediates. *Journal of Pharmacology and Experimental Therapeutics* **1981,** 218, (3), 739-749.
10. Gobert, A. P.; Semballa, S.; Daulouede, S.; Lesthelle, S.; Taxile, M.; Veyret, B.; Vincendeau, P., Murine macrophages use oxygen- and nitric oxide-dependent mechanisms to synthesize S-nitroso-albumin and to kill extracellular trypanosomes. *Infection and Immunity* **1998,** 66, (9), 4068-4072.
11. Persichini, T.; Colasanti, M.; Lauro, G. M.; Ascenzi, P., Cysteine nitrosylation inactivates the HIV-1 protease. *Biochemical and Biophysical Research Communications* **1998,** 250, (3), 575-576.
12. delaTorre, A.; Schroeder, R. A.; Bartlett, S. T.; Kuo, P. C., Differential effects of nitric oxide-mediated S-nitrosylation on p50 and c-jun DNA binding. *Surgery* **1998,** 124, (2), 137-141.
13. Broillet, M. C.; Firestein, S., Direct activation of the olfactory cyclic nucleotide-gated channel through modification of sulfhydryl groups by NO compounds. *Neuron* **1996,** 16, (2), 377-385.

14. Broillet, M. C.; Firestein, S., beta subunits of the olfactory cyclic nucleotide-gated channel form a nitric oxide activated Ca^{2+} channel. *Neuron* **1997,** 18, (6), 951-958.
15. Tenneti, L.; DEmilia, D. M.; Lipton, S. A., Suppression of neuronal apoptosis by S-nitrosylation of caspases. *Neuroscience Letters* **1997,** 236, (3), 139-142.
16. Li, J. R.; Billiar, T. R.; Talanian, R. V.; Kim, Y. M., Nitric oxide reversibly inhibits seven members of the caspase family via S-nitrosylation. *Biochemical and Biophysical Research Communications* **1997,** 240, (2), 419-424.
17. Caballero, A. E., Endothelial dysfunction in obesity and insulin resistance: A road to diabetes and heart disease. *Obesity Research* **2003,** 11, (11), 1278-1289.
18. Mano, T.; Masuyama, T.; Yamamoto, K.; Naito, J.; Kondo, H.; Nagano, R.; Tanouchi, J.; Hori, M.; Inoue, M.; Kamada, T., Endothelial dysfunction in the early stage of atherosclerosis precedes appearance of intimal lesions assessable with intravascular ultrasound. *American Heart Journal* **1996,** 131, (2), 231-238.
19. Shah, V.; Wiest, R.; Garcia-Cardena, G.; Cadelina, G.; Groszmann, R. J.; Sessa, W. C., Hsp90 regulation of endothelial nitric oxide synthase contributes to vascular control in portal hypertension. *American Journal of Physiology-Gastrointestinal and Liver Physiology* **1999,** 277, (2), G463-G468.
20. Tooke, J. E., Perspectives in diabetes microvascular function in human diabetes - a physiological perspective. *Diabetes* **1995,** 44, (7), 721-726.
21. Fang, K. Z.; Ragsdale, N. V.; Carey, R. M.; MacDonald, T.; Gaston, B., Reductive assays for S-nitrosothiols: Implications for measurements in biological systems. *Biochemical and Biophysical Research Communications* **1998,** 252, (3), 535-540.
22. Tyurin, V. A.; Liu, S. X.; Tyurina, Y. Y.; Sussman, N. B.; Hubel, C. A.; Roberts, J. M.; Taylor, R.; Kagan, V. E., Elevated levels of S-nitrosoalbumin in preeclampsia plasma. *Circulation Research* **2001,** 88, (11), 1210-1215.
23. Murai, J. T.; Muzykanskiy, E.; Taylor, R. N., Maternal and fetal modulators of lipid metabolism correlate with the development of preeclampsia. *Metabolism-Clinical and Experimental* **1997,** 46, (8), 963-967.
24. Roberts, J. M., Preeclampsia: What we know and what we do not know. *Seminars in Perinatology* **2000,** 24, (1), 24-28.
25. Lavi, S.; Prasad, A.; Yang, E. H.; Mathew, V.; Simari, R. D.; Rihal, C. S.; Lerman, L. O.; Lerman, A., Smoking is associated with epicardial coronary endothelial dysfunction and elevated white blood cell count in patients with chest pain and early coronary artery disease. *Circulation* **2007,** 115, (20), 2621-2627.
26. Rassaf, T.; Bryan, N. S.; Kelm, M.; Feelisch, M., Concomitant presence of N-nitroso and S-nitroso proteins in human plasma. *Free Radical Biology and Medicine* **2002,** 33, (11), 1590-1596.
27. Gladwin, M. T.; Wang, X. D.; Reiter, C. D.; Yang, B. K.; Vivas, E. X.; Bonaventura, C.; Schechter, A. N., S-Nitrosohemoglobin is unstable in the reductive erythrocyte environment and lacks O^{-2}/NO-linked allosteric function. *Journal of Biological Chemistry* **2002,** 277, (31), 27818-27828.
28. Mayer, B.; Schrammel, A.; Schmidt, K.; Pfeiffer, S., Quantitative determination of S-nitrosothiols by electrochemical measurement of copper-catalyzed release of

nitric oxide. *Naunyn-Schmiedebergs Archives of Pharmacology* **1998,** 357, (4), R50-R50.

29. Pfeiffer, S.; Schrammel, A.; Schmidt, K.; Mayer, B., Electrochemical determination of S-nitrosothiols with a clark-type nitric oxide electrode. *Analytical Biochemistry* **1998,** 258, (1), 68-73.
30. Schulz, K.; Kerber, S.; Kelm, M., Reevaluation of the griess method for determining NO/NO^{2-} in aqueous and protein-containing samples. *Nitric Oxide-Biology and Chemistry* **1999,** 3, (3), 225-234.
31. Cook, J. a.; Kim, S. Y.; Teague, D.; Krishna, M. C.; Pacelli, R.; Mitchell, J. B.; Vodovotz, Y.; Nims, R. W.; Christodoulou, D.; Miles, A. M.; Grisham, M. B.; Wink, D. A., Convenient colorimetric and fluorometric assays for S-nitrosothiols. *Analytical Biochemistry* **1996,** 238, (2), 150-158.
32. Ishibashi, T.; Tashimo, O.; Yoshida, J.; Tsuchida, H.; Nishio, M., Interference by ultrafiltration with Saville's method (absorbance at 540 nm) in determination of low-molecular weight S-nitrosothiols. *Nitric Oxide-Biology and Chemistry* **2004,** 11, (1), 78-78.
33. Tashimo, O.; Ishibashi, T.; Yoshida, J.; Tsuchida, H.; Nishio, M., Interference with Saville's method in determination of low-molecular weight S-nitrosothiols by ultrafiltration. *Nitric Oxide-Biology and Chemistry* **2003,** 9, (3), 148-152.
34. Tsikas, D., Measurement of physiological S-nitrosothiols: a problem child and a challenge. *Nitric Oxide-Biology and Chemistry* **2003,** 9, (1), 53-55.
35. Stamler, J. S.; Toone, E. J., The decomposition of thionitrites. *Current Opinion In Chemical Biology* **2002,** 6, (6), 779-785.
36. Szacilowski, K.; Stasicka, Z., S-nitrosothiols: Materials, reactivity and mechanisms. *Progress In Reaction Kinetics And Mechanism* **2001,** 26, (1), 1-58.
37. Cha, W.; Lee, Y.; Oh, B. K.; Meyerhoff, M. E., Direct detection of S-nitrosothiols using planar amperometric nitric oxide sensor modified with polymeric films containing catalytic copper species. *Analytical Chemistry* **2005,** 77, (11), 3516-3524.
38. Cha, W.; Meyerhoff, M. E., S-nitrosothiol detection via amperometric nitric oxide sensor with surface modified hydrogel layer containing immobilized organoselenium catalyst. *Langmuir* **2006,** 22, (25), 10830-10836.
39. Lee, Y.; Yang, J.; Rudich, S. M.; Schreiner, R. J.; Meyerhoff, M. E., Improved planar amperometric nitric oxide sensor based on platinized platinum anode. 2. Direct real-time measurement of NO generated from porcine kidney slices in the presence of L-arginine, L-arginine polymers, and protamine. *Analytical Chemistry* **2004,** 76, (3), 545-551.
40. Lee, Y.; Oh, B. K.; Meyerhoff, M. E., Improved planar amperometric nitric oxide sensor based on platinized platinum anode. 1. Experimental results and theory when applied for monitoring NO release from diazeniumdiolate-doped polymeric films. *Analytical Chemistry* **2004,** 76, (3), 536-544.
41. Wang, P. G.; Xian, M.; Tang, X. P.; Wu, X. J.; Wen, Z.; Cai, T. W.; Janczuk, A. J., Nitric oxide donors: Chemical activities and biological applications. *Chemical Reviews* **2002,** 102, (4), 1091-1134.

42. Hou, Y. C.; Guo, Z. M.; Li, J.; Wang, P. G., Seleno compounds and glutathione peroxidase catalyzed decomposition of S-nitrosothiols. *Biochemical And Biophysical Research Communications* **1996,** 228, (1), 88-93.
43. Stamler, J. S.; Loscalzo, J., Capillary Zone Electrophoretic detection of Biological thiols and their S-nitrosated derivatives. *Analytical Chemistry* **1992,** 64, (7), 779-785.
44. Stamler, J. S.; Simon, D. I.; Osborne, J. A.; Mullins, M. E.; Jaraki, O.; Michel, T.; Singel, D. J.; Loscalzo, J., S-Nitrosylation of proteins with nitric-oxide - Synthesis and characterization of biologically-active compounds. *Proceedings of the National Academy of Sciences of the United States of America* **1992,** 89, (1), 444-448.
45. Birringer, M.; Pilawa, S.; Flohe, L., Trends in selenium biochemistry. *Natural Product Reports* **2002,** 19, (6), 693-718.
46. Nygard, B.; Ludvik, J.; Wendsjo, S., Voltammetry of organic ditellurides in protic media. Mercury assisted chemical pre-reactions with catalytic effects. *Electrochimica Acta* **1996,** 41, (10), 1655-1660.
47. Giustarini, D.; Milzani, A.; Colombo, R.; Dalle-Donne, I.; Rossi, R., Nitric oxide and S-nitrosothiols in human blood. *Clinica Chimica Acta* **2003,** 330, (1-2), 85-98.
48. Rossi, R.; Giustarini, D.; Milzani, A.; Colombo, R.; Dalle-Donne, I.; Di Simplicio, P., Physiological levels of S-nitrosothiols in human plasma. *Circulation Research* **2001,** 89, (12), E47.
49. Stamler, J. S., S-nitrosothiols in the blood - Roles, amounts, and methods of analysis. *Circulation Research* **2004,** 94, (4), 414-417.
50. Meyer, D. J.; Kramer, H.; Ozer, N.; Coles, B.; Ketterer, B., Kinetics and equilibria of S-nitrosothiol-thiol exchange between glutathione, cysteine, penicillamines and serum-albumin. *Febs Letters* **1994,** 345, (2-3), 177-180.
51. Stamler, J. S.; Jaraki, O.; Osborne, J.; Simon, D. I.; Keaney, J.; Vita, J.; Singel, D.; Valeri, C. R.; Loscalzo, J., Nitric-oxide circulates in mammalian plasma primarily as an S-nitroso adduct of serum-albumin. *Proceedings of the National Academy of Sciences of the United States of America* **1992,** 89, (16), 7674-7677.
52. Broillet, M. C., S-Nitrosylation of proteins. *Cellular and Molecular Life Sciences* **1999,** 55, (8-9), 1036-1042.
53. Noble, D. R.; Williams, D. L. H., Formation and reactions of S-nitroso proteins. *Journal of the Chemical Society-Perkin Transactions 2* **2001**, (1), 13-17.
54. Wang, K.; Wen, Z.; Zhang, W.; Xian, M.; Cheng, J. P.; Wang, P. G., Equilibrium and kinetics studies of transnitrosation between S-nitrosothiols and thiols. *Bioorganic & Medicinal Chemistry Letters* **2001,** 11, (3), 433-436.
55. Brand, M. J. D.; Rechnitz, G. A., Computer approach to ion-selective electrode potentiometry by standard addition methods. *Analytical Chemistry* **1970,** 42, (11), 1172-1177.
56. Midgley, D., Systematic and random errors in double known addition potentiometry - a review. *Analyst* **1993,** 118, (11), 1347-1354.
57. Musameh, M.; Moezzi, N.; Schauman, L. M.; Meyerhoff, M. E., Glutathione peroxidase-based amperometric biosensor for the detection of S-nitrosothiols. *Electroanalysis* **2006,** 18, (21), 2043-2048.

Chapter 7

Conclusions and Future Directions

7.1. Conclusions

The research in this dissertation has introduced a new strategy for preparing the biomaterials to improve their hemocompatibility. The polymers possessing appended catalytic sites, where the catalyst can liberate NO from endogenous S-nitrosothiols (RSNOs) to nitric oxide (NO) in the presence of reducing agents such as free thiols (RSHs) already present in blood, are able to provide elevated NO levels at the polymer/blood boundary. Hence, these new types of polymeric materials are termed NO generating polymers (NOGPs). Owing to the variety of vasoprotective activities of NO,[1-4] as observed for healthy endothelial cells (EC),[5] the NOGPs may offer surfaces that are resisted to thrombus formation, smooth cell proliferation, and bacterial infection, etc.[1-4]

7.1.1. NO generating catalysts

Two distinctive catalysts have been employed in this research. One was the metal ion-based NO generating catalyst, Cu(II)-cyclen (cyclen; 1,4,7,10-tetraazacyclododecane) as described in Chapters 2 and 3. The incorporation of the catalytic redox chemistry between Cu(II)/Cu(I) and RSNO/RSH[6] into the polymeric phase made it possible for this type of NOGP to catalyze spontaneous NO generation in contact with blood.

The other catalyst was the organoditelluride (RTeTeR)-based species that has been discovered in this work to be a NO generating catalyst (see Chapter 4). The catalytic mechanism of this species (5,5'-ditelluro-2,2'-dithiophenecarboxylic acid, DTDTCA) was studied in detail. Mechanistic studies indicate that: DTDTCA (ArTeTeAr) is reduced by thiolate (RS^-) to afford telluro-sulfide (ArTeSR) intermediate and tellurolate ($ArTe^-$), and then $ArTe^-$ decomposes RSNO to produce NO, RS^-, and ½ (ArTeTeAr); ArTeSR is again reduced by RS^- to form $ArTe^-$ and RSSR (the rate-limiting step). The organoditelluride compound is also known to participate in a disproportion reaction of ArTeSR to ½ (ArTeTeAr) and ½ (RSSR)[7,8] and the oxidation of $ArTe^-$ to ½ (ArTeTeAr) mediated by oxygen[9] (see Chapter 4).

7.1.2. Polymer matrices

The low molecular weight (LMW) endogenous RSNO/RSH species (e.g., S-nitrosoglutathione (GSNO), S-nitrosocysteine (CySNO), glutathione (GSH), and cysteine (CySH)) can easily diffuse into the polymeric phase and react with the catalytic sites in the NOGPs. Therefore, in order to maximize the catalytic efficiency of the NOGPs, the catalytic sites were created in both the surface and bulk phases of the polymers through homogeneous reactions with the polymers and the NO generating catalysts. In these immobilization steps, the covalent attachments were performed to minimize the potential catalyst leaching. In addition, because the hydrophilic polymer would be beneficial to provide a good environment for the substrates to diffuse into (and thus the catalytic efficiency could be maximized) a variety of hydrophilic polymers were employed in this study such as hydrogel types of polymers and hydrophilic polyurethanes (PU).

For example, a Cu(II)-cyclen complex modified with a polymerizable functional group, a methacrylate moiety, was crosslinked with poly(2-hydroxyethyl methacrylate) (pHEMA), a representative classic hydrogel,[10-12] yielding a new type of functional hydrogel containing the NO generating catalyst (Chapter 2). Further, a biomedical grade polymer, hydrophilic thermoplastic PU[13-15] modified with free amine groups was conjugated with the another cyclen monomer appended with a free carboxylic acid to afford the PU-based NOGP (Chapter 3). The new RTeTeR species (DTDTCA) was also linked to various polymers including thermoplastic PU and poly(allylamine hydrochloride) (PAH), as well as the interpenetrating polymer network (IPN) using a cellulose membrane and the DTCTCA-tethered PAH (Chapters 5 and 6).

7.1.3. Catalytic NO generation of the NOGP

The NO generation of the various NOGPs newly developed in this research was measured by two specific techniques; chemiluminescence NO analyzer (NOA) and amperometric RSNO sensor[16, 17] (see Chapters 2 – 6).

To demonstrate the catalytic activities of the NOGPs, typical procedures for the NOA experiments were performed. When a given small sized NOGP was immersed into the endogenous RSNO/RSH species in PBS buffer, pH7.4, the baseline NO level was increased and reached to a steady-state NO level; then, by removing the piece of the NOGP from the reaction solution, the NO level returned to the original baseline. The catalytic reaction mediated by the NOGP was further confirmed by continuing the insertion/removal processes via the NOA measurements. Indeed, the catalytic NO generation properties of a variety of the NOGPs developed in this work were successfully demonstrated by the NOA measurements.

To demonstrate the spontaneous NO generation mediated by the NOGPs in contact with blood, an amperometric RSNO sensor configuration,[16, 17] in which an NO sensor is modified with the various NOGPs, was used. The RSNO sensors were fabricated by mounting a thin film of given NOGP onto the distal tip of a planar NO sensor.[18, 19] Because the NOGP film in the RSNO sensor provides a catalytic layer responsible for the NO generation, the RSNO species in the sample solution that diffuse into the catalytic layer decomposes to NO, and the NO levels within this layer are locally increased in proportional to the RSNO levels. Hence, the NO oxidation reaction occurs at the platinized platinum anode and yields a current signal that is in proportional to the RSNO concentrations in the sample solutions. The NO sensors modified with "blank" polymers (without any NO generating catalysts) were used for control experiments, and did not yield RSNO responses. The RSNO sensors modified with the various NOGPs successfully demonstrated their ability to spontaneously generate NO when in contact with fresh blood.

As an application example of the organoditlluride-based NOGPs, more detailed studies of a given amperometric RSNO sensor design[16, 17] based on using a DTDTCA-tethered PAH were carried out for the direct detection of various RSNO species (see Chapter 6). This proposed RSNO sensor could reversibly detect low molecular weight (LMW) endogenous GSNO and/or CySNO at 0.1 μM levels. Both GSNO and CySNO yield comparable responses. The remarkable feature of this new RSNO sensor is a very long operational lifetime (up to a month) probably due to the excellent stability of DTDTCA-linked PAH in the outer dialysis membrane of the device (see Chapter 6).

7.1.4. Potential catalyst leaching

To investigate the potential catalyst leaching from the NOGPs, various soaking experiments were carried out. In this work, after soaking the NOGPs in a given solution, such as the excess amount of GSNO/GSH or the animal blood, for certain time periods, the catalyst content either in the polymer or the solution was analyzed primary by inductively coupled plasma-high resolution mass spectrometry (ICP-HRMS).

In the case of Cu(II)-cyclen based NOGPs, due to the strong metal binding affinities of RSH and/or RSSR[20, 21] (formed during the NO generation reactions), the excess amount of GSNO/GSH caused the significant loss of copper in the films of the NOGPs (ca. 30 % loss of copper for 15 d, see Chapter 2), resulting in the considerable decrease in the NO flux (see Chapters 2 and 3). However, after soaking in sheep plasma, no significant changes in the NO fluxes were observed (Chapters 2 and 3). These data indicate that the blood components may not influence the demetalation and/or deactivation of copper catalysts in the Cu(II)-cyclen based NOGPs, while the LMW endogenous RSH and/or RSSR species may be largely responsible for the demetalation processes from these polymeric materials.

The catalyst leaching from the organditelluride-immobilized polymer was also examined by measuring the tellurium (Te) amount in the solution after soaking in excess GSNO/GSH (see Chapter 5). First, the one side-tethered RTeTeR species (among two carboxylic acid groups in DTDTCA) can be easily released from the polymeric matrix, and this process is likely responsible for the 10 % loss of Te after soaking for 1 d. Then, the disconnection of the ditelluride bond during the catalytic reaction also causes the physically crosslinked polymers and/or low molecular weight polymers (> 50k, the

molecular weight cutoff of the cellulose membrane employed in this IPN) to further fragment to dissolve in the solution phase, yielding the additional 10 % loss over 2 weeks. In fact, the rate of Te loss was opposite to the GSH/GSNO levels in the solution phase (see Chapter 5). This experiment proposes the good stability of the DTDTCA in the polymer matrix during this redox cycle, allowing it to exhibit long-term catalytic activity (see Chapter 6).

7.2. Future directions

7.2.1. Coatings for stents

Vascular stents to reduce the restenosis (re-occlusion of blood vessel) compared to balloon angioplasty (enlarging an artery partially blocked by atherosclerotic plaque),[22, 23] however, it has been reported that stent stenosis (in-stent restenosis) occurs in about 10 - 60 % of cases[24-27] due mainly to the neointimal hyperplasia[22, 28] resulting from the inflammatory reactions. This process is quite complex and not fully understood, but it is known that the main mediator is the excessive proliferation of vascular smooth muscle cells.[22, 29] Since NO plays a key role in inhibiting the vascular smooth muscle cell proliferation *in vivo*, the NOGPs may offer an approach in such medical devices to enhance their hemocompatiblitiy.

For example, to make the Cu(II)-cyclen complex-based NOGP more applicable as a coating for stents, the modified intermediate, cyclen-N-propyl methacrylate (**3**) (see **Scheme 7.1**) that have been synthesized in this research (see Chapter 2) may be useful to anchor such coatings on metal surfaces. **Scheme 7.1** shows how this intermediate can be

employed in the surface modification of commercial stents. Based on the proposed scheme and using the key intermediate, this work will be further conducted by Dr. Lahann and his researchers at the Department of Chemical Engineering in the University of Michigan as well as the researchers in Michigan Critical Care Consultants Inc. (MC3, Inc.) in Ann Arbor.

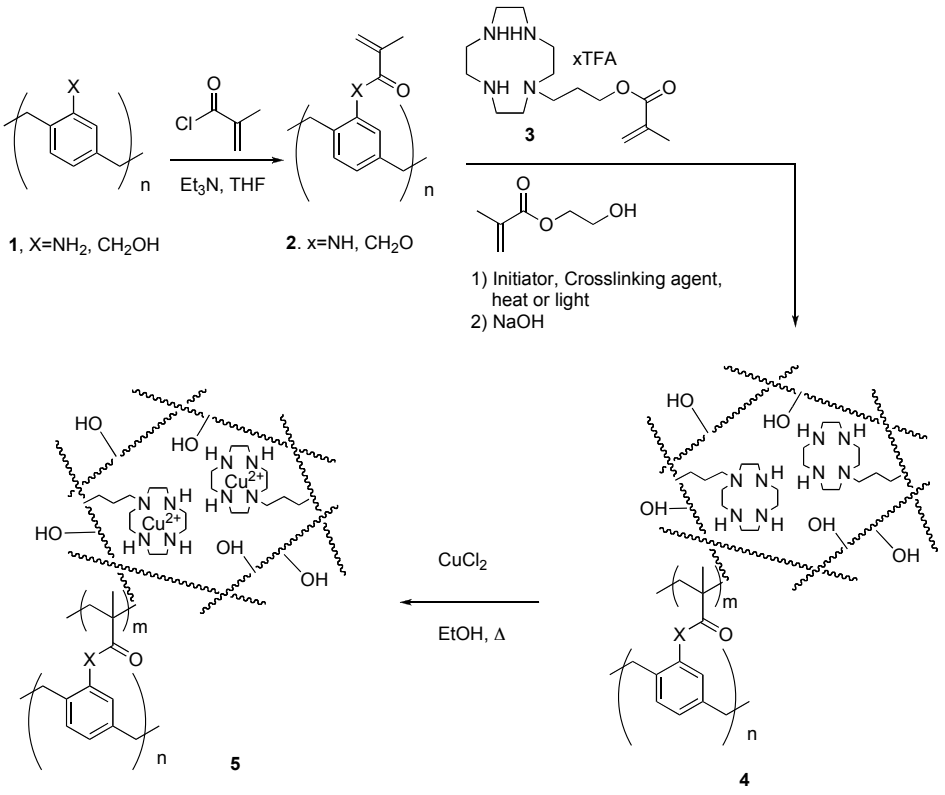

Scheme 7.1 The proposed scheme for the anchoring the Cu(II)-cyclen complex on the surface of stent coated with the functionalized poly-*para*-xylylene (PPX) (**2**) using the cyclen-N-propyl methacrylate monmer (**3**) developed in this research (see **Scheme 2.1** in Chapter 2).

In this proposed scheme, an ultra-thin polymer coating (~ 200 nm) is formed on the surface of a stainless steel stent using functionalized poly-*para*-xylylene (PPX) monomers[30] (**1**) (hydroxy methyl-PPX, or amino-PPX, see **Scheme 7.1**) via the chemical

vapor deposition (CVD)[31] process. This polymer can be further derivatized with an anchoring methacrylate group (**2**). Thus, the polymerization of the intermediate (**3**) on the surface of the stent coated with the functionalized polymer **2** will afford another hydrogel layer containing the modified cyclen. Copper ion incorporation into the surface polymer **4** will result in the final NO generating polymer coating **5**.

7.2.2. Coatings for indwelling sensors

The development of an implantable glucose sensor that can continuously monitor glucose levels of the diabetic patients *in vivo* is an important biomedical goal.[32-36] The major barriers are identified to be the inflammatory responses of the body causing the sensors to yield unreliable analytical results and/or decreasing their sensitivities.[37, 38] NO is a naturally occurring anti-inflammatory agent;[39] thus a locally elevated NO level at the implanted sensor's surface could be achieved by a thin coating of a suitable NOGP, and this may maintain the proper function of the sensor for extended time periods.

To evaluate the effectiveness of the NOGPs in such application, a needle-type subcutaneous glucose sensor coated with the NOGPs will be tested in this laboratory. For example, thermoplastic polyurethanes (PUs) tailored with the Cu(II)-cyclen complex (see Chapter 3) has a good solubility in organic solvents such as THF. Thus, this NOGP composed of biomedical PU matrix affords various benefits in terms of the process as well as sterilization. This new NOGP will be dip-coated on the needle-type indwelling glucose sensors to form a thin protective layer that can provide the locally increased NO levels at the polymer/blood interface. Prior to use, it will be tested to see how the NOGP coatings could affect the functions of the glucose sensors by comparing the control sensors coated with the "blank" polymers (without the NO generating catalyst).

7.2.3. Catalytic layers for amperometric S-nitrosothiol sensors

As presented in Chapter 6, the amperometric RSNO sensors[16, 17] outfitted with an organoditelluride-tethered polymer have already been shown to be useful to directly detect the various RSNO species. In addition, very interesting results were observed regarding the transnitrosation effects as well as the size-limit of detecting RSNO species (only LMW RSNO species can be reversibly detected). In order to measure all RSNO levels in biological samples including the LMW RSNO species such as GSNO and CySNO, and high molecular weight (HMW) RSNO species such as S-nitrosoalbumin (AlbSNO) and S-nitrosohemoglobin (HbSNO), new approaches must be considered. Originally, the catalytic layer has been designed to be located between the gas permeable membrane (GPM) and outer dialysis membrane (see **Figure 6.1** in Chapter 6). Hence, the MWCO of dialysis membrane determines the sizes of analytes that can diffuse into the catalytic layer, and then to be detected. Therefore, one potential strategy to accomplish this goal is to modify the configurations of the catalytic layers in the proposed RSNO sensor, in which the immobilized catalytic layer will be tethered at the outmost layer; that is, not over the GPM, but the outer surface of the dialysis membrane. Then, this catalytic layer likely reacts with all RSNO species regardless of the molecular sizes. In addition, it would be interesting to observe how the different configurations of the catalytic layers in the proposed RSNO sensors will result in the amperometric responses to the transnitrostations between RSNOs/RSHs species with various their levels.

7.3 Considerations for future research and applications of NOGPs

The fundamental idea of creating NOGPs was successfully demonstrated mainly via use of appropriate synthetic chemistry in this thesis work. Both Cu(II)-cyclen-based and organoditelluride-based NOGPs clearly exhibit catalytic NO production from the naturally occurring RSNO species under physiological conditions as well as spontaneous NO generation when in contact with fresh animal blood. Hence, these NOGPs have the potential to become useful biomaterials to enhance the hemocompatible of blood contacting devices for long-term applications.

Among major concerns, however, that must be addressed before such NOGPs can be seriously considered for clinical applications, is the catalyst leaching (copper ions or organotellurium/tellurium species in this work) into the contacting biological fluids. Although the Cu(II)-cyclen complex has a high copper ion binding stability, the complete prevention of metal ion leaching from such a metal-ligand complexed polymeric material is not possible, since there is always a low equilibrium concentration of copper ions present that can interact with the biological environment. As shown in this work, catalyst leaching when soaking the Cu(II)-cyclen-based NOGPs in solutions containing excess of GSH/GSNO resulted in a significant decrease of copper content of the polymer (25 – 35 %) after 15 days. This loss was coupled with a substantial reduction in the NO generating capability (more than 50 %) of the polymer. It is likely that the copper ions mostly at the surface of polymer are leached out under such conditions; however, the majority of copper ions within the interior of the polymeric phase are still able to decompose RSNOs to NO.

In the case of the organoditelluride-based NOGP, Te leaching is relatively low, provided the polymer is properly prepared (e.g., by pre-treatment with excess RSH to remove uncoupled halves of the DTDTCA species). Tellurium leaching is minimal due to the good redox stability of the prepared organoditelluride species (DTDTCA). In fact, the catalytic function of the final polymer was well maintained (ca. one month) as demonstrated by the amperometric RSNO sensor equipped with such a DTDTCA-based NOGP (see Chapter 6). Considering the high toxicity of tellurium and potential toxicity of organotellurium species compared to the copper ions, the copper-ligand based NOGP is more likely suitable for the application of medical devices, and the organoditelluride-based NOGP would be more useful for *in vitro* applications, including the preparation of RSNO sensors.

For *in vivo* applications of NOGPs (e.g., coatings for extracorporeal circuits, vascular grafts, etc.), the side effects that may be caused by the additional production of NO and consumption of endogenous RSNOs via NOGPs need to be considered as well. The therapeutic window of NO (ranges between effective and toxic dosage) has not been examined in any detail. Further the levels of endogenous RSNO levels (reported to be ranged from a few nM to sub-mM) as well as the possibility of individual differences in these values are not yet understood. Based on the recent animal studies in our laboratory, extracorporeal circuits coated with NOGPs possessing a relatively large surface area caused rapid consumption of the endogenous RSNOs (after 1 h), suggesting that production of endogenous RSNOs was much slower than consumption by the NOGP coated circuit. Hence, the supplementation of the animal with exogenous RSNO may be

necessary to observe the optimal benefit of the NOGP coating to reduce thrombus and platelet loss. In the extracorporeal circuit application, this is quite feasible.

All questions with respect to the longer-term NO generation capability as well as the side effects (including the potential toxicity) that may occur by the employment of NOGP must be answered by clinical investigations, first with appropriate animal models, and then potentially in human studies. The good news derived from this dissertation work is that chemistry can enable development of a variety of NOGPs and tune their NO generating properties by adjusting the amount of NO generating catalyst loaded in the polymer matrix. To achieve the ultimate goal of clinical *in vivo* application of these new NOGP materials, many scientists including chemists, biologists, biomedical engineers, as well as clinical researchers will need to collaborate closely to answer the many fundamental physiology and practical questions that remain.

7.5. References

1. Krejcy, K.; Schmetterer, L.; Kastner, J.; Nieszpaurlos, M.; Monitzer, B.; Schutz, W.; Eichler, H. G.; Kyrle, P. A., Role of nitric-oxide in hemostatic system activation in-vivo in humans. *Arteriosclerosis Thrombosis and Vascular Biology* **1995,** 15, (11), 2063-2067.
2. Samama, C. M.; Diaby, M.; Fellahi, J. L.; Mdhafar, A.; Eyraud, D.; Arock, M.; Guillosson, J. J.; Coriat, P.; Rouby, J. J., Inhibition of platelet-aggregation by inhaled nitric-oxide in patients with acute respiratory-distress syndrome. *Anesthesiology* **1995,** 83, (1), 56-65.
3. Sarkar, R.; Webb, R. C., Does nitric oxide regulate smooth muscle proliferation? A critical appraisal. *Journal of Vascular Research* **1998,** 35, (3), 135-142.
4. Isenberg, J. S., Nitric oxide modulation of early angiogenesis. *Microsurgery* **2004,** 24, (5), 385-391.
5. Huang, P. L.; Huang, Z. H.; Mashimo, H.; Bloch, K. D.; Moskowitz, M. A.; Bevan, J. A.; Fishman, M. C., Hypertension in mice lacking the gene for endothelial nitric-oxide synthase. *Nature* **1995,** 377, (6546), 239-242.
6. Mcaninly, J.; Williams, D. L. H.; Askew, S. C.; Butler, A. R.; Russell, C., Metal-ion catalysis in nitrosothiol (RSNO) decomposition. *Journal of the Chemical Society-Chemical Communications* **1993**, (23), 1758-1759.
7. Dong, Z.; Liu, J.; Mao, S.; Huang, X.; Yang, B.; Ren, X.; Luo, G.; Shen, J., Aryl thiol substrate 3-carboxy-4-nitrobenzenethiol strongly stimulating thiol peroxidase activity of glutathione peroxidase mimic 2, 2'-ditellurobis (2-deoxy-b-cyclodextrin). *Journal of the American Chemical Society* **2004,** 126, (50), 16395-16404.
8. Mugesh, G.; Panda, A.; Kumar, S.; Apte, S. D.; Singh, H. B.; Butcher, R. J., Intramolecularly coordinated diorganyl ditellurides: Thiol peroxidase-like antioxidants. *Organometallics* **2002,** 21, (5), 884-892.
9. Engman, L.; Cava, M. P., Organotellurium compounds. 6. Synthesis and reactions of some heterocyclic lithium tellurolates. *Organometallics* **1982,** 1, (3), 470-473.
10. Ramakrishna, S.; Mayer, J.; Wintermantel, E.; Leong, K. W., Biomedical applications of polymer-composite materials: a review. *Composites Science and Technology* **2001,** 61, (9), 1189-1224.
11. Midha, R.; Munro, C. A.; Dalton, P. D.; Tator, C. H.; Shoichet, M. S., Growth factor enhancement of peripheral nerve regeneration through a novel synthetic hydrogel tube. *Journal of Neurosurgery* **2003,** 99, (3), 555-565.
12. Montheard, J. P.; Chatzopoulos, M.; Chappard, D., 2-Hydroxyethyl methacrylate (HEMA) - chemical-properties and applications in biomedical fields. *Journal of Macromolecular Science-Reviews In Macromolecular Chemistry and Physics* **1992,** C32, (1), 1-34.
13. Zdrahala, R. J.; Zdrahala, I. J., Biomedical applications of polyurethanes: A review of past promises, present realities, and a vibrant future. *Journal of Biomaterials Applications* **1999,** 14, (1), 67-90.

14. Gunatillake, P. A.; Martin, D. J.; Meijs, G. F.; McCarthy, S. J.; Adhikari, R., Designing biostable polyurethane elastomers for biomedical implants. *Australian Journal of Chemistry* **2003,** 56, (6), 545-557.
15. Francois, P.; Vaudaux, P.; Nurdin, N.; Mathieu, H. J.; Descouts, P.; Lew, D. P., Physical and biological effects of a surface coating procedure on polyurethane catheters. *Biomaterials* **1996,** 17, (7), 667-678.
16. Cha, W.; Lee, Y.; Oh, B. K.; Meyerhoff, M. E., Direct detection of S-nitrosothiols using planar amperometric nitric oxide sensor modified with polymeric films containing catalytic copper species. *Analytical Chemistry* **2005,** 77, (11), 3516-3524.
17. Cha, W.; Meyerhoff, M. E., S-Nitrosothiol detection via amperometric nitric oxide sensor with surface modified hydrogel layer containing immobilized organoselenium catalyst. *Langmuir* **2006,** 22, (25), 10830-10836.
18. Lee, Y.; Yang, J.; Rudich, S. M.; Schreiner, R. J.; Meyerhoff, M. E., Improved planar amperometric nitric oxide sensor based on platinized platinum anode. 2. Direct real-time measurement of NO generated from porcine kidney slices in the presence of L-arginine, L-arginine polymers, and protamine. *Analytical Chemistry* **2004,** 76, (3), 545-551.
19. Lee, Y.; Oh, B. K.; Meyerhoff, M. E., Improved planar amperometric nitric oxide sensor based on platinized platinum anode. 1. Experimental results and theory when applied for monitoring NO release from diazeniumdiolate-doped polymeric films. *Analytical Chemistry* **2004,** 76, (3), 536-544.
20. Baek, H. K.; Cooper, R. L.; Holwerda, R. A., Stability of the Cu(II)-S bond in mercapto amino-acid complexes of [2,2',2''-tris(dimethylamino)triethylamine]copper(II) and [tris(2-pyridylmethyl)amine]copper(II). *Inorganic Chemistry* **1985,** 24, (7), 1077-1081.
21. Gilbert, B. C.; Silvester, S.; Walton, P. H., Spectroscopic, kinetic and mechanistic studies of the influence of ligand and substrate concentration on the activation by peroxides of Cu-I-thiolate and other Cu-I complexes. *Journal of the Chemical Society-Perkin Transactions 2* **1999**, (6), 1115-1121.
22. Bennett, M. R.; O'Sullivan, M., Mechanisms of angioplasty and stent restenosis: implications for design of rational therapy. *Pharmacology & Therapeutics* **2001,** 91, (2), 149-166.
23. Horlitz, M.; Sigwart, U.; Niebauer, J., Fighting restenosis after coronary angioplasty: contemporary and future treatment options. *International Journal of Cardiology* **2002,** 83, (3), 199-205.
24. Fenton, S. H.; Fischman, D. L.; Savage, M. P.; Schatz, R. A.; Leon, M. B.; Baim, D. S.; King, S. B.; Heuser, R. R.; Curry, R. C.; Rake, R. C.; Goldberg, S., Long-term angiographic and clinical outcome after implantation of balloon-expandable stents in aortocoronary saphenous-vein grafts. *American Journal of Cardiology* **1994,** 74, (12), 1187-1191.
25. Fischman, D. L.; Leon, M. B.; Baim, D. S.; Schatz, R. A.; Savage, M. P.; Penn, I.; Detre, K.; Veltri, L.; Ricci, D.; Nobuyoshi, M.; Cleman, M.; Heuser, R.; Almond, D.; Teirstein, P. S.; Fish, R. D.; Colombo, A.; Brinker, J.; Moses, J.; Shaknovich, A.; Hirshfeld, J.; Bailey, S.; Ellis, S.; Rake, R.; Goldberg, S., A randomized comparison of coronary-stent placement and balloon angioplasty in the treatment

of coronary-artery disease. *New England Journal of Medicine* **1994,** 331, (8), 496-501.

26. Serruys, P. W.; Dejaegere, P.; Kiemeneij, F.; Macaya, C.; Rutsch, W.; Heyndrickx, G.; Emanuelsson, H.; Marco, J.; Legrand, V.; Materne, P.; Belardi, J.; Sigwart, U.; Colombo, A.; Goy, J. J.; Vandenheuvel, P.; Delcan, J.; Morel, M. A., A comparison of balloon-expandable-stent implantation with balloon angioplasty in patients with coronary-artery disease. *New England Journal of Medicine* **1994,** 331, (8), 489-495.
27. Tilli, F. V.; Aliabadi, D.; Kinn, J. M.; Kaplan, B. M.; Benzuly, K. H.; Safian, R. D., Real life stenting: A comparison of target vessel revascularization in benestent-stress lesions to non benestent-stress lesions. *Circulation* **1996,** 94, (8), 1934-1934.
28. Lowe, H. C.; Schwartz, R. S.; Mac Neill, B. D.; Jang, L. K.; Hayase, M.; Rogers, C.; Oesterle, S. N., The porcine coronary model of in-stent restenosis: Current status in the era of drug-eluting stents. *Catheterization and Cardiovascular Interventions* **2003,** 60, (4), 515-523.
29. Kavurma, M. M.; Khachigian, L. M., ERK, JNK, and p38 MAP kinases differentially regulate proliferation and migration of phenotypically distinct smooth muscle cell subtypes. *Journal of Cellular Biochemistry* **2003,** 89, (2), 289-300.
30. Lahann, J.; Langer, R., Novel poly(p-xylylenes): Thin films with tailored chemical and optical properties. *Macromolecules* **2002,** 35, (11), 4380-4386.
31. Gorham, W. F., A new general synthetic method for preparation of linear poly-P-xylylenes. *Journal of Polymer Science Part a-1-Polymer Chemistry* **1966,** 4, (12PA), 3027-3039.
32. Clarke, W. L.; Santiago, J. V., Characteristics of a new glucose sensor for use in an artificial pancreatic beta cell. *Artificial Organs* **1977,** 1, (2), 78-82.
33. Garg, S. K.; Schwartz, S.; Edelman, S. V., Improved glucose excursions using an implantable real-time continuous glucose sensor in adults with type 1 diabetes. *Diabetes Care* **2004,** 27, (3), 734-738.
34. Shichiri, M.; Kawamori, R.; Yamasaki, Y., Needle-type glucose sensor. *Methods in Enzymology* **1988,** 137, 326-334.
35. Shichiri, M.; Kawamori, R.; Yamasaki, Y.; Hakui, N.; Abe, H., Wearable artificial endocrine pancreas with needle-type glucose sensor. *Lancet* **1982,** 2, (8308), 1129-1131.
36. Wilkins, E.; Atanasov, P., Glucose monitoring: State of the art and future possibilities. *Medical Engineering & Physics* **1996,** 18, (4), 273-288.
37. Anderson, J. M., Mechanisms of inflammation and infection with implanted devices. *Cardiovascular Pathology* **1993,** 2, (3), S33-S41.
38. Gifford, R.; Kehoe, J. J.; Barnes, S. L.; Kornilayev, B. A.; Alterman, M. A.; Wilson, G. S., Protein interactions with subcutaneously implanted biosensors. *Biomaterials* **2006,** 27, (12), 2587-2598.
39. Kim, S. F.; Huri, D. A.; Snyder, S. H., Inducible nitric oxide synthase binds, S-nitrosylates, and activates cyclooxygenase-2. *Science* **2005,** 310, (5756), 1966-1970.